Ground vibration during the bentonite tunnelling process

B. M. New

GROUND VIBRATION DURING THE BENTONITE TUNNELLING PROCESS

by

B M NEW

being a thesis submitted in partial fulfilment of the requirements for the degree of Master of Science in the University of Durham

July 1977

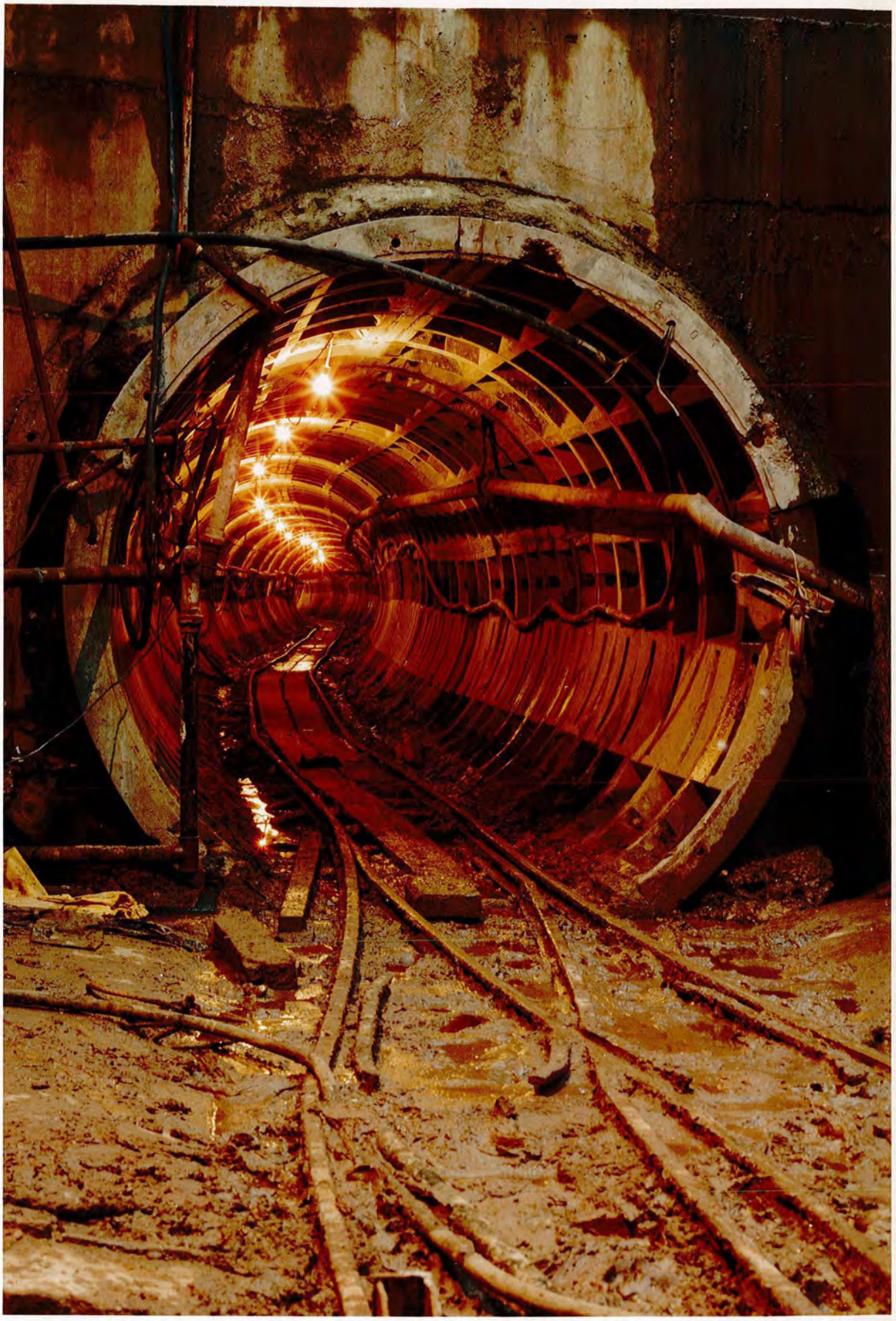

THE TUNNEL PORTAL

GROUND VIBRATION DURING THE BENTONITE TUNNELLING PROCESS

ABSTRACT

The research was carried out during the bentonite shield tunnel drive for the Acton Grange trunk outfall sewer at Warrington, Cheshire. This tunnel is driven through cohesionless Drift deposits beneath a built-up urban environment, with a cover of less than 6m. The environmental effects of the ground vibration caused by the excavation process are investigated with particular regard to ground settlement by compaction. The geology of the area and the technical and commercial factors which led to the choice of the bentonite tunnelling system are described.

Previous work on compaction by vibration is critically reviewed and methods to assess a soil's potential for compaction are given. The vibration instrumentation is described and relevant wave propagation theory is developed with emphasis on body waves from underground sources.

Vibration data were recorded from transducers located in boreholes, on the pavement surface, on the tunnelling machine and on the concrete tunnel lining. These records were processed to characterise the vibrations in terms of peak particle velocities, frequency spectra and spatial attenuation.

The maximum measured ground vibration (expressed in terms of resultant peak particle velocity) was 3.90 mm/s. The vibration was

characterised by random high velocity particle motions resulting from impacts between the machine's disc cutters and glacial boulders in the tunnel face. Surface and subsurface settlement measurements were made along the tunnel line and structural damage to property above the tunnel was observed.

Laboratory tests and other field data showed that the ground in this area was likely to settle at levels of vibration lower than those measured from the tunnelling machine.

The vibration caused by the excavation process caused ground compaction which contributed to ground settlement and the ensuing damage to the overlying structures. The vibration was not likely to have damaged these properties directly but did cause considerable nuisance to the residents.

ACKNOWLEDGEMENTS

The work presented in this thesis formed part of a research programme carried out by Tunnels Division of the Transport and Road Research Laboratory during the construction of a trunk outfall sewer at Warrington, Cheshire. The project was carried out jointly with Durham University and was supervised by Dr P B Attewell (Reader in Engineering Geology, Durham University) and Mr M P O'Reilly (Head of Tunnels Division, TRRL).

The research was carried out by permission of the Warrington New Town Development Corporation and their main contractor for the works, Edmund Nuttall Ltd. In particular the author would like to thank Mr P Wild (of WNTDC), Mr C Bishop, Mr A Finch, Mr D Thornton and Mr D Sharrocks (of Edmund Nuttall Ltd) for their valuable assistance on site, the provision of tunnel survey data and the most useful discussions regarding the tunnel construction.

The author expresses his gratitude to Mr G West and Mr A S Nagarkatti for their assistance with this research and to Mr D A Barratt and the other members of Tunnels Division who provided the ground settlement data.

TABLE OF CONTENTS

		Page No
Abstract		i
Acknowledgements		iii
Table of Contents		iv
List of Figures		viii
List of Tables		x
List of Plates		xi
List of Appendices		xii
Chapter 1	Ground vibration in tunnelling	1
1.1	The significance of ground vibration in civil engineering	1
1.2	Soft ground tunnelling	3
1.2.1	The need and technique	3
1.2.2	Surface disturbance	4
1.2.3	The opportunity for research	5
1.3	Thesis structure	6
Chapter 2	The bentonite tunnelling process and geology at Warrington	8
2.1	The Acton Grange trunk outfall sewer (AGTOS)	8
2.1.1	The social and civil engineering requirements	8
2.1.2	The contract	10
2.2	The slurry shield system	13
2.3	Site location and geology	18
2.3.1	The geology of the area	18
2.3.2	The site	21

Page No

2.4 Tunnelling problems associated with the site geology 30

2.4.1 Introduction 30

2.4.2 The presence of boulders 31

2.4.3 Loose ground 33

Chapter 3 Ground vibration: Its transmission and effect 38

3.1 Introduction 38

3.2 The transmission of wave energy 40

3.3 Settlement due to vibration in sands 47

3.3.1 Introduction 47

3.3.2 Saturated sands 47

3.3.3 Compaction 48

3.3.4 Measuring soil compaction 49

3.3.5 The effect of frequency and direction of vibration on settlement 53

3.4 The thresholds of tolerance to ground vibration 56

3.4.1 Urban structures 56

3.4.2 Human perception 57

Chapter 4 The measurement, recording and processing of the vibration data 62

4.1 Transducers 62

4.1.1 Measured variables 62

4.1.2 Geophones 63

4.1.3 Geophone location 65

4.1.4 In-tunnel measurements 67

4.2 Signal conditioning, monitoring and recording 69

4.2.1 Conditioning and monitoring 69

4.2.2 Recording 73

4.3 Processing 75

Page No

4.3.1 Objectives and system choice 75

4.3.2 The spectrum analysis of field data .. 78

Chapter 5 Vibration caused by the tunnelling process 81

5.1 Introduction 81

5.2 Borehole measurements of machine induced vibration 82

5.2.1 The type of vibration and peak particle velocities 82

5.2.2 The spectral distribution of particle velocity 93

5.2.3 Other borehole measurements 99

5.3 Surface vibration measurements 101

5.3.1 Vibration measurements in No 54 Ellesmere Road 101

5.3.2 Pavement vibration measurements 103

5.3.3 Disturbance by noise 104

5.4 In-tunnel vibration 105

Chapter 6 Ground settlement 108

6.1 Soil density assessment 108

6.2 Laboratory tests of vibration induced settlements 111

6.3 Ground settlement at Sections A and B 115

6.3.1 Introduction 115

6.3.2 Surface settlement 116

6.3.3 Sub-surface settlements 118

6.3.4 Structural damage due to settlement .. 122

6.4 Disturbances due to ground treatment 126

Chapter 7 Conclusions and recommendations 132

7.1 Introduction 132

7.2 Vibration induced ground settlement 132

Page No

7.3 The direct effect of vibrations 135

7.3.1 Damage to structures 135

7.3.2 Nuisance to residents 135

List of references 137

LIST OF FIGURES

FIGURE	TITLE	Page No.
2.1	The bentonite tunnelling system	14
2.2	Area location map with adjacent geological boundaries	19
2.3	Warrington tunnel, stratigraphy of rocks in Ellesmere Road boreholes	20
2.4	Site map	23
2.5	Site plan: Section A	24
2.6	Site plan: Section B	25
2.7	Grading curves of ground at New Cross and Warrington with 'envelope of suitable ground'.....	27
2.8	Grading curves at Section A (depth at A2 6.0m, and at A6 6.5m)	28
2.9	Grading curves at borehole B6 (depth 4.5m and 6.0m)	29
2.10	Proposed route of ship canal (1883)	36
3.1	Theoretical wave velocity derived from Gassman (after Winter 1972)	43
3.2	Velocity versus depth (after Fountain and Owen 1967)	43
3.3	Relation between initial tangent modulus and all-round pressure for sand	46
3.4	The relations between SPT values, relative density and relative compaction	54
3.5	Vibration thresholds; damage to buildings and human sensitivity	58
4.1	Equipment schematic	72
5.1	Typical spectra with tabulated values	83
5.2	Typical data sheet	84
5.3	Typical UV chart record derived from cassette tape	85
5.4	Typical UV chart record (Borehole A7)	86
5.5	UV chart record showing typical vibrations induced by the excavation process	88

FIGURE	TITLE	Page No.
5.6	Peak particle velocity (N-S) v tunnel face distance	90
5.7	Peak particle velocity (E-W) v tunnel face distance	91
5.8	Peak particle velocity (Vert) v tunnel face distance	92
5.9	Average (N-S) amplitude spectra for various tunnel face-borehole A7 distances	94
5.10	Average (E-W) amplitude spectra for various tunnel face-borehole B7 distance	95
5.11	Relative amplitude (N-S) in 5 bandwidths v tunnel face-borehole A7 distance	98
5.12	Lining segment dropping into invert during construction of ring 1075 (Borehole A7)	100
6.1	*In situ* density test results and BS (Heavy) compaction curve	110
6.2	Surface settlement at Section A	120
6.3	Surface settlement at Section B	121
6.4	Sub-surface settlement	123
B.1	Vector diagram for harmonic motion	154
B.2	Force-damped motion magnification factor for various levels of damping	154

LIST OF TABLES

TABLE	TITLE	Page No
2.1	Standard Penetration Tests in Borehole A6	26
3.1	Resonant frequency of vibrator on various types of soil (after Terzaghi and Peck 1967)	56
5.1	Peak particle velocities at borehole A7	89
5.2	Peak particle velocities at borehole B7	89
5.3	Values of relative amplitude in 100 Hz bandwidths derived from average spectra at borehole A7	97
5.4	Peak particle velocities in cellar of No. 54 Ellesmere Road	103
5.5	In-tunnel vibrations	107
6.1	Results of *in situ* density measurements	109
6.2	Laboratory vibration induced settlements	113
6.3	Surface settlements above tunnel axis	119
6.4	Surface slopes of settlement profiles	119
6.5	Settlements due to drilling grout holes	131

LIST OF PLATES

PLATE	TITLE	Page No.
Frontispiece	The portal	
2.1	View of tunnel showing placement of dry weather flow channel	9
2.2	The bentonite tunnelling machine	16
2.3	The bentonite surface separation plant	17
2.4	Glacial deposits removed from the tunnel face	32
2.5	Ellesmere Road during the construction of the Manchester Ship Canal in 1890	35
4.1	Borehole terminal box	66
4.2	Pavement mounted geophone array	68
4.3	General view inside mobile laboratory	70
4.4	Monitoring and recording equipment	71
4.5	Processing equipment	80
5.1	General view at Section A	102
6.1	Laboratory shake table rig	112
6.2	Structural damage at Section B	125
6.3	The drill rig	127
6.4	Nos 29-32 Ellesmere Road during ground treatment .	129
6.5	Nos 29-32 Ellesmere Road after ground treatment ..	130

LIST OF APPENDICES

APPENDIX	TITLE	Page No
A	Bentonite	146
B	Harmonic particle motion	148
C	Travelling wave motion	158
D	Physical properties of a granular soil	164
E	Processed data from borehole A7	166
F	Processed data from borehole B7	168
G	Supplementary processed data	170
H	Simplified analysis of simple harmonic motion	172

CHAPTER 1

GROUND VIBRATION IN TUNNELLING

1.1 The significance of ground vibration in civil engineering

The viability of civil engineering construction techniques will often depend upon their effects on existing structures, and recently increasing importance has been given to the preservation of 'environmental amenity' both during and subsequent to completion of the works. A major contributor to structural and environmental damage may be vibrational energy transmitted either through the ground or, in the form of sound, through the air. Steffens (1974), Whiffin and Leonard (1971) and Roberts (1969) have produced useful documents reviewing vibration and its effects. Each work contains an extensive range of references.

Engineers must consider two basic sources of vibration. The first, and potentially most severe in character, is natural ground movement resulting from seismic activity. This problem is present in various degrees of severity throughout the world. Certain areas around the great faults in the earth's crust, and associated with plate margins, are particularly subject to devastating earthquakes, whilst here in the British Isles very little consideration need generally be given to seismic activity. The second group comprises man-made vibrations which, when referred to civil engineering, may usefully be sub-divided into 'operational' and 'constructional' sections.

Ground movement and noise from road, rail and air traffic (Steffens 1974) have caused widespread concern to large groups of the community

and illustrate 'operational' problem areas which concern civil engineers.

Vibration and noise from 'constructional' sources will generally be of a transient nature as few constructions *actually* go on indefinitely. The disturbance caused, however, may result in permanent damage to property, and substantial nuisance to the surrounding population (Koch 1953; Bender 1972). Both these factors may prevent the works from continuing efficiently, so resulting in additional costs or even curtailment of activity. Pakes (1976) reports restrictions imposed on the construction of a tunnel due to disturbance of the local population.

Explosive blasting (Snodgrass and Siskind 1974; Duvall and Fogelson 1962; Taylor 1975) and piling operations (Wiss 1967; Sior 1961; Luna 1967) have in the past been the cause of greatest concern, but in recent years the scale of construction has become larger and the plant utilised has grown even more rapidly as economic pressures force greater emphasis on mechanised rather than labour intensive techniques. These developments have resulted in the use of plant which is larger, heavier, noisier and which dissipates large amounts of energy into the ground. Examples of damage and nuisance have been attributed to even relatively small amplitude vibrations and consequently almost any source may be regarded with suspicion. The work of Jackson (1967) is widely quoted in the literature and points out the difficulties in assessing the true effects of vibrations and the response of humans to them. Claims of damage derive from many sources and whilst it may be straightforward to prove some claims, others are sometimes difficult to deal with and an effective numerate capability to relate 'cause and effect' would be highly desirable.

1.2 Soft ground tunnelling

1.2.1 The need and technique

As the urban areas of this country expand, their needs in terms of transport, water supply, sewerage and the provision of other utilities, demand the construction of tunnels (BRE/TRRL 1974). These tunnels must be driven through a variety of geological strata but as the majority of the conurbations within the British Isles are underlain with weak sedimentary formations some emphasis has been placed on developing soft ground tunnelling techniques. A comprehensive background to these techniques may be obtained from the works of Peck (1969), Bartlett and King (1975), Donovan (1968) and Szechy (1973). Any construction technique employed to tunnel beneath existing structures should cause the minimum of disturbance to the inhabitants above. A system that caused structural damage or other substantial disturbances would not be acceptable.

The extent of mechanisation in tunnelling has increased in recent years and in suitable ground conditions it is now usual for tunnel drives of over 1 km to be driven by mechanical digger shields or tunnelling machines. Driving tunnels through non-cohesive materials, such as sand and gravel, was originally carried out by miners skilled in techniques which involved the close timbering of the tunnel face within a shield. Progress by this method was often slow and a run-in of ground could cause considerable damage to surface buildings. If the tunnel level was below the water table it was necessary to use compressed air, which added considerably to the hazard and cost of underground workings.

Recently other approaches to the problem have been made, most of which involve some alteration to the properties of the ground. Treatment

of the ground by chemical and cementitious grouts, ground freezing and ground water lowering, have all been used with varying degrees of success. All these techniques tend to be time consuming and expensive, and whenever possible tunnel lines have been chosen to avoid non-cohesive ground. It is problems of this type that led to the construction of London's underground in the London Clay rather than the overlying Thames gravels. Cut and cover systems are rarely viable in densely populated areas as their construction will often result in unacceptable levels of disruption.

The requirement is for a tunnelling machine which may be used in non-cohesive ground above or below the water table without disturbing overlying property, preferably without the use of compressed air.

Various types of machine have been designed to meet this need, and the bentonite tunnelling machine described in Chapter 2 is currently employed on the first commercial works using such a technique in this country.

1.2.2 Surface disturbance

Any method of tunnel construction will dissipate energy into the surrounding ground in the form of vibration. This energy may cause disturbance at the surface either directly by shaking the overlying property, or indirectly by causing settlement which may undermine it. In certain types of construction, ground heave may also occur but vibration is not likely to be responsible. Tunnelling operations are often based on shift working, and if the tunnel has little cover then the noise created may disturb the local population, particularly at night.

Little, if any, work has been undertaken to investigate the effects of vibration from the tunnelling process, although information is available on vibrations produced when the tunnel is operational (Bean and Page 1976; Anon 1974). Many studies have reported the settlements (Peck 1969) caused by tunnel and mining excavations, but again little work is available which directly relates these settlements to vibration. Information on earthquake induced settlements and damage (Terzaghi and Peck 1967; Holmes 1965) is widely reported but unfortunately this is not easily related to tunnelling as the amplitude, frequency and duration of energy from such tremors is not similar to that produced by tunnelling machines.

1.2.3 The opportunity for research

The construction of a trunk outfall sewer at Warrington provided an excellent opportunity to study the effects of vibration on an environment likely to be adversely affected. The construction contract was awarded to Edmund Nuttall Ltd by the Warrington New Town Development Corporation, with certain financial support to be provided by the National Research and Development Corporation (for full details see Chapter 2). Agreement was obtained from the parties concerned for Tunnels Division of the Transport and Road Research Laboratory to undertake a programme of geotechnical research during the construction of the tunnel. In view of their expertise in the field of ground vibration, the Engineering Geology Laboratories of Durham University were contracted to set up and carry out the vibration measurement programme. The co-operation of both contractor and customer proved most important in the conduct of the research, particularly where access to the tunnel and engineer's log sheets were required.

The tunnel is driven beneath an urban area in Drift sand deposits with a cover of less than six metres. Such a construction might be expected to cause considerable ground settlement, a proportion of which might be attributed to compaction caused by vibration. A principal aim of the bentonite tunnelling process chosen to complete the work is to reduce settlements caused by the flow of material into the tunnel, to a minimum. If this objective is achieved, then settlements caused by compaction may assume a dominant rôle. Also, as the cutting head of the bentonite tunnelling machine is well coupled to the ground mass by a thixotropic slurry, the transmission of energy into the ground might be increased, so accentuating any tendency to cause compaction of the ground.

An early impression was that the shallow overburden would offer a low attenuation facility to the vibration caused by the tunnelling, and so investigation of the direct effect to the surface environment was also desirable.

1.3 Thesis structure

This thesis presents work which falls into three principal areas of study:

a) The geology at Warrington and the choice of the bentonite tunnelling process.

b) The collection and processing of vibration records on, and in the ground surrounding the bentonite tunnelling machine. A chapter on the vibration instrumentation is included and wave propagation theory is developed with particular emphasis on body waves from underground sources.

c) The effects of the vibrations.

Where appropriate the research is discussed within the relevant section of the text and Chapter 7 provides the overall conclusions and recommendations in a concise form.

CHAPTER 2

THE BENTONITE TUNNELLING PROCESS AND SITE GEOLOGY AT WARRINGTON

2.1 The Acton Grange trunk outfall sewer (AGTOS)

2.1.1 The social and civil engineering requirement

The present population of Warrington is expected to almost double in the next fifteen years, rising to around 220,000 by 1991. The Warrington New Town Development Corporation, set up under the 1965 New Towns Act, was faced with the immediate problem of improving and expanding the sewerage system of the town. New development was not possible until the sewerage capacity had been increased. The AGTOS contract provides replacement of the existing overloaded trunk sewer, and will avoid the need to discharge crude sewage into the Manchester Ship Canal. The full scheme comprises several works, the principal of which is the construction of 1350 m of 2440 mm internal diameter main tunnel. The tunnel is lined with strengthened bolted concrete segments, and is shown in Plate 2.1. The dry weather flow channel is installed subsequent to the main drive and the erection of the primary lining.

It is necessary that the tunnel passes beneath a densely built-up urban area and the design brief laid down certain broad requirements:

i The optimisation of the relief given to the existing sewerage network.

PLATE 2.1 VIEW OF TUNNEL SHOWING PLACEMENT OF DRY WEATHER FLOW CHANNEL

ii The avoidance of working directly beneath houses.

iii The minimisation of disruption to road traffic.

iv The minimisation of environmental disturbance.

2.1.2 The contract

The 'cut and cover' technique for the construction of shallow tunnels was not considered as the disruption caused by such work would have been substantial and unacceptable. The sewer had, therefore, to be constructed as a bored tunnel. The site investigation indicated that the Drift deposits could not be excavated with a conventional tunnelling machine, and that a hand driven tunnel in compressed air would be the appropriate solution. Other methods, mentioned in Chapter 1, were considered but discarded on economic or technical grounds. The compressed air technique had certain elements of risk due to the shallow depth of the tunnel and its proximity to old property, services, and the Manchester Ship Canal. It is the author's view that these risks may have proved greater even than expected. Experience from another site in the same locality reveals difficulties that were encountered in maintaining even low air pressures with a cover of more than double that of the AGTOS tunnel. The possibility of huge air losses and blow-outs may have made the system impracticable and dangerous.

The new bentonite tunnelling process appeared to present a solution to the problems mentioned above, the contractor having developed the machine on an experimental contract at New Cross in South London (Boden and McCaul 1974). The experiment had shown that the process was technically viable and had given certain costing information. Before

the process could be used widely on a commercial scale the contractor needed to obtain a suitable contract founded on a sound commercial basis.

Contract documents were prepared so as to allow the bentonite tunnelling process to be proposed as a method. A conventional tender based on compressed air working was also submitted by the contractor. At a figure of £1,098,000 the bentonite process tender was some £79,000 in excess of the lowest bid received. However, it was decided to proceed with this tender on the following grounds:

i Ground movements and other detrimental effects were likely to be reduced.

ii Health risks due to the use of compressed air were greatly reduced.

iii The possibility of large air losses and their effect on the environment was removed.

iv The diameter of tunnel offered by the contractor was larger than that required and may have future advantages.

v The financial risk to the client was quantified.

vi The commercial application of the process could help to advance national technology.

With hindsight some of these advantages may not have been fulfilled whilst others manifested themselves as disadvantages in a different form.

It should be noted that owing to the circumstances (particularly the novelty of the tunnelling system) the contractor submitted his proposal with the bentonite tunnelling machine at cost.

A 'cost reimbursable contract' was formulated between the client and contractor, and was based on the following safeguards and incentives:

i A 'target estimate' based on the 'conventional tender' was produced to give the contractor a financial incentive to minimise the cost of the scheme.

ii If the final account is less than the 'target estimate' the difference between the actual 'cost of the works' and the 'target estimate' will be shared qually between contractor and client.

iii If the final account exceeds the 'target estimate' the contractor will receive the actual 'cost of the works' up to the 'maximum cost'.

iv A 'maximum cost' based on the bentonite tender was placed in the contract; the contractor having to absorb any excess.

The form of contract assisted the contractor with financing the work, particularly in its early stages, but retained the penalty of possible financial loss. The National Research and Development Corporation helped

the contractor financially in three ways:

i Contribution to Head Office overheads.

ii Sharing of development costs.

iii The underwriting of 50 per cent of any expenditure over and above the maximum cost of works payable by the client.

2.2 The slurry shield system

A full description of the bentonite tunnelling system has been published by Bartlett, Biggart and Triggs (1973). The following brings out its most important aspects which may be seen diagrammetically in Figure 2.1.

The system is intended as an alternative to the use of other systems described earlier for tunnelling in cohesionless soils. The machine can be used without bentonite where ground conditions permit, spoil being removed either directly from the face hopper by conveyor or as a pumped slurry. The machine was invented by British civil engineering consultants Mott, Hay and Anderson and developed under a research contract from NRDC in association with Robert Priestly Ltd. Edmund Nuttall Ltd are the contractors using the system.

The cutter head, fitted either with disc or pick cutters depending on ground conditions, rotates within a sealed plenum chamber which is filled with a thixotropic bentonite slurry (see Appendix A) under pressure. When the soil is of a suitable permeability this slurry penetrates into

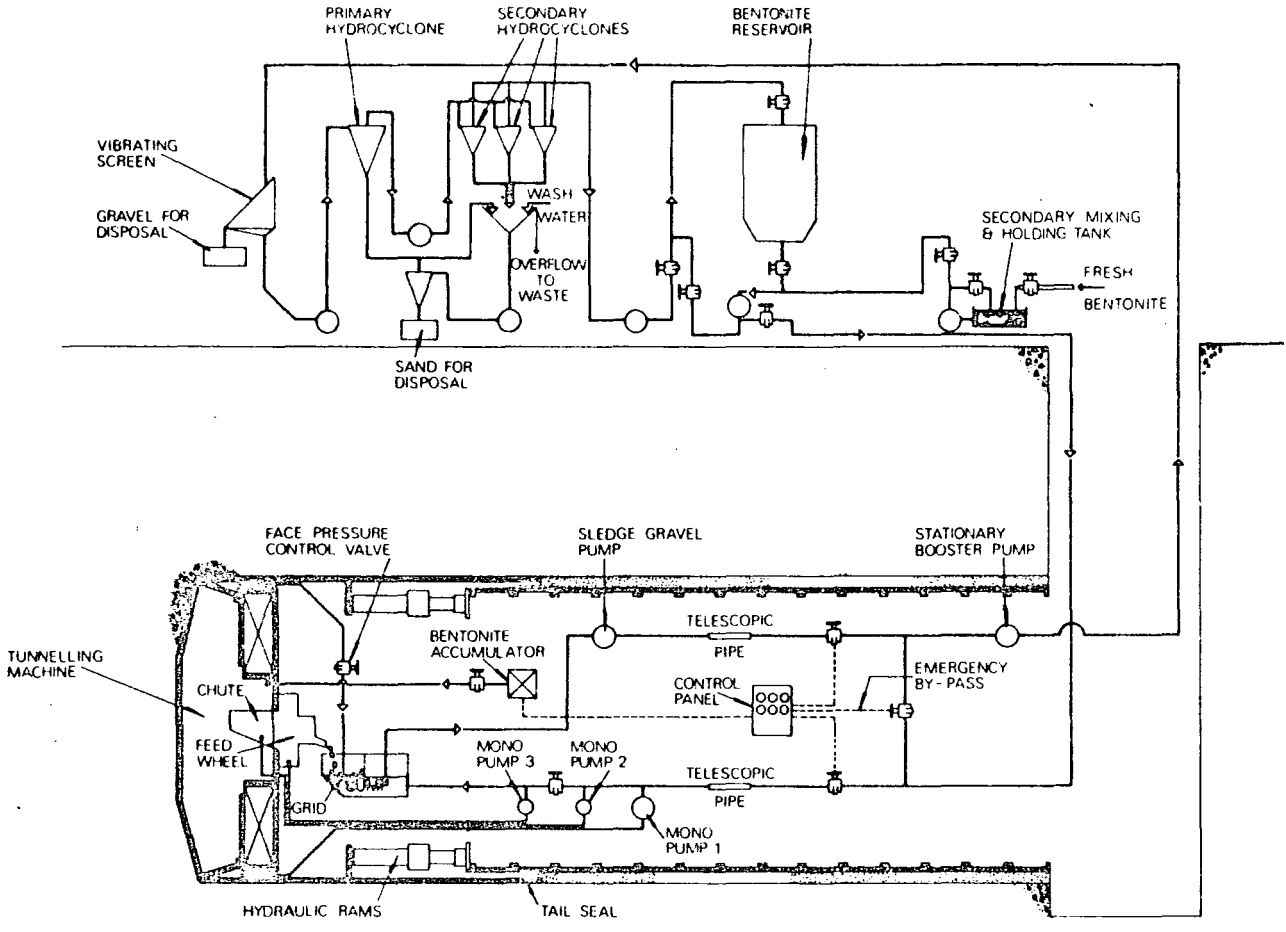

Fig. 2.1 THE BENTONITE TUNNELLING SYSTEM
(after Walsh and Biggart 1976)

the ground sealing and stabilising the face. The pressure surcharge provided also assists face support. Rotation of the cutting head removes spoil from the face and discharges it through the hopper into the extraction feedwheel which allows discharge to a sump at atmospheric pressure without loss of plenum chamber pressure. The material is passed through a 50 mm grid before entry to the sump to remove any large pieces of spoil. Plate 2.2 shows the front of the tunnelling machine with the lining erector in the foreground. The slurry is pumped from the face to a surface separation plant (shown in Plate 2.3), which consists of a vibrating screen followed by a series of hydrocyclones. The cleaned bentonite slurry is returned to a storage silo for re-use.

The British bentonite system was first used on an experimental basis at a site in New Cross, South London (Boden and McCaul 1974). The tunnel was sited such that it may be incorporated as a running tunnel for the proposed Fleet Line underground extension in due course. A description of the works involved may be found in Bartlett, Biggart and Triggs 1973. These trials showed the potential qualities of the system and formed the practical background which allowed the tender for the AGTOS tunnel to be formulated.

Other slurry shield systems have been used in Japan and Germany. Japanese engineers are credited with having introduced the idea of liquid-supported tunnel faces as early as 1961. Many systems of this type have been tried in Japan but most seem to use sea water under pressure to support the ground rather than bentonite.

The German company, Wayss and Freytag, have developed the Hydroschild bentonite system which also relies on the stabilising properties of

Plate 2.2 THE BENTONITE TUNNELLING MACHINE

Plate 2.3 THE BENTONITE SURFACE SEPARATION PLANT

bentonite. The pressure of the supporting liquid, however, is controlled by the insertion of an air cushion located behind a partial diaphragm wall in the plenum chamber. This technique is claimed to be more effective and simpler than the British system where the face pressure is maintained by pressure regulating valve located in the shield crown. A fuller description of the German and Japanese systems has been reported by Jacob (1976).

2.3 Site location and geology

2.3.1 The geology of the area

Warrington is in North East Cheshire (see Figure 2.2) and the tunnel is located approximately 2 km south of the town centre. The tunnel line runs for 1.4 km parallel to and about 20 m south of the Manchester Ship Canal.

The local geology is consistent with that of the plains of West and South Lancashire and Cheshire, and is floored with red rocks of Triassic age. The Triassic system comprises three series, the Upper, Middle and Lower. This system was originated in Germany and in this country the marine Middle Series, the Muschelkalk, is absent. The Upper beds comprise Keuper Marl and Keuper Sandstone and are present within 1 km to the south of the tunnel line. The Lower series is referred to as Bunter Sandstone generally, and the Upper Mottled Sandstone in particular is the bed through and above which the tunnel is driven. A stratigraphy is given in Figure 2.3. It should be noted that this fine-grained rock may vary in coherence from a moderately firm stone to a soft sand which may be readily excavated and used as a building sand. Unfortunately, 6-inch series geological maps do not exist for this area.

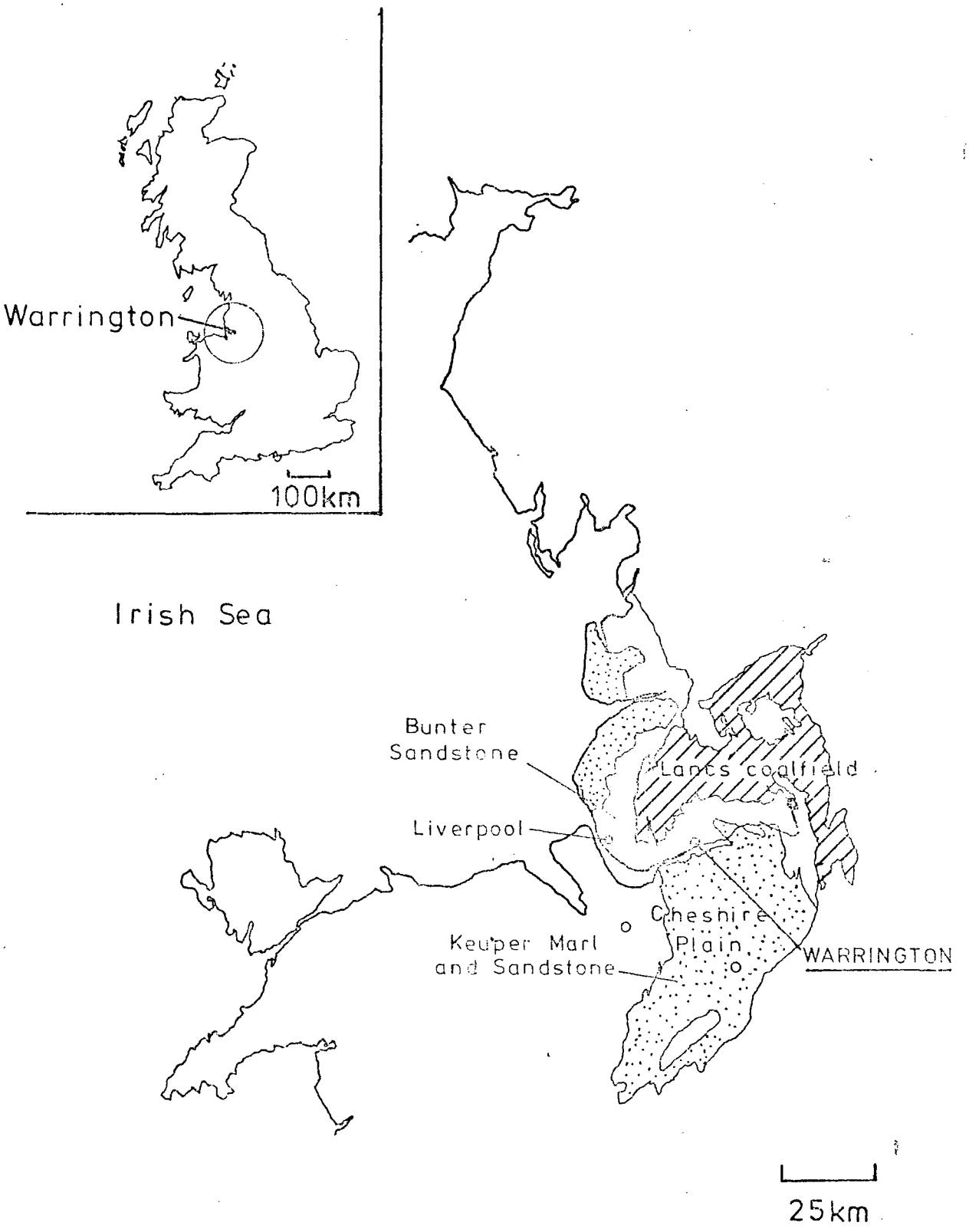

Fig. 2.2. AREA LOCATION MAP WITH ADJACENT GEOLOGICAL BOUNDARIES

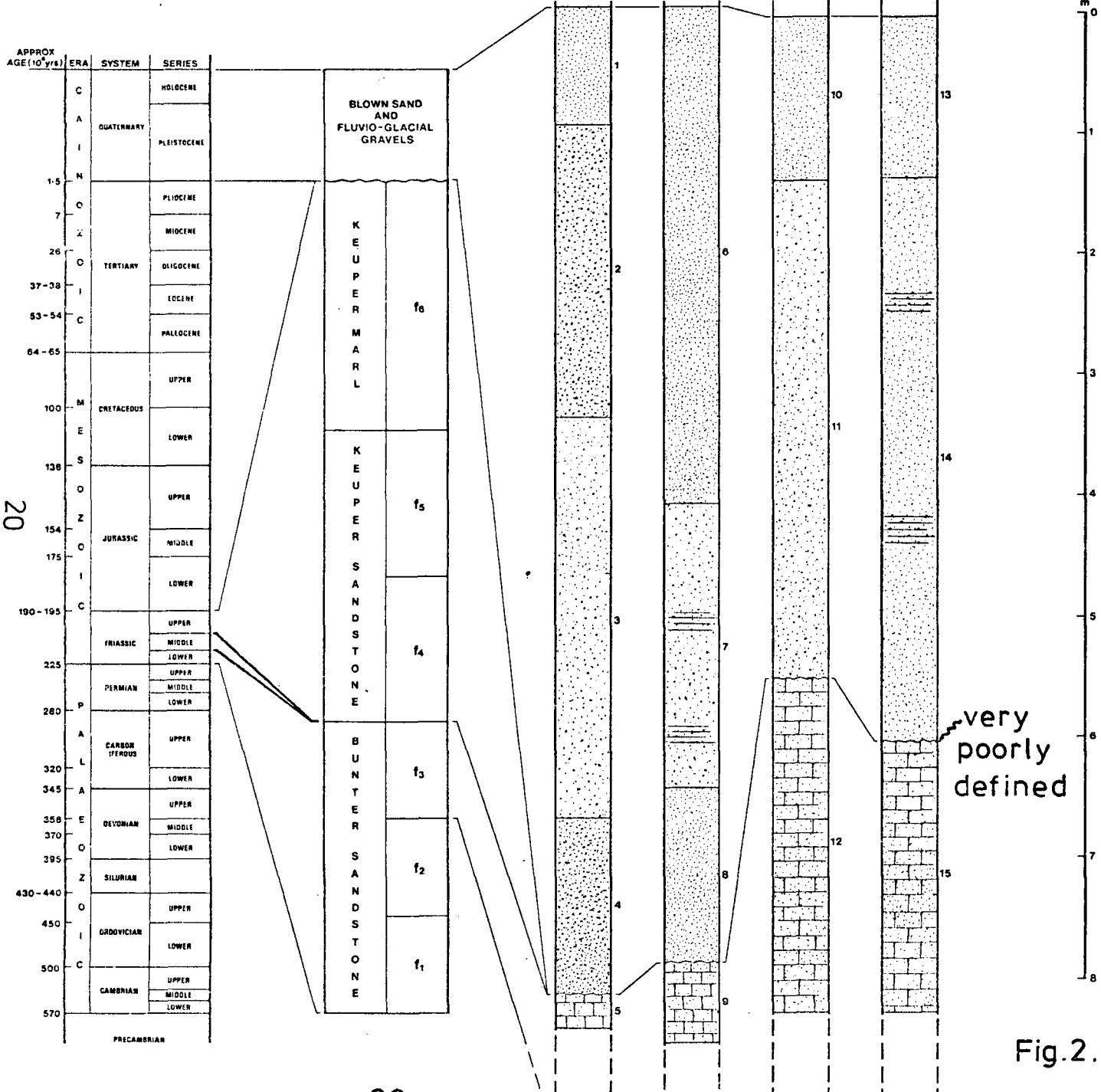

DESCRIPTION OF STRATA

The strata shown in these successions show Pleistocene and Recent blown sands and fluvio-glacial gravels resting uncomformably on Triassic Sandstone of Bunter age

DESCRIPTION OF LITHOLOGIES

1 Brown medium to fine SAND with occasional fine to medium gravel and clinker fragments
2 Brown medium to coarse SAND and fine to coarse GRAVEL
3 Brown medium to coarse SAND with much fine to medium gravel — BOREH
4 Red-brown slightly silty fine to coarse SAND with much fine to coarse gravel and red sandstone chippings
5 Highly weathered red-brown fine to medium grained SANDSTONE

6 Brown fine to coarse SAND with occasional fine gravel and ash fragments and a layer of medium to coarse gravel at the base
7 Brown medium to coarse SAND with much medium to coarse gravel and a layer of black ash material interspersed with reddish-brown clay layers — BOREH
8 Red-brown silty fine SAND
9 Red-brown completely weathered SANDSTONE

10 Fine to coarse SAND
11 Brown fine to coarse SAND and some fine to medium gravel with occasional ash fragments, increasing gravel content towards base becoming slightly silty with occasional red-brown clay balls — BOREH
12 Red-brown completely weathered slightly silty SANDSTONE

13 Fine SAND
14 Grey-brown slightly silty fine to coarse SAND with occasional gravel and red-brown clay balls increasing fine to medium gravel content towards the base — BOREH
15 Red-brown completely weathered SANDSTONE

Borehole logs by Nuttall Geotechnical Services Ltd

Fig.2.3 WARRINGTON TUNNEL, STRATIGRAPHY OF ROCKS IN ELLESMERE RD BOREHOLES

The Downall Green fault passes close to the tunnel portal and its influence is clearly visible in the exposed rock at this point. To the east of the fault the Upper Mottled Sandstone is shown dipping at about 5^0 to the SSE which is closely normal to the direction of the tunnel. This sandstone is overlain with Blown Sands (Shirdley Hill Sand) and fluvio-glacial gravels. The Shirdley Hill Sands extend some ten or twelve miles inland from Liverpool and form a horizontal sheet obscuring minor features of the country and only rarely appear as moundy dunes. Undifferentiated marine alluvium is also present in this area of the Mersey valley. A full description of the area geology may be found in the British Regional Geology series (Wray 1948).

From this existing geological data it was predicted that the deposits along the line of the sewer might vary between moderately firm sandstone and recent sands of aeolian origin with some Pleistocene deposits between them. The varied and difficult nature of this geology had great influence on the choice of the tunnelling system chosen for the contract.

2.3.2 The site

The initial site investigations depended almost entirely on information derived from boreholes along the proposed line of the tunnel. These boreholes confirmed broadly the lithologies shown by the Geological Survey data but for reasons explained later in this chapter did not reveal certain features which led to serious tunnelling problems. It was on the basis of this geological data that the contractor decided to use the bentonite tunnelling system. Because of the nature of the lithologies, the tunnelling operations were divided into three distinct categories:

1. The first 230 metres were to be driven in fairly coherent sandstone and the machine was to be fitted with disc cutters and operated as a conventional full face shield machine.

2. The next 150 metres comprised a mixed face of sandstone and non-cohesive Drift sands. These deposits were cementiciously and chemically consolidated, and again the machine was to be used in a conventional manner.

3. From just beyond shaft 6 (see Figure 2.4) the tunnel was in the Drift deposits entirely and the machine was to be converted to its slurry shield rôle to deal with the non-cohesive soils. It was this part of the tunnel drive that is the subject of the research described in this thesis.

It was decided to carry out the research programme of vibration and settlement studies at the two sections designated A and B shown on the site map Figure 2.4. Larger scale plans, Figures 2.5 and 2.6, give fuller details of the borehole locations and other measuring points. Transducers were installed in boreholes at each section and, during the sinking of these, stratigraphical logs were taken. A stratigraphy and descriptions of the lithologies found in these boreholes are given in Figure 2.3. The first 1 m of the ground was excavated as a pit to reveal any services, and each borehole log in Figure 2.3 was overlain by about ½ m of fill material in the form of tarmac, sand and sandstone boulders. The boreholes were sunk by a 1 ton Pilcon Wayfarer percussion rig operated by a two-man crew. The work was carried out by Nuttall

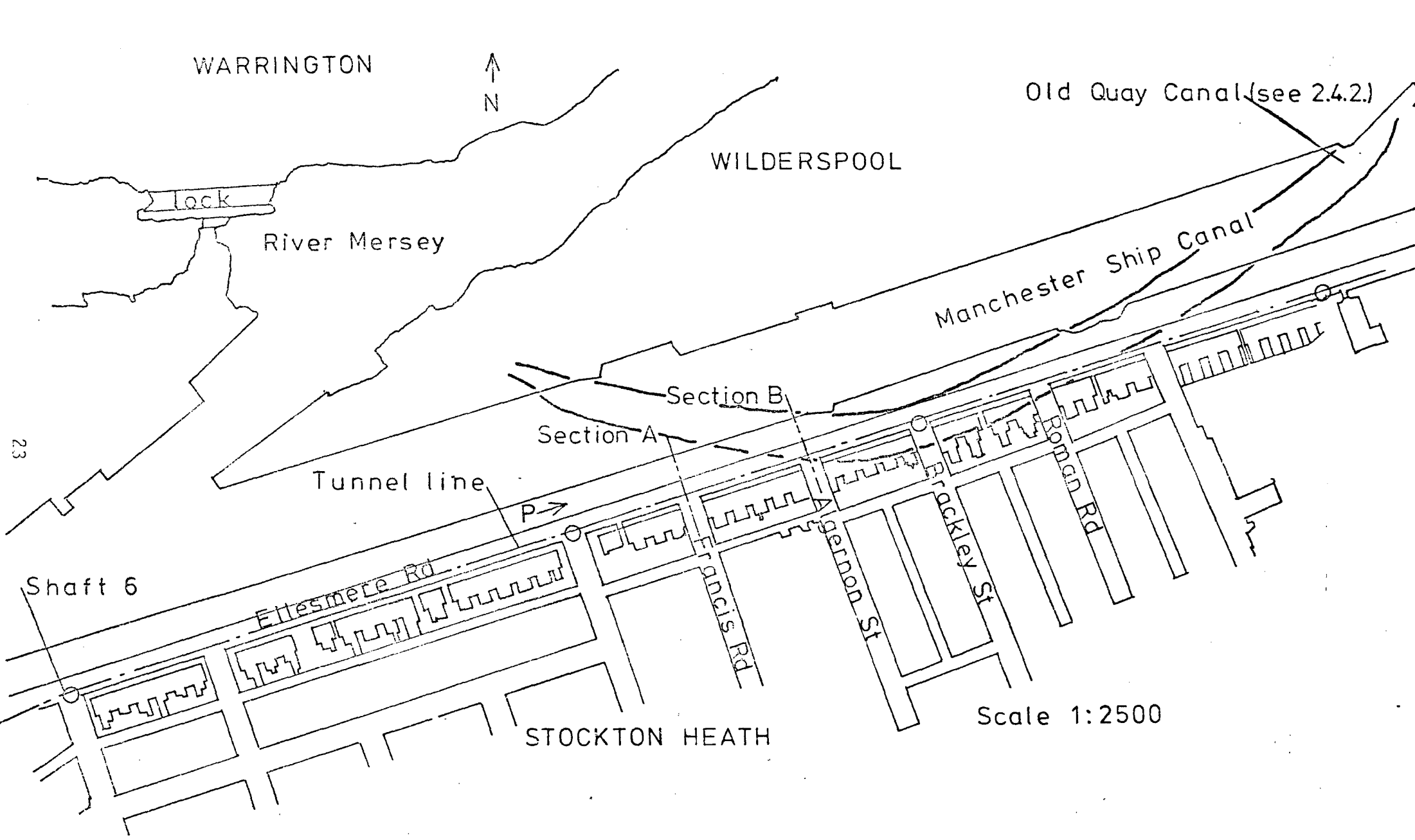

Fig. 2.4 SITE MAP

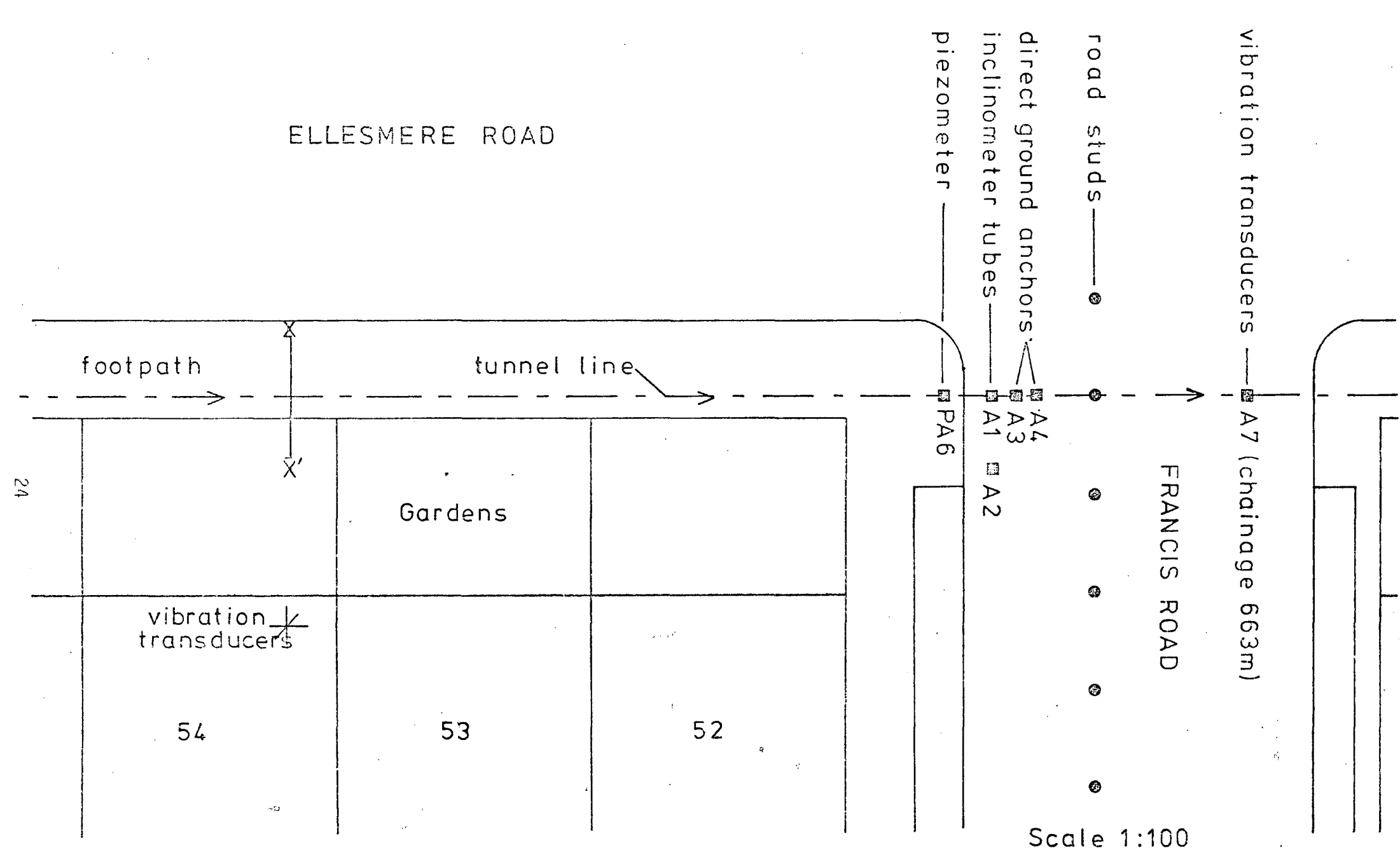

Fig. 2.5. SITE PLAN : SECTION A

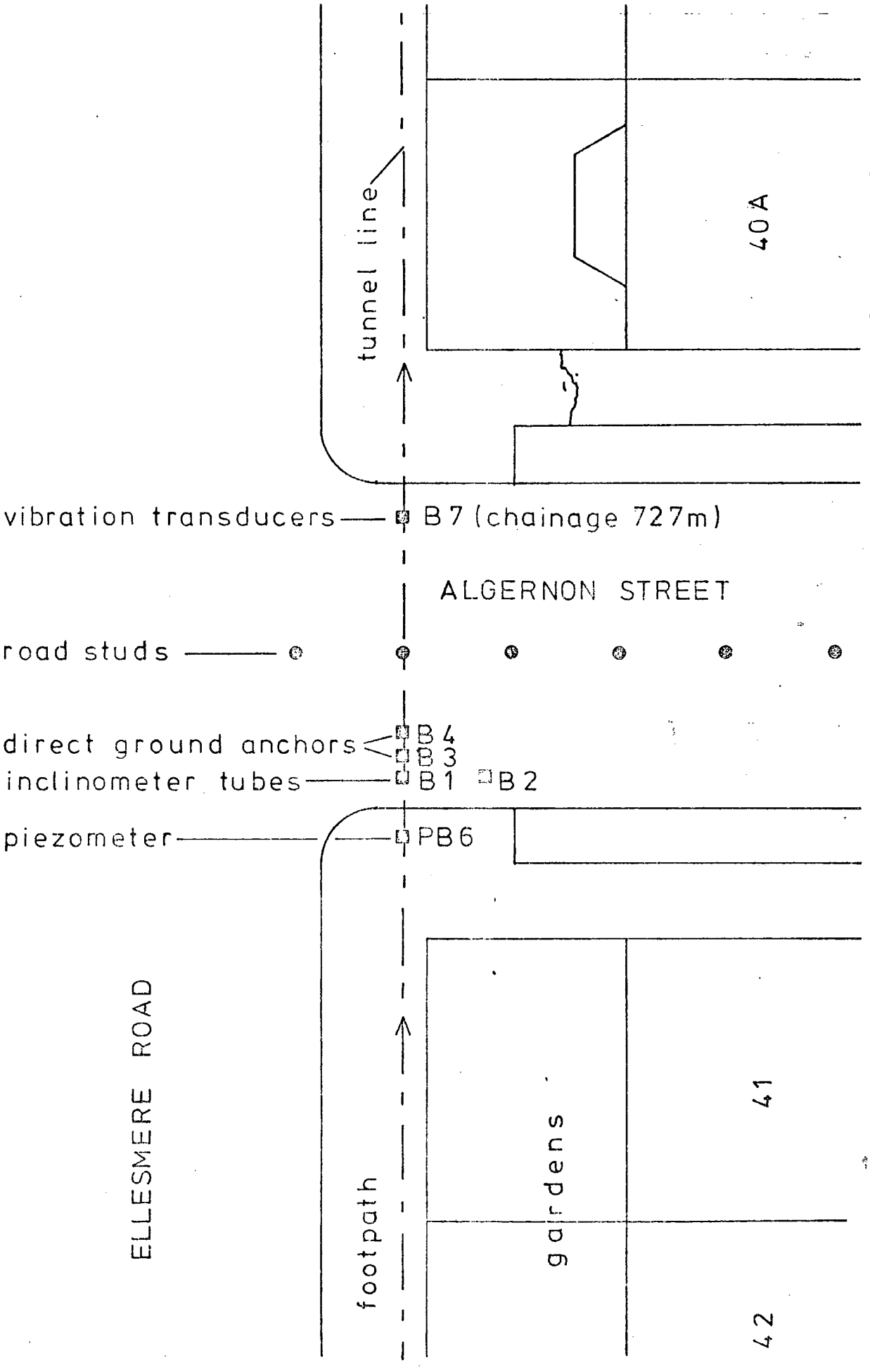

Fig.2.6 SITE PLAN : SECTION B

Geotechnical Services. It immediately became clear that the boundary between the sandstone and the overlying non-cohesive deposits was poorly delineated.

Figure 2.7 shows an 'envelope of suitable ground" for the bentonite system (*after* Walsh and Biggart 1976) together with a typical grading curve for the sands at Warrington and New Cross. Figures 2.8 and 2.9 show the extremities in grading found at sections A and B respectively. Another borehole log (not given here) some 60 metres east of Section B revealed an even coarser grading; this curve was designated C2 depth 7 m. The grading in A2 at 6 m and C2 at 7 m, together with comments on the log sheets referring to 'cobbles', might have given at least an idea that the coarseness of the ground might subsequently lead to problems with the machine. It should be noted that the presence of erratic boulders of igneous rock derived from the Southern Uplands of Scotland and the Lake District is common everywhere in the Lancashire and Cheshire plains (see Wray 1948 page 70).

Standard Penetration Tests (SPT)(BS 1377: 1975) were carried out during the boring of borehole A6 and the results shown in Table 2.1.

Table 2.1
Standard penetration tests in Borehole A6

Depth m from	to	SPT blows/ft	Relative Density (*after* Terzaghi and Peck 1967)
2.00	2.45	16	medium dense
3.00	3.45	15	medium dense
4.00	4.45	10	loose-medium dense
7.75	8.20	51	very dense
8.75	8.89	(a)	very dense

(a) 62 blows for 300 mm penetration, then no further penetration.

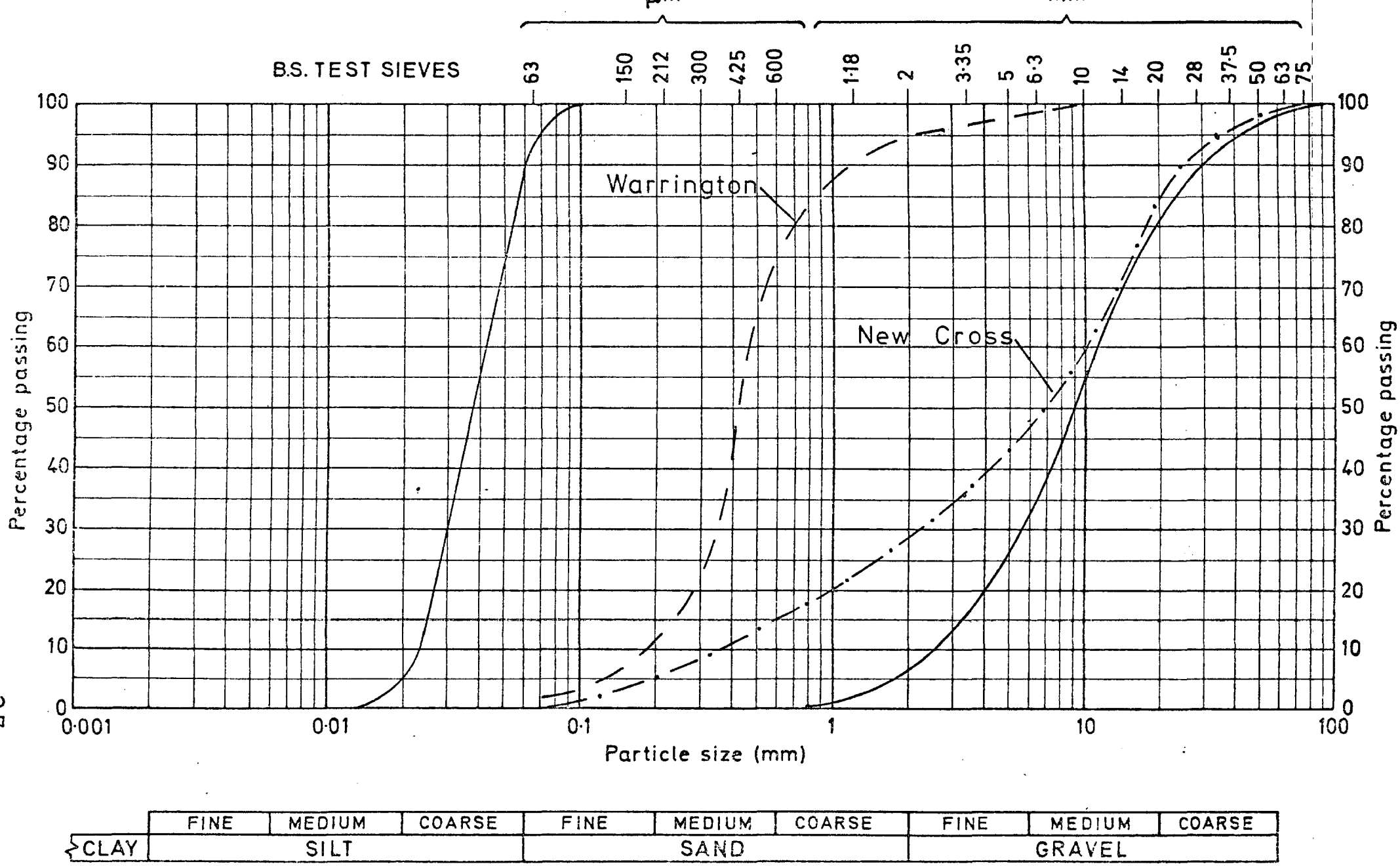

	FINE	MEDIUM	COARSE	FINE	MEDIUM	COARSE	FINE	MEDIUM	COARSE
CLAY	SILT			SAND			GRAVEL		

Fig. 2.7. GRADING CURVES OF GROUND AT NEW CROSS AND WARRINGTON WITH 'ENVELOPE OF SUITABLE GROUND'

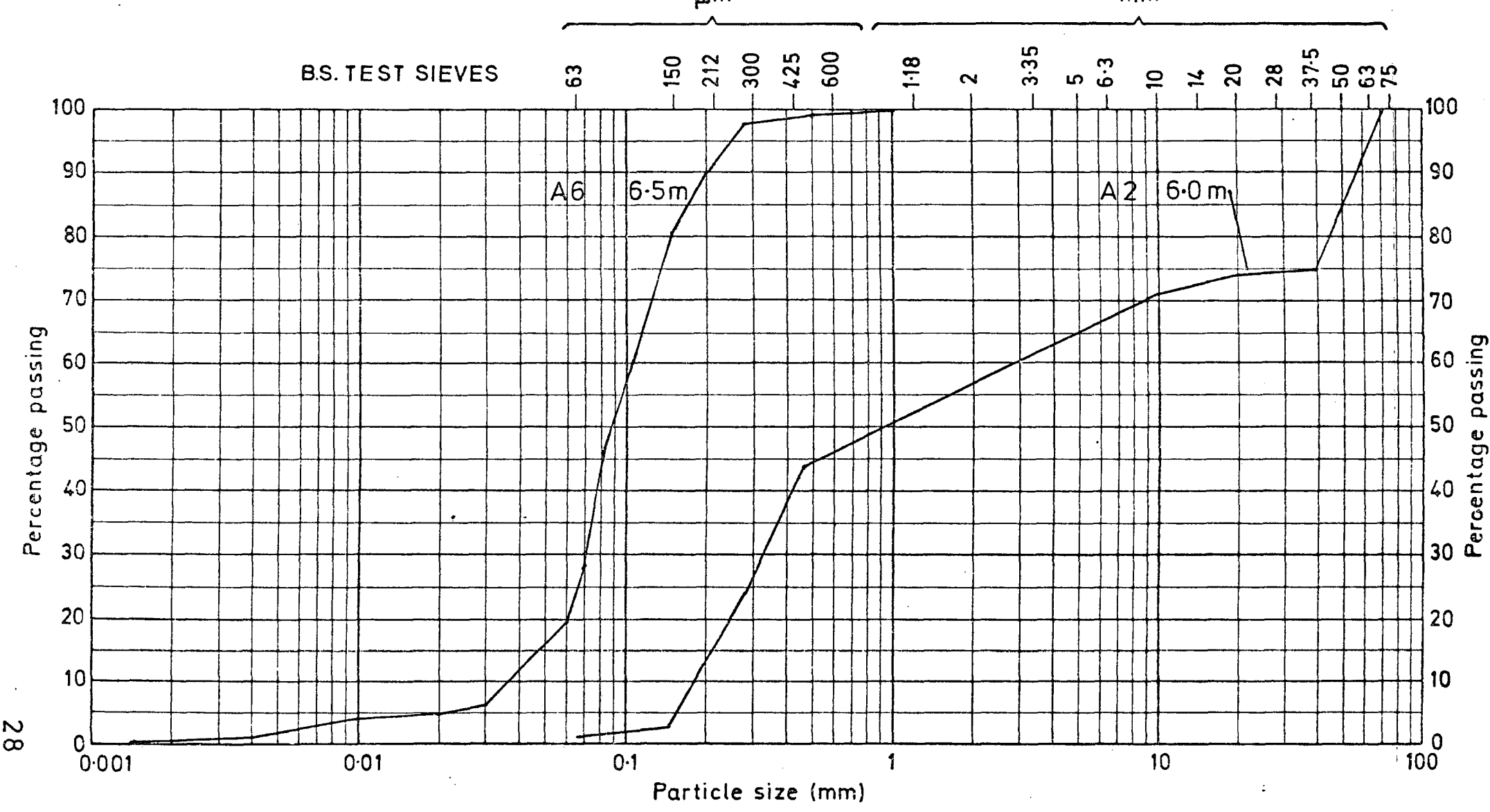

Fig.2.8 GRADING CURVES AT SECTION A (depth at A2,6·0 m and at A6, 6·5 m)

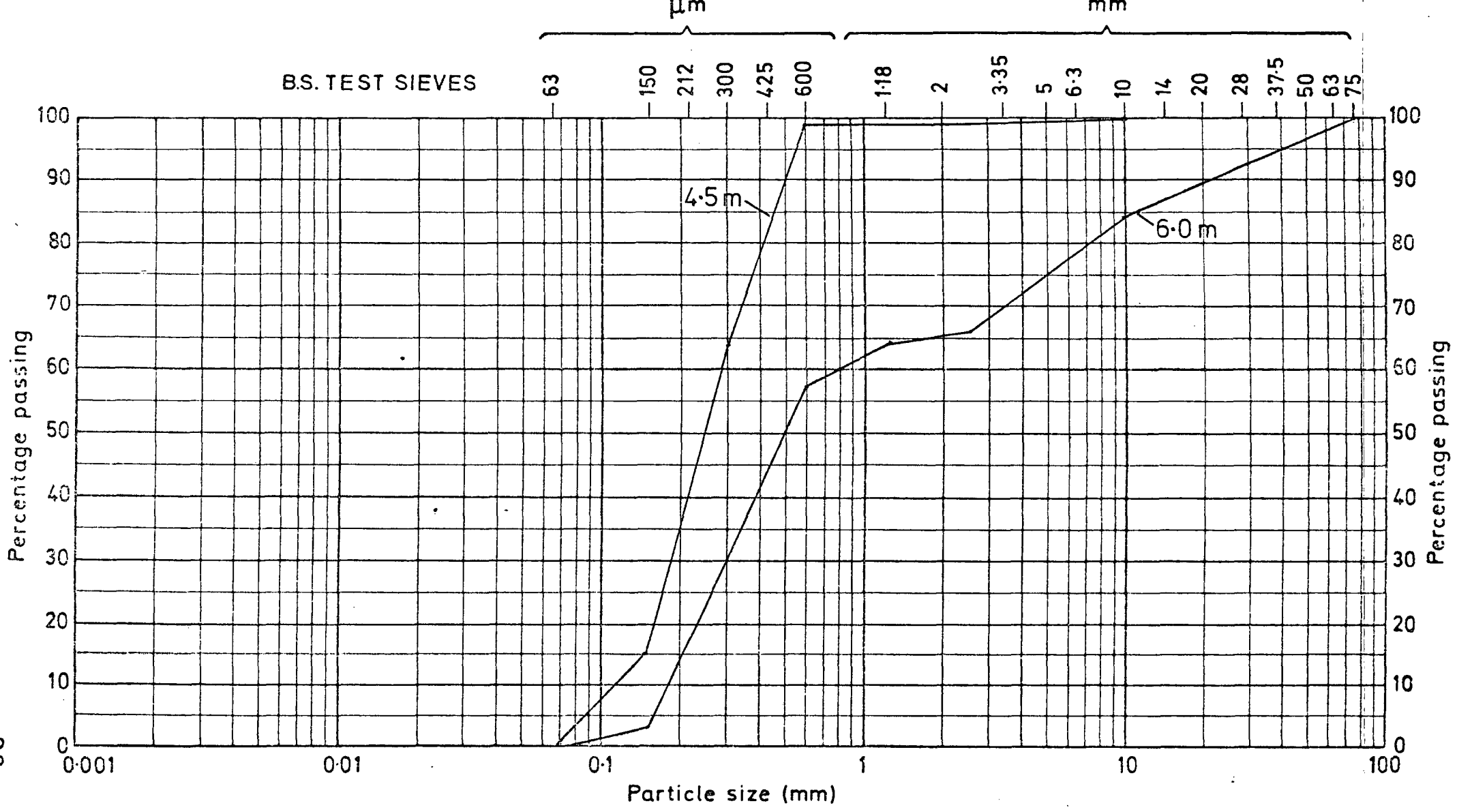

	FINE	MEDIUM	COARSE	FINE	MEDIUM	COARSE	FINE	MEDIUM	COARSE
CLAY	SILT			SAND			GRAVEL		

Fig. 2.9. GRADING CURVES AT BOREHOLE B6 (depth 4·5 m and 6·0 m)

Of the 12 boreholes at sections A and B, SPT values were taken only at A6, although the contractor had access to other SPT values from boreholes on the other side of Ellesmere Road. It is understood that these borehole results were similar to those at A6.

The level of the water table derived from borehole logs at sections A and B was approximately 5-6 m below the road surface. It seems unlikely however that the water table was standing significantly above the tunnel invert (about 7 m down) when the tunnel face passed Sections A and B owing to the drought of the previous summer (1976). It should be noted that the water surface in the adjacent ship canal is at about tunnel invert level and there was no indication of ground water seepage on the banks at this time.

2.4 Tunnelling problems associated with the site geology

2.4.1 Introduction

During the tunnel drive from portal to section B there were two major difficulties involving the site geology which were not predicted by either client or contractor. The first was the presence of boulders in the lower levels of the Drift deposits and the second the occurrence of very loose ground at chainage 744 m.

Two other minor problems were encountered early in the machine drive:

(a) The contractor claimed that the quality of the rock was harder and more abrasive than had been expected and had

caused excessive wear to the disc cutters. This problem was overcome by the use of special discs with hard rims.

(b) The combination of water and the small debris size of the excavated rock caused slurry problems with the conveyor. It was, therefore, decided to convert to hydraulic disposal early on in the rock drive.

2.4.2 The presence of boulders

The following is a direct quotation from a paper written jointly by representatives of the client and the contractor. 'Unexpectedly at ring 457 the tunnelling machine encountered boulders at the face. The boulders were up to 500 mm in size and caused great difficulty in excavating and steering of the machine'. It should be noted that at approximately ring 457 the Drift deposits began to occur in the tunnel crown, increasing steadily until a full face of Drift occurred at about chainage 350 m. Besides general damage to the cutting head the boulders caused blockages in the chute and the slurry disposal system which could not, of course, deal with such material. The tunnelling was enabled to continue to shaft 6 by the manual removal from the face of the large debris. Plate 2.4 shows some of the granite and dolerite boulders removed in this way. At shaft 6 the machine was fitted with a new head of the fully plated type and disc cutters with tungsten carbide tyres.

This remedy was immediately successful. It seems that the close plating and disc array binds the boulders into a matrix in the face until they are smashed into pieces small enough to pass through the 100 mm

Plate 2.4 GLACIAL DEPOSITS REMOVED FROM TUNNEL FACE

slots in the head. It is also possible that some boulders are thrust aside by the rotary action and the conical shape of the machine head. During the bentonite drive the large debris was removed by hand from the 50 mm grid between the feedwheel and slurry sump. This system proved successful although occasional blockages still occurred when elongated fragments penetrated the grid and fouled the pumps or pipes.

The method of breaking down the boulders at the face during the excavation process had a crucial effect on the vibrational energy put into the ground by the machine.

2.4.3 Loose ground

During the night shift on 6 October 1976, at ring 1180 (chainage 720-730) a 'loss' of some 12,000-15,000 gallons (55,000-68,000 litres) of bentonite from the face occurred in a short space of time. Tunnelling proceeded for one week, during which time it became apparent that structural damage was occurring to the houses close to the tunnel line; large settlements also took place above the tunnel. It was decided that owing to the presence of loose ground it would be necessary to stop the tunnel drive until further ground information was obtained. It was generally agreed that in these very loose conditions the settlements were likely to be due to compaction caused by vibration rather than ground loss at the face. It should be noted that up to this time little damage had occurred to houses close to the tunnel line and the measured settlements were small (Barratt 1976). A further point of interest is that, for several metres before the large loss of bentonite, very few boulder fragments or cobbles had been found on the slurry sump grid.

The presence of changed ground conditions stimulated a search of documents held in the town library. This investigation revealed that this area had once been used to obtain sand and that several sand pits were probably worked close to the tunnel line. The Ordnance Survey map also revealed the presence of the, now buried, Old Quay Canal. The Cheshire Mid-Division sheet, surveyed in 1877, shows clearly the canal and areas of sand excavation. Figure 2.4 shows the position of the filled Old Quay Canal superimposed on the recent map. The intersection point between the tunnel and the filled canal occurs almost exactly where the loss of bentonite took place, and the houses indicated were the first to be structurally damaged by settlement (No 40A at corner of Algernon Street). From this evidence it was accepted that the presence of the filled canal was in a large part responsible for the problems.

After further research, the present author is not convinced that the filled canal is definitely the cause of the loose ground. Figure 2.10 shows the proposed route of the Manchester Ship Canal (circa 1883) and Plate 2.5 shows the construction of this part of the Canal in 1890. This photograph was taken from the point marked P in Figure 2.4 looking in an easterly direction. It should be noted that it was proposed that the Old Quay Canal would fall in its entirety inside the boundaries of the new Ship Canal. It is possible to recognise and accurately locate several important features on Plate 2.3 by using the tower of St Thomas's Church (on extreme right) and the roof and chimney of the Old Greenalls Brewery (still lovely beer!) on the left skyline as sighting points. The plate is dated 1888-90 by the author as the first houses (seen under construction) in Ellesmere Road were built at this time. Other information (Leech 1895) reveals that it was not until 4 July 1887 that Bridgewater Undertakings, which included the Old Quay Canal, was purchased by the Manchester Ship Canal Company. It also appears that it was not

PLATE 2.5 ELLESMERE ROAD DURING THE CONSTRUCTION OF THE MANCHESTER SHIP CANAL IN 1890

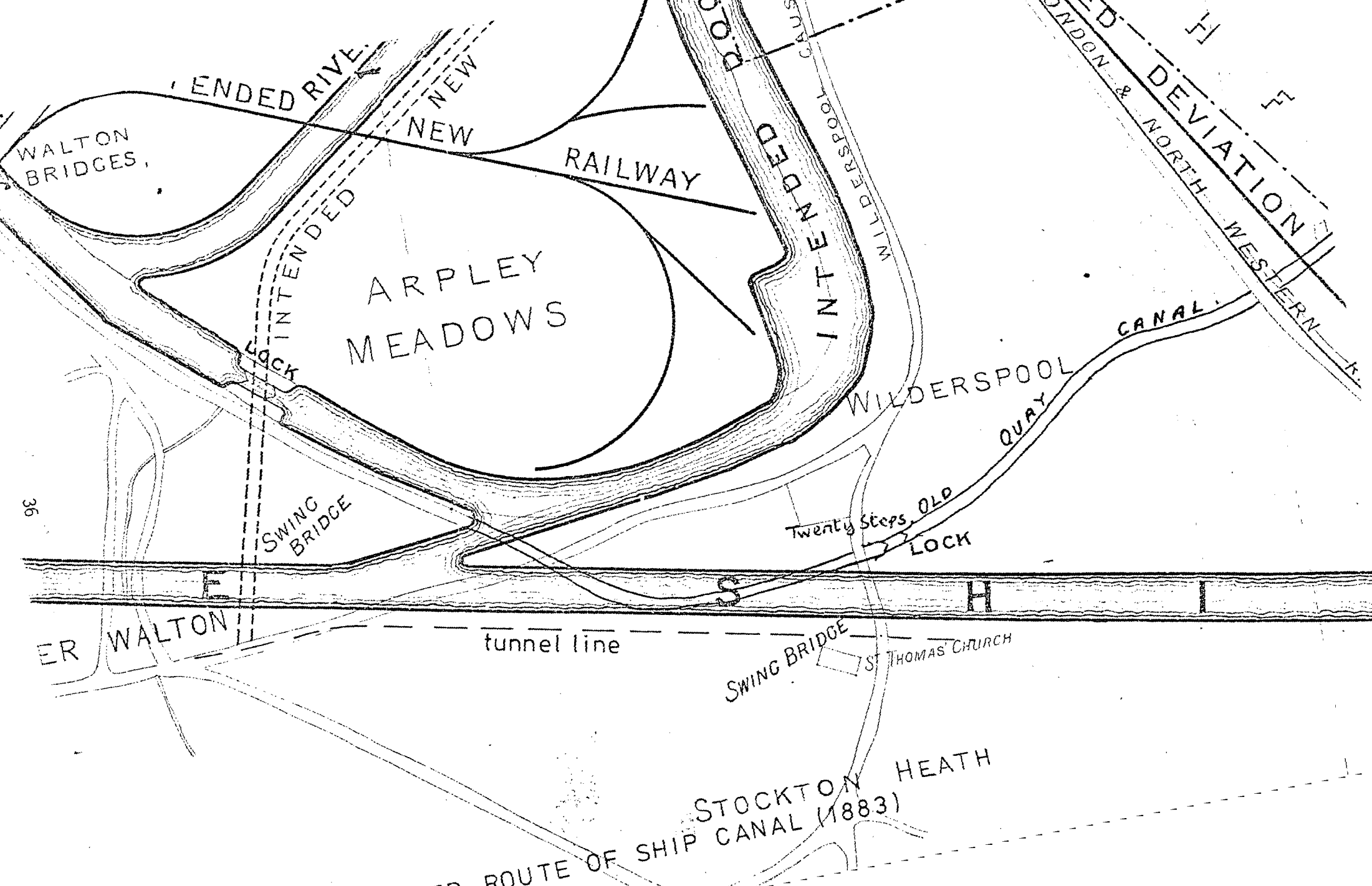
ENDED RIVE
NEW
NEW
RAILWAY
WALTON
BRIDGES.
INTENDED
ARPLEY
MEADOWS
LOCK
INTENDED
WILDERSPOOL CAUSEWAY
LONDON & NORTH WESTERN
DEVIATION
WILDERSPOOL
CANAL
QUAY
Twenty Steps, OLD
LOCK
SWING
BRIDGE
E
S
H
I
ER WALTON
tunnel line
SWING BRIDGE
ST THOMAS CHURCH
STOCKTON HEATH
ROUTE OF SHIP CANAL (1883)
36

until August 1888 that the Old Quay Canal was closed below Twenty Steps Lock.

Plate 2.3 shows no sign that the Old Quay Canal was located beneath the newly constructed Ellesmere Road. It does not seem likely that within a period of 1-2 years the canal was closed, drained, filled, a road built and vegetation established as shown by the photograph. It seems more likely that the railway line which appears to follow a curve from Twenty Steps Bridge (centre-right background) away to and probably beneath Tom Paines Bridge (extreme left) was located at the start of the main Ship Canal excavations in the floor of the then existing Old Quay Canal. It is possible that the position of the Canal was not mapped very accurately in the 1877 survey. Indeed, the shape of the canal shown in the Ordnance Survey map bears very close resemblance to a freehand sketchmap (circa 1820) showing the canal running across Arpley meadows.

As a result of encountering loose fill, further SPT values were obtained in boreholes along the line of the tunnel for some 150 m ahead of the tunnel face. These tests confirmed that the ground at and around the tunnel level was very loose indeed, SPT values of between 1 and 10 being very common. As a result of these 'real time' site investigation results it was decided to treat the loose ground with cementitious and chemical grout before any further tunnelling took place. In practical terms the cause of the loose ground was of little or no consequence, but the lessons learned from the encounter may influence future thinking on the use of tunnelling machines in non-cohesive materials. The incident also emphasises the need to anticipate disturbed ground conditions in urban and industrial areas.

CHAPTER 3

GROUND VIBRATION: ITS TRANSMISSION AND EFFECT

3.1 Introduction

The theory of wave propagation in solids was developed during the 19th century and since that time theoretical mechanisms for most types of wave behaviour have been postulated. The bulk of manageable theory has in common some combination of assumptions regarding fundamental material properties. These are that the material is:

1. homogeneous
2. isotropic
3. linearly elastic
4. spatially infinite or corresponding to a true half-space or having some clearly defined boundary conditions.

When related to some types of materials (for example, most metals) the assumptions are often almost wholly valid and lead to accurate theoretical analysis of static and dynamic material behaviour. Unfortunately, rocks and soils are rarely either homogeneous or isotropic, and the limit of their linear elasticity will often be difficult to specify reliably in dynamic terms. Attempts to analyse the dynamic behaviour of geological materials are often frustrated because simplifying assumptions are not allowable and the resulting theory becomes unmanageable and/or unusable in a civil engineering context. Such difficulties, however, rarely deter the diligent geophysicist. However, wave theory may have a rôle to play in the context of the problems presented in this thesis in two well defined areas:

(a) The interpretation of field measurements.

(b) To supplement and extend the value of field measurements in order to develop a quantitative model which may be used for predictive purposes beyond the immediate vicinity of the measurements.

This thesis is concerned with soil particle and wave dynamics in varied materials in their natural state with superposition of man-made inhomogeneities and boundary conditions.

If used in isolation, in a predictive rôle to determine the effect of vibration on the Warrington environment, theoretical approaches alone would have proved to be inadequate. However, when used in a qualified manner the theory developed below provides for fuller understanding and rationalisation of the field measurements than would otherwise have been possible.

Valiant but often fruitless attempts have been made to quantify the effects of vibration on structures and the human senses. Human beings and structures both exhibit extremely varied thresholds of distress, rendering any attempt to quantify the physical levels at which problems begin a difficult task. Nevertheless, it is recognised that some general guidance must be given and this type of research may provide important case-history information which will allow reasonable limits to be set in future. Section 3.4 reviews some previous work in this area where relevant to the problems of the Warrington environment.

3.2 The transmission of wave energy

The theory covering the propagation of waves is thoroughly covered by several excellent texts (Jaeger and Cook 1976; Timoshenko and Goodier 1970; Kolsky 1963; and Volterra and Zachmanoglou 1965). However, there is, to the author's knowledge, no single text which developes from first principles a united theory covering all the aspects of wave propagation required by this thesis. Appendices B and C have, therefore, been included as supplementary references to the standard texts and form an important part of this work. A book written specifically for engineers by Timoshenko, Young and Weaver (1974) may also be found useful in understanding the fundamentals of wave motion.

Making the assumptions given in 3.1 it may be shown that a material may support two types of body wave motion:

1. A wave of dilatation which will propagate with a velocity $C_p = (\lambda + 2G/\rho)^{\frac{1}{2}}$. (These waves are often described as compressional and have a particle motion in the direction of wave propagation.)

   where G is modulus of rigidity
   λ is Lamé's constant
   and ρ is bulk density

2. A wave of distortion which propagates with a velocity $C_s = (G/\rho)^{\frac{1}{2}}$. These waves are often described as shear waves and have a particle motion in a plane normal to the direction of wave propagation.

If a surface is introduced creating an elastic half space the material may support two further types of wave, namely Rayleigh and Love waves (Bullen 1963; Kolsky 1963). These waves are guided by the surface and are characterised by an exponential decrease in particle amplitude with increasing distance from the boundary. Miller and Purdsey (1954) studied theoretically the distribution of waves in a homogeneous, isotropic, elastic half-space. Their investigation dealt with the generation of small stress waves in a bed of soil by the use of a circular disc oscillating vertically on the surface. Except in the region close to the source (a distance of about 2 or 3 disc diameters) the body waves were found to be unimportant compared with the Rayleigh waves in regard to surface effects. They confirmed that the body waves decayed in proportion to the square of the distance from the source, while the Rayleigh waves decayed in proportion to the square root of the distance. Calculations of the partition of energy between the various elastic waves gave 67 per cent for the Rayleigh waves,26 per cent for shear waves and 7 per cent for compressional waves. Surface waves play an important role in the study of earthquakes, where, diverging parallel to the surface only, they acquire dominating importance with increasing distance from the source.

This thesis is concerned with a source (a tunnelling machine) wholly contained within a geologic material and the wave energy of interest is that close to the source,where the disturbance to the structure of the material will be greatest. The theory developed in the Appendices is largely common to all types of wave motion but in certain instances is specifically concerned with body waves which are most relevant to the site measurements.

Appendix B develops the equations for free, damped and force-damped harmonic vibrations, and Appendix C develops and extends this theory to travelling waves within a solid. Expressions are derived from first principles describing particle motion, material strain, attenuation and energy propagation due to travelling waves.

It is important to emphasise that wave velocities are dependent on the elastic properties of the material and upon its density. Therefore we may use measured changes in wave velocity to reveal changes in the condition or composition of a soil. It has been shown (Whitman 1970) that the principal factors affecting the velocity in a soil are the confining pressure (usually from the overburden) and the water content. White and Sengbush (1953) used theory developed by Gassmann (1951) to predict the wave velocity in sand with varying overburdens. Figure 3.1 gives the theoretical curves which have been closely confirmed by field measurements with overburdens of between 10 and 100 ft. Note the predicted rapid increase in velocity with depth especially within the first few meters and the steep increase in compressional wave velocity below the water table. Gassmann's theory (based on assemblies of spheres) predicts that the vertical velocity will be different from the horizontal as the vertical stress from an overburden is greater than the horizontal stress. Duffy and Mindlin (1957) provide the most comprehensive treatment of this problem because they include tangential contact pressures in addition to the normal contact pressures considered in earlier work.

On a small scale, however, Figure 3.2 (after Fountain and Owen) shows that field variation of velocity with depth is not necessarily at all uniform in sand and Gassmann's theory should be viewed with some caution, particularly when low overburden stresses are involved.

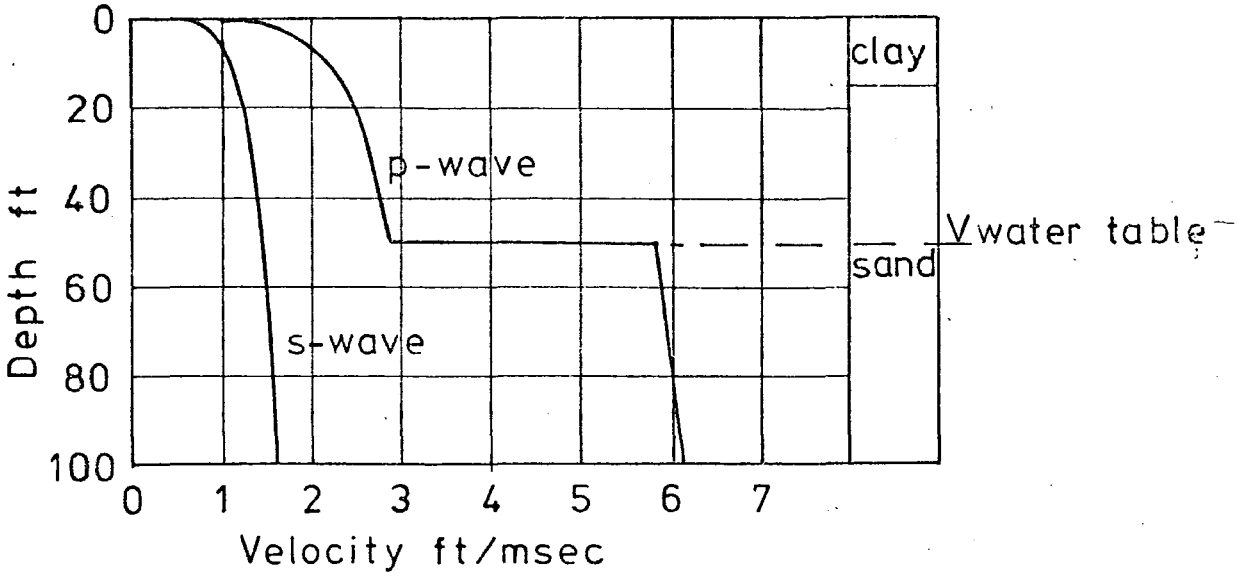

Fig.3.1 THEORETICAL WAVE VELOCITY DERIVED FROM GASSMAN (after Winter 1972)

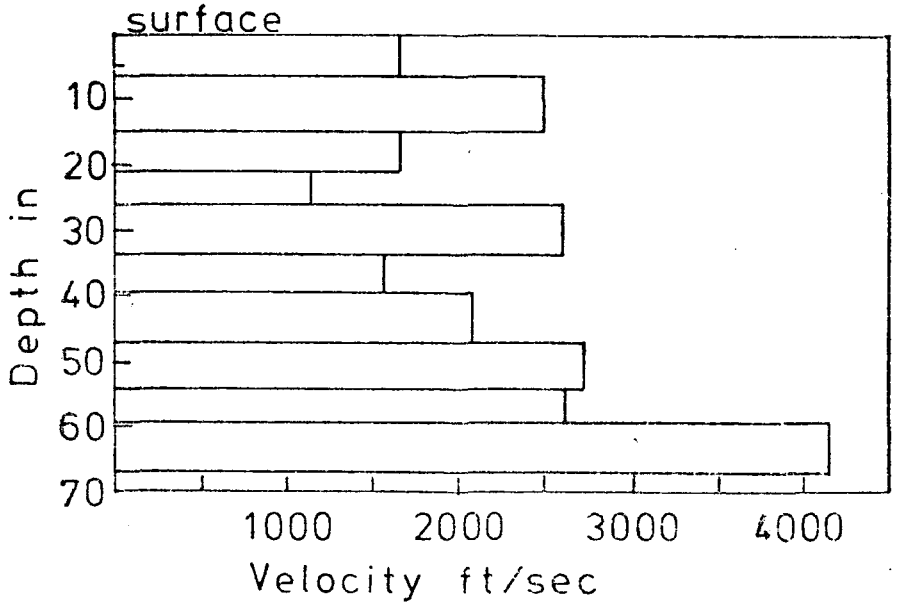

Fig.3.2 VELOCITY vs DEPTH
(after Fountain and Owen 1967)

Hardin and Richart (1963) have carried out laboratory tests, using the resonant column method, to evaluate compressional and shear wave velocities in sand and crushed quartz silt. (This work contains a useful review of previous experimental and theoretical studies). The variables considered were the confining pressure, void ratio, and grain characteristics of the materials and the results may be summarised as follows:

(a) The wave velocities for the sands varied with approximately the $\frac{1}{4}$ power of the confining pressure.

(b) For a given confining pressure the void ratio was the most significant variable.

(c) The wave velocity varied almost linearly with the void ratio.

(d) The effects of relative density, grain size, and gradation entered only through their effects on void ratio.

An excellent critical review of existing knowledge of the dynamic behaviour of soils and foundations has been published by Jones *et al* (1966).

Terzaghi and Peck (1967) reproduce Figure 3.3 (*after* Scheidig 1931) which describes the initial tangent modulus E_i for loose and dense sand against variation of 'consolidation pressure', p_c. It is clear from these relations that seismic velocity will increase far more sharply with increasing overburden in dense sands than loose material.

Biot (1956) considered the three-dimensional propagation of waves in porous saturated solids and concludes that two compressional waves with differing velocities may be present. Winter (1972) asserts that (for body waves) there is no velocity dispersion below 50k Hz but that the velocity of both shear and compressional waves decreases slightly with increasing amplitude.

The mechanism by which waves are attenuated in geological materials is one of the most poorly understood aspects of rock and soil dynamics. The causes for the reduction in amplitude of a wave, other than that due to geometrical spreading, are often collectively described as internal friction. Kolsky (1963) states that 'at present there is no satisfactory theory of internal friction in solids, and more experimental data are required'. Measurements available at the present time indicate that attenuation constants are largely dependent on frequency so that high frequencies are attenuated more rapidly than low frequencies. Attewell and Ramana (1966) conducted a review of published data on sedimentary rocks and concluded that the spatial attenuation coefficient α was approximately proportional to the frequency for P & S waves where $10^0 < f < 10^7$. Winter (1972) gives typical 'absorption coefficients' (in $dB/_{ft}$) of 0.00012f for shale and 1.2 + 0.002f in dry silty clay.

Internal friction ultimately results in heating of the material but it is not fully understood whether this is caused by scattering, frictional, viscous or other phenomena. A concise review on internal friction in rocks is given by Bradley and Fort (1966) and it concludes that frictional losses account for most of the energy lost by elastic waves travelling through a solid.

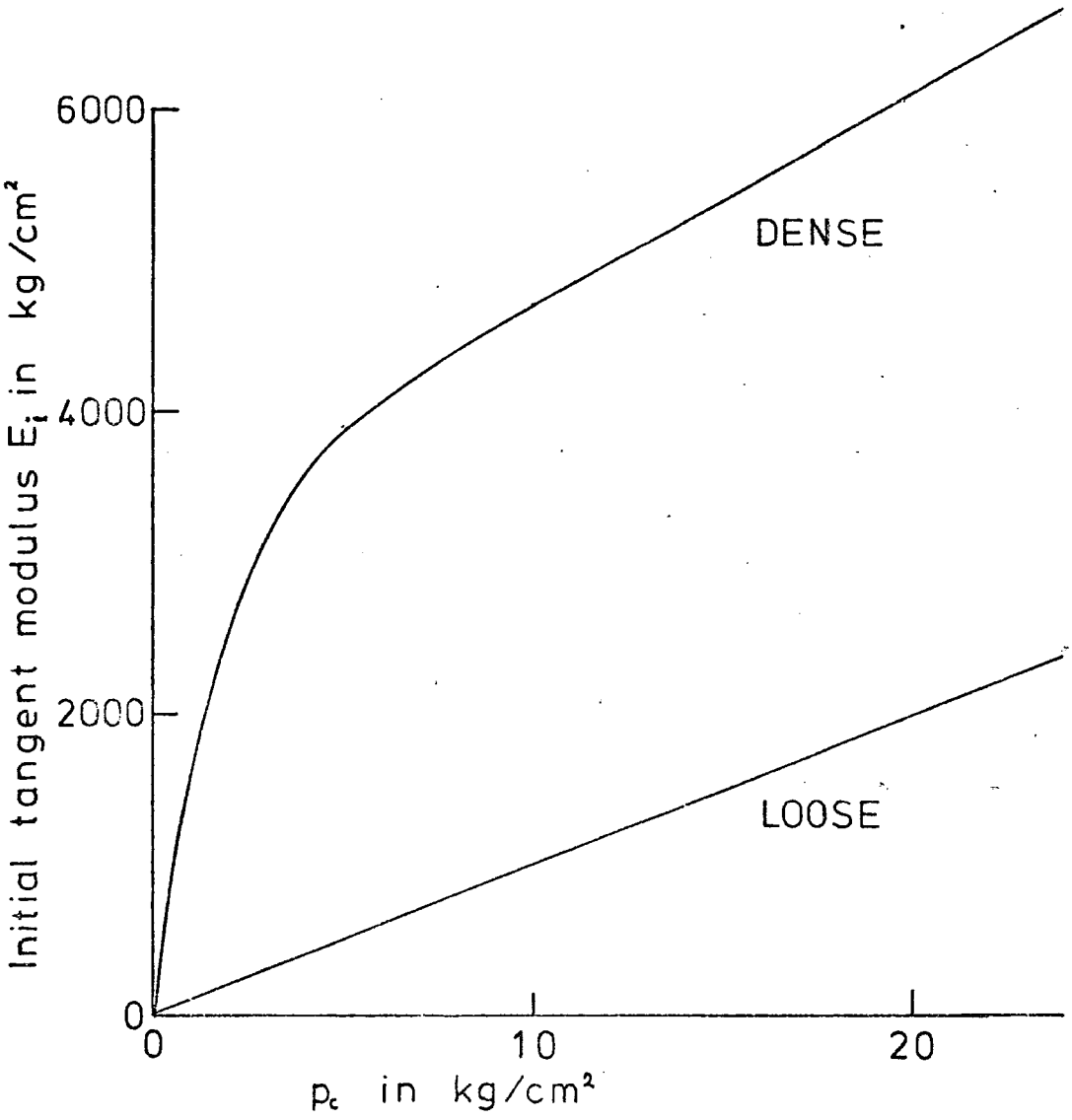

Fig. 3.3 RELATION BETWEEN INITIAL TANGENT MODULUS AND ALL-ROUND PRESSURE FOR SAND (after Scheidig 1931)

3.3 Settlement due to vibration in sands

3.3.1 Introduction

During the excavation of a tunnel in a cohesionless material, ground settlements will almost inevitably occur. This section is concerned with that part of the settlement that might be caused by energy input from the construction process, so re-ordering the grain structure to a more compact form with the consequent loss of bulk volume.

3.3.2 Saturated sands

At the Warrington site we are principally concerned with an unsaturated material and any loss of bulk volume caused by vibrations will be referred to as compaction. However, as the bentonite tunnelling process is also suited for use in saturated materials it is relevant to consider liquefaction effects. Liquefaction occurs when the pore water pressure increases to the point where it is equal to the total normal stress. At this threshold the shear strength falls to zero and the material behaves as a fluid. Liquefaction usually results from dynamic changes of stress or strain within a material that is poorly drained and relatively loose. During the liquefaction process the grains may be totally supported by the fluid and the combined effects of dynamic and gravitational forces will re-order the grains to a denser form. This may occur in almost any cohesionless material but obviously is most prevalent in loose sands and gravels.

Bodies of loose saturated sands are particularly subject to liquefaction during earthquakes with durations long enough for the occurrence of a large number of oscillations involving repeated reversals

of shearing strains of large amplitude. The process of vibroflotation (Terzaghi and Peck 1967; Basore and Boitano 1969) is based on liquefaction effects and is frequently used to increase the density of loose ground to reduce settlements subsequent to construction. In dense sands rapid deformations may have the reverse effect of liquefaction. When such a dense saturated sand is deformed the void ratio is increased and if there is no time for seepage into the sand the water can no longer fill the voids. As a result the pore water is put in tension (negative pore water pressure) thereby increasing the pressure between the grains and causing a temporary increase in strength (Seed and Lundgren 1954).

3.3.3 Compaction

The term 'compaction' is generally understood to mean the increase in the dry density of a soil by a dynamic load. It should not be confused with 'consolidation' which is the gradual decrease in void volume caused by the action of a continuous static load over a period of time. In cohesive saturated soils consolidation is accompanied by the gradual expulsion of water and air out of the soil voids with a consequent decrease in soil volume. A great deal has been written on compaction and its relation to other soil parameters such as dry density, porosity, void ratio, relative compaction and relative density (Attewell and Farmer 1976; Jumikis 1967; Terzaghi and Peck 1967).

Most laboratory and field investigations have been directed at either the settlements caused by large ground movements, usually earthquakes (Lee and Albaisa 1974; Silver and Seed 1971), or the deliberate compaction of ground for civil engineering purposes (RRL 1952, Basore and Boitano 1969; Forssblad 1965). Very little, if any, work has been done to investigate the compaction effects of relatively high frequency seismic

energy generated below the ground surface. Even the extensive laboratory studies are difficult to interpret in this context as the frequency and duration of the wave energy is not similar to that from the tunnelling machine. Papers by D'Appolonia (1970) and Brumund and Leonards (1972) both contain useful bibliographies related to settlements caused by dynamic loadings from blasting, earthquakes, surface compaction machinery and laboratory sources.

3.3.4 Measuring soil compaction

Although it is difficult to gain specific information from previous work there are several general points which are helpful when considering the potential compaction of a soil. It is the degree of looseness of a cohesionless soil which determines its ultimate settlement potential. This factor is often very difficult to measure in the field, and may be specified in several ways (see Appendix D for definitions of soil properties). RRL (1952) defines 'relative compaction' as the ratio of the field dry density to the maximum dry density obtained in the BS compaction test (test 12 or 13 of BS 1377: 1975) expressed as a percentage. This work goes on to say that a better scale on which to compare the efficiency of compaction plant may be obtained by a ratio including the 'loose density' of the soil.

$$\frac{\text{Field dry density - Loose dry density}}{\text{Maximum dry density - Loose dry density (from BS compaction test)}} \times 100 \text{ per cent}$$

Kolbuszewski (1965) suggests that the relative porosity N_R is the best way of expressing the state of sand in the field where

$$N_R = \frac{n_{max} - n_f}{n_{max} - n_{min}}$$

where

n_{max} = maximum porosity

n_{min} = minimum porosity

n_f = field porosity

However, the most usual method is to use relative density RD which is defined by the equation:

$$RD = \frac{e_{max} - e_f}{e_{max} - e_{min}}$$

where

e_{max} = maximum void ratio

e_{min} = minimum void ratio

e_f = field void ratio

Attewell and Farmer (1976) extend this to give

$$RD = \frac{\gamma_{dmax}}{\gamma_{df}} \left(\frac{\gamma_{df} - \gamma_{dmin}}{\gamma_{dmax} - \gamma_{dmin}} \right) = \frac{(n_{max} - n)(1 - n_{min})}{(n_{max} - n_{min})(1 - n)}$$

where

γ_{dmax} = maximum dry density

γ_{dmin} = minimum dry density

γ_{df} = field dry density

From the above equations it is clear that two sands of identical field void ratio, porosity or bulk dry density are not necessarily in

the same state of compaction. Variations in the particle size, shape, grading and specific gravity will all result in changes in the possible stacking geometry and/or bulk density.

The values obtained from the formulae above will also be to some extent dependent on the methods used to obtain the 'loose' and 'dense' states. These conditions are usually obtained by some form of fast dry pouring and wet rodding or vibrating respectively. Under such conditions typical void ratios range between 0.2 to 1.2, porosities vary from 20 per cent to 50 per cent, and dry densities vary from 1.2 to 2.2 Mg/m^3 for granular soils.

The factors affecting the accurate measurement of relative density were exhaustively dealt with at a conference (Selig and Ladd 1973), where papers on almost every aspect of relative density were presented. Many of the papers presented to this conference expressed considerable reservations and cast grave doubts on the usefulness of the relative density approach. A complete study by Tavenas *et al* (1973) concludes that 'the concept of relative compaction is significantly better than the relative density, in terms of accuracy and practicability of the result. It is often considered that a major advantage of the relative density over the relative compaction is that the relative density magnifies small variations of the *in situ* density, thus allowing a better control of such variations, particularly on compaction works. From the present findings, this supposed major advantage appears to be a major disadvantage, since the relative density also magnifies the errors on the unit weights to such an extent that the computed result is barely better than that obtained by a pure guess. Therefore, the use of relative compaction can only be encouraged, not only in compaction specifications but also in the analysis of natural deposits'.

Poulos and Hed (1973) conclude that per cent compaction (relative compaction) is related to the potential settlements of a fill and that per cent compaction is a considerably more useful parameter than is relative density for measuring degree of denseness.

The present author concludes that owing to difficulties discussed in the references above, and in particular due to the errors introduced by the 'loose density' measurement, that relative compaction should be used to assess the settlement potential of a soil.

It should be noted that relative compaction gives an indication of the maximum possible settlement as it involves the ratio of field dry density (at field moisture content) with maximum dry density at optimum moisture content.

If we wish to assess the maximum compaction settlement possible without variation of field moisture content, then the ratio of field dry density (γ_{df}) to maximum dry density at field moisture content (γ_{fmax}) will give a better indication of likely settlements.

$$RC_f = \gamma_{df}/\gamma_{fmax}$$

where RC_f is termed the relative compaction at field moisture content.

This relative compaction value at field moisture content reflects the difference in objective between a tunnelling engineer who knows closely when dynamic compaction forces will be imposed on a soil, and the road engineer who must design his subgrade to be suitable at any moisture content. Whilst the tunnelling engineer must be aware of the maximum possible settlement, it is the maximum likely under a given set of circumstances which will be of primary importance.

For site investigation purposes the state of compaction of a granular soil is often derived from Standard Penetration Test (SPT) values (see test 19 BS 1377). Figure 3.4 is derived from several sources in an attempt to correlate SPT values with relative compaction. The relation between relative compaction (RC) and relative density (RD) was derived from the work of Lee and Singh (1971) who reviewed data from some 47 different soils and concluded that RC = 80 + 0.2 RD. Further confirmation of this formulation was obtained from work on granular fill materials by Poulos and Hed (1973). Their Fill II material was similar to the Warrington sand in size and grading and their conclusions regarding the linearity of the relations between relative compaction and relative density are interpreted numerically.

The qualitative description applied to relative density is attributed to Terzaghi and Peck (1967). Unfortunately many authors seem to overlook the fact that SPT values are heavily dependent on vertical effective stress whereas relative density is not. It is, therefore, unwise to relate SPT values to relative densities unless the confining stress is defined.

The correlation between SPT value, relative density and vertical effective stress was derived from the work of Gibbs and Holtz (1957). This qualitative link between differing numerical indices may be found useful when interpreting site investigation data.

3.3.5 The effect of frequency and direction of vibration on settlement

It is known that an infinite and uniform mass of soil has no natural or preferred frequency of vibration (Whiffin and Leonard 1971). However,

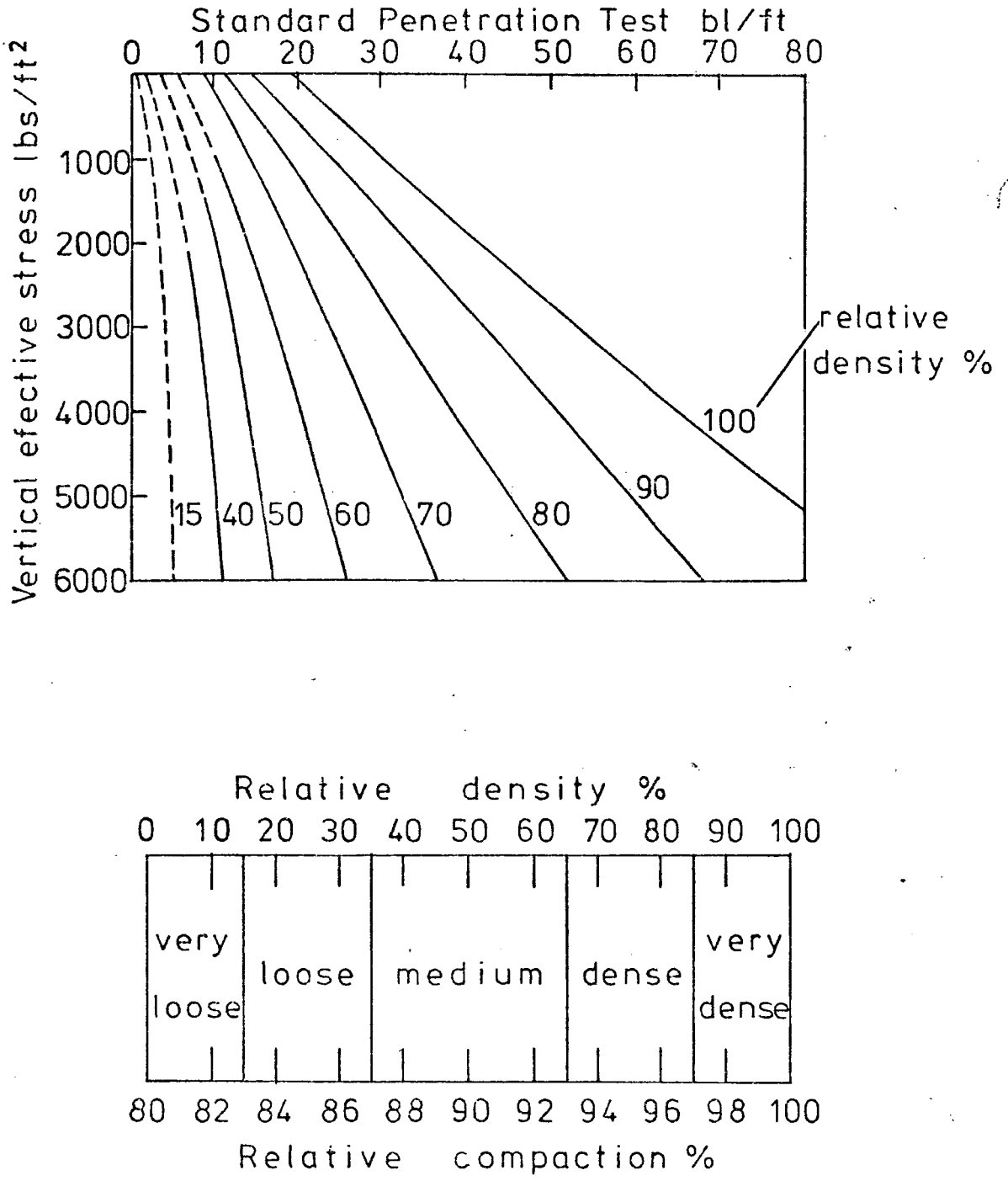

Fig.3.4 THE RELATIONS BETWEEN S.P.T. VALUES, RELATIVE DENSITY AND RELATIVE COMPACTION

it has been suggested by Barkan (1962) and others that soil has a natural frequency and that vibrations at this frequency are likely to occur when the material is loaded by a sudden impulse. This idea stems from Lorenz (1938) and others who measured the frequency at which a vibrator placed on the soil surface generated the greatest vertical amplitude. However, the frequency corresponding to maximum amplitude is not a characteristic of the soil alone because it depends on the mass of the vibrator and its mechanical properties, the distribution of the load over its base, the coupling between the vibrator and the soil as well as the stiffness and density of the soil. The boundary conditions will also have an important rôle in determining the nature of the vibrations.

Table 3.1 (*after* Terzaghi and Peck 1967) gives a list of 'resonant frequencies' of vibrators on various materials. From these results it would appear likely that the interaction of the tunnelling machine with the soil-boulder material may give rise to resonances at about 20-30 Hz.

Important work has been carried out by Pyke et al (1975) to investigate the difference between uni- and multi-directional shaking of sands. Their work was concerned with earthquake type vibrations and concludes that 'tests on samples of dry sand subjected to shaking in one, two and three dimensions have shown that the settlements caused by combined horizontal motions are about equal to the sum of the settlements caused by the components acting separately. While vertical accelerations less than 1 g cause no settlement if acting alone, vertical accelerations superimposed on horizontal accelerations also cause a marked increase in the settlements! This work provided useful guidance in the design and interpretation of laboratory studies reported in Chapter 6 (Section 6.2).

Table 3.1
Resonant frequency of vibrator on various types of soil (after Terzaghi and Peck 1967, page 129)

Supporting soil or rock	Frequency Hz
Loose fill	19.1
Dense artificial cinder fill	21.3
Fairly dense medium sand	24.1
Very dense mixed grained sand	26.7
Dense pea gravel	28.1
Soft limestone	30.0
Sandstone	34.0

3.4 The thresholds of tolerance to ground vibration

3.4.1 Urban structures

Vibrational energy may be transmitted from the ground into a structure through its foundations. The possibility or degree of damage resulting from such vibrations will depend on the natural frequencies, the damping characteristics and the inherent strength of the structure as well as on the amplitude and frequency of the forcing vibrations. Steffens (1974) gives a comprehensive account relating damage criteria from many sources to structural vibrations. Roberts (1969) has made a survey of information on vibrations produced by civil engineering processes and Whiffin and Leonard (1971) have produced a similar but more complete work on traffic induced vibrations. The three papers above each contain useful bibliographies on this subject.

National and international standardising authorities throughout the world have been reluctant to issue any firm standards related to vibration damage thresholds owing to the extreme complexity and independence of the

many factors involved for almost any example. However, the German provisional standard Vornorm DIN 4150 dated September 1975, is now available and gives a positive guide for those seeking recommendations regarding maximum vibration levels acceptable under various conditions. It is, as might be expected, a very conservative document and many may question the low thresholds given.

Figure 3.5 shows damage thresholds given by Whiffin and Leonard which relate to traffic induced vibrations and by DIN 4150 which apply particularly to blasting vibrations.

3.4.2 Human perception

Often the fears expressed concerning vibration damage are a result of the extreme sensitivity of the human body to vibration especially in the low frequency range of 1 to 100 Hz. The direct action of vibrations on people is to produce physiological effects on the body and psychological reactions, and, although the two often go together, the extreme sensitivity of the human senses may provoke varied and sometimes irrational behaviour patterns. Pyschological differences between people often lead to diverse interpretations but these are even more difficult to assess as it is almost impossible to predict emotional reactions. Human reaction is more likely to be influenced by previous experience and understanding than by the actual level of vibration itself; a person's state of health, temperament and age will all contribute to this reaction. Soliman (1968) and Guignard and Guignard (1970) have written useful surveys of published work on human response to vibration. Figure 3.5 shows the curves (heavy solid lines) with subjective description (in capitals) produced by Reiher and Meister (1931) and which are still regarded as a useful basis for interpreting levels from most sources of vibration. More recently Dieckmann (1958) showed the importance of exposure time on tolerance in

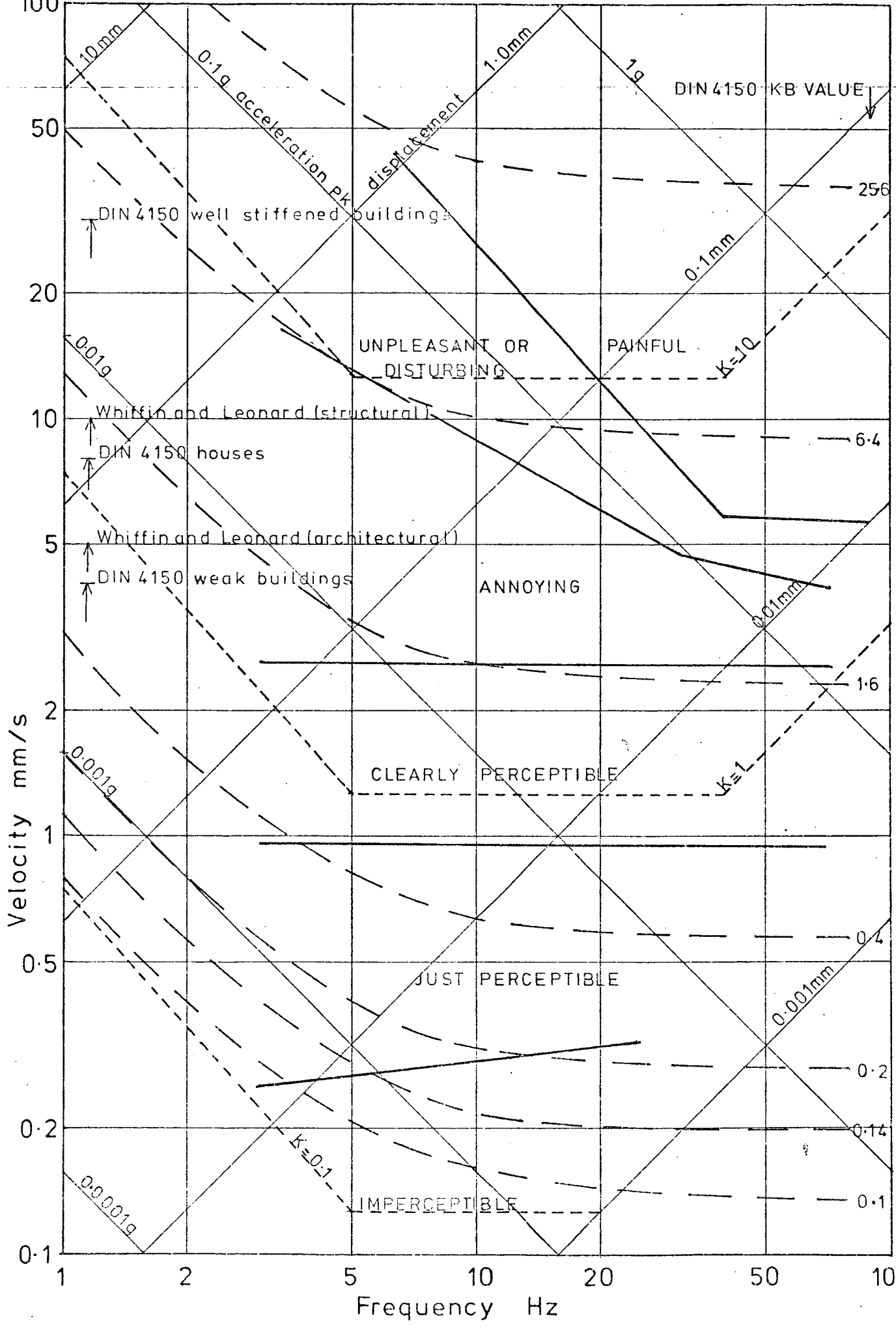

Fig. 3.5. VIBRATION THRESHOLDS: DAMAGE TO BUILDINGS AND HUMAN SENSITIVITY

the series of curves shown in Figure 3.5 (fine dashed lines with K values) for exposure to vertical sinusoidal vibrations. The K values were obtained from:

0-5 Hz : $K = 0.001\ Af^2$ (proportional to acceleration)

5-40 Hz : $K = 0.005\ Af$ (proportional to velocity)

40-200 Hz : $K = 0.2\ A$ (proportional to displacement)

where A = Amplitude in microns and f = frequency in hertz. The tolerances for various values of K were defined by:

K = 0.1 : the lower limit of perception

K = 1.0 : vibrations permitted in industry for any period of time

K = 10 : allowable in industry for a short time

K = 100 : the upper limit of strain for man

It should be noted that the threshold of perception is slightly lower than that of Reiher and Meister. Dieckmann also produced tolerance curves for exposure to vibrations in a horizontal direction. These show a greater sensitivity by people to lateral vibrations at frequencies below 4 Hz than to vertical motion.

The recent provisional standard DIN 4150 uses a classification based as follows:

$$KB = V\beta f \Big/ \left[1 + \left(\frac{f}{f_o} \right)^2 \right]^{\frac{1}{2}}$$

where V = maximum velocity mm/s

f = frequency

f_o = reference frequency of 5.6 Hz

and $\beta = 0.13$

This German standard gives a table of acceptable values related to the particular environment. For areas described as 'general residential' the KB guide values are as follows:

	Vibration continuous or repeated with intervals	Infrequently occurring vibration
Day	0.2	4
Night	0.15	0.15

Two other standards in this area are worthy of mention; the I.S.O. Standard 2631-1974 (currently subject to amendment), and the BSI 'draft for development DD 32 : 1974'.

Apart from helping to define thresholds of perception and annoyance, tolerance scales alone do not provide sufficient information for defining limits for tunnelling generated vibrations as they are only applicable to situations where vibration is an accepted part of the environment. A different type of criterion has to be considered in areas where vibration does not normally occur or is at a very low level. Vibration may then be considered as intrusive. It is the unpredictability and unusual nature of a source rather than the level itself which is likely to provoke complaint. The effect of intrusion tends to be psychological rather than physiological and is more of a problem at night when occupants of buildings expect no unusual disturbance from external sources.

A second type of involvement of people with vibrations is in interpreting the effect on buildings or their contents. Not surprisingly, this is particularly true where the person concerned is the owner. Even the slightest disturbances from an unusual source may excite anxiety and draw attention to minor cracking of plaster or similar effects which

were pre-existing or may have otherwise gone un-noticed. The provision of information, education, and reassurance seem to be the main requirements in these difficult circumstances.

CHAPTER 4

THE MEASUREMENT, RECORDING AND PROCESSING OF THE VIBRATION DATA

4.1 Transducers

4.1.1 Measured variables

It was decided at an early stage that the vibrations to be measured would be expressed in terms of their frequency and peak particle velocity. A review of current literature revealed that this is the most usual approach, although acceleration-frequency and displacement-frequency descriptions are also found. In the context of structural damage vibrations are generally expressed in terms of particle velocity although the relevant parameter to human perception is related to the frequency range involved. At frequencies below 10 Hz acceleration seems to be the dominant factor, whilst at frequencies between 10 and 50 Hz velocity criteria are appropriate. At frequencies above 50 Hz displacement is the more important factor. Studies on the effect of vibration on settlements of sands commonly use acceleration as a criterion. These studies are, however, usually at the low frequencies which are associated with earthquakes. Sinusoidal vibrations are uniquely defined (for zero phase) when any two of the four parameters maximum acceleration, velocity, displacement and frequency are specified. Use of velocity-frequency parameters allows single process derivation of acceleration, by differentiation, and of displacement by integration.

Most measurements were made with arrays of three mutually perpendicular transducers to enable maximum particle velocities to be calculated

if required by vector summation as follows:

$$V_{res} = (V^2_{vert} + V^2_{n-s} + V^2_{e-w})^{\frac{1}{2}}$$

where V_{res} = Maximum resultant velocity

V_{vert} = Maximum vertical velocity

V_{n-s} = Maximum velocity in a north-south direction

V_{e-w} = Maximum velocity in an east-west direction

It should be noted that if all component velocities are equal in magnitude and in phase then

$$\frac{V_{res}}{\sqrt{3}} = V_{vert} = V_{n-s} = V_{e-w}$$

Calculation of resultant velocity in this way provides an inherent factor of safety as it is unlikely that maximum velocities recorded individually from the three transducers will occur simultaneously. By measuring in all three directions it was possible to observe the direction of maximum vector amplitude. Provided that analysis is performed on the vector component in the direction of maximum particle velocity the error can never be greater than 42.3 per cent of the maximum possible resultant. In practice, owing to the random phase and lower amplitudes of the sub-dominant vibrations, any error incurred by considering only this vector is likely to be significantly less than 42.3 per cent.

4.1.2 Geophones

Velocity type geophones were used for all surface and borehole measurements. These transducers were manufactured by Walker-Hall-Sears

Inc of Houston, Texas, and supplied by Fenning Environmental Products of Luton. The 'horizontal' and 'vertical' type geophones were of WHS type Z-2CA and had the following principal specifications:

Natural frequency	14 Hz
Intrinsic voltage sensitivity	0.62 V/in/sec (24.41 mV/mm/sec)
Field shunt resistance	560 Ω
Field damping ratio	0.61
Field sensitivity	14.89 mV/mm/sec

The geophones were checked in the Engineering Geology Laboratories at Durham University before installation (Handsley 1975) and all were found to be of closely similar sensitivity. At the conclusion of the field work some geophones were recovered from the site and their sensitivities were confirmed at about 15 mV/mm/sec. This value is in close agreement with that expected for these geophones and is used for all particle velocity calculations. It should be noted that the recovered geophones were in a poor condition having been in the ground for some two years. The geophone cases were opened and their type number (Z-2CA) positively confirmed.

Low frequency ground motion (below 10 Hz) was monitored by Bell and Howell accelerometers and was found to be negligible during the periods of interest.

The choice of the geophone type of transducer proved to be particularly satisfactory, their relative simplicity contributing to the field reliability, a feature so important in this type of application. Although peizoelectric accelerometers have certain advantages of specification (in particular better low and high frequency response) they would have proved

more expensive, and they are also subject to temperature drift problems. Further, they are not completely self-generating like the geophones and they require a stable power supply which is not always conveniently available in the field.

4.1.3 Geophone location

Arrays of three mutually perpendicular geophones were placed at four levels in boreholes at sections A and B. These boreholes were directly above the tunnel crown and were designated A7 and B7 respectively (See Figures 2.5 and 2.6). Each group of three geophones was mounted and potted in an epoxy resin compound by the technical staff at the Engineering Geology Laboratories in Durham University. Special measures were taken to dissipate the high temperatures generated during the process of resin curing. Care was also taken during cable coupling to ensure, as far as possible, that water ingress was inhibited and that differential ground movements along the cable lengths would not cause breakage. When assembled the geophone packages were carefully lowered into the prepared boreholes, taking care that the correct orientation about both vertical and horizontal axes was rigorously preserved. The borehole was then backfilled with the excavated material and tamped to restore the ground to as near its original condition as possible. This procedure was repeated until all four arrays had been installed in each borehole. The colour coded wiring was then terminated in a diecast box situated in a 12" cast iron road box, as shown in Plate 4.1. Connection to the processing and recording equipment was then simply a matter of removing the road cover and plugging directly into the Plessey type socket on the terminal box as shown.

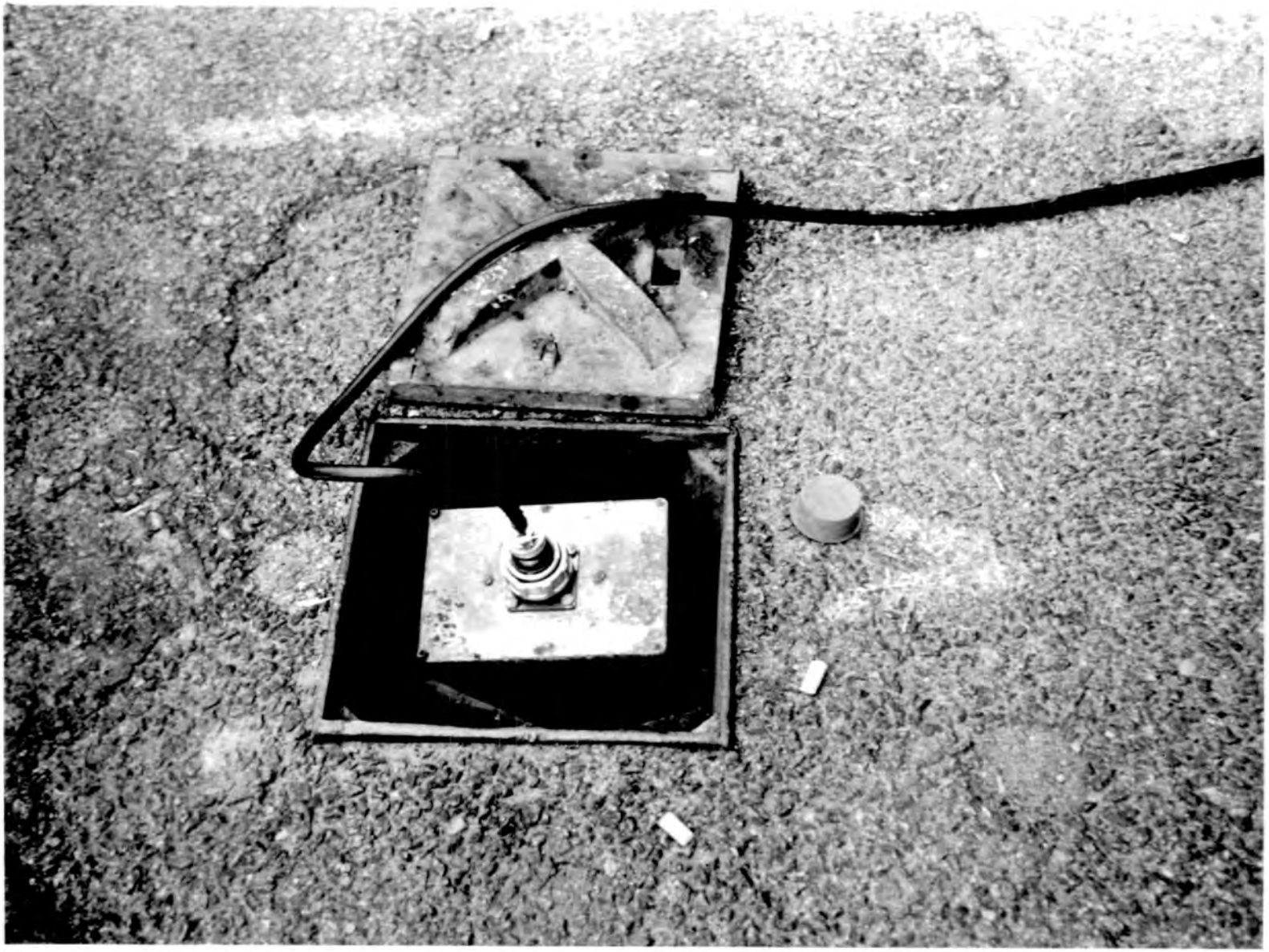

PLATE 4.1 BOREHOLE TERMINAL BOX

The level of each transducer array expressed as depth below the road surface is as follows:

	Borehole A7	Borehole B7
Level 1	0.20 m	0.20 m
Level 2	1.00 m	1.00 m
Level 3	2.25 m	2.25 m
Level 4	3.67 m	3.69 m

Some measurements were made with a three geophone array mounted on the pavement above the tunnel axis (as shown in Plate 4.2). These geophones were screwed to an alloy block which was 'fixed' to the pavement with Plasticene. Various other methods were tried but this proved to be the simplest and most effective. This system was also used when taking a series of measurements on the floor of the basement at No 54 Ellesmere Road (see Section 5.3).

4.1.4 In-tunnel measurements

A different approach from that used on the surface had to be taken when making vibration measurements in the tunnel. The equipment used had to be fully portable and suitable for use in difficult environmental conditions. The equipment chosen was a model 2100 portable vibration analyser produced by Environmental Equipments Ltd of Wokingham, Berkshire. Plate 6.1 shows the equipment (centre left). This equipment employs a piezoelectric accelerometer with magnetic mounting and provides meter read-out in terms of acceleration, velocity or displacement. It also incorporates a narrow-band tuneable filter, which allows measurement of each variable at any particular frequency. Two tuned filter bandwidths are available at ±5 per cent and ±2½ per cent of the centre frequency.

PLATE 4.2 PAVEMENT MOUNTED GEOPHONE ARRAY

This facility was most useful when isolating the predominant frequencies at various locations within the tunnel and on the tunnelling machine.

The actual locations at which vibration measurements were obtained are listed in Table 5.5, together with the vibration data.

4.2 Signal conditioning, monitoring and recording

4.2.1 Conditioning and monitoring

Conditioning and monitoring equipment was housed in a mobile laboratory parked close to the borehole and was supplied with mains electrical power from a nearby lamp-post. The importance of this arrangement should not be overlooked, since a reliable, relatively noise-free source of ample power was vital when using relatively sensitive electronic equipment. Plate 4.3 gives a general view in the mobile laboratory and Plate 4.4 shows a close-up of some of the equipment within. A diagrammatic layout of the equipment is given in Figure 4.1. From the borehole terminal box a single 25 way Plessey connector and cable assembly carried the geophone signals into the van and terminated in a 12 channel patch panel, each channel relating to geophone as shown in the diagram. The geophone output was fed into an amplifier type 1-190 made by Bell and Howell. This differential amplifier is designed specifically for use with instrumentation magnetic tape and ultra-violet chart recorders. The amplifiers are designed for multi-channel operation and being separately mains energised with isolation of signal earth, allow complete system flexibility. Twelve channels of amplification were required and their specification is as follows:

PLATE 4.3 GENERAL VIEW INSIDE MOBILE LABORATORY

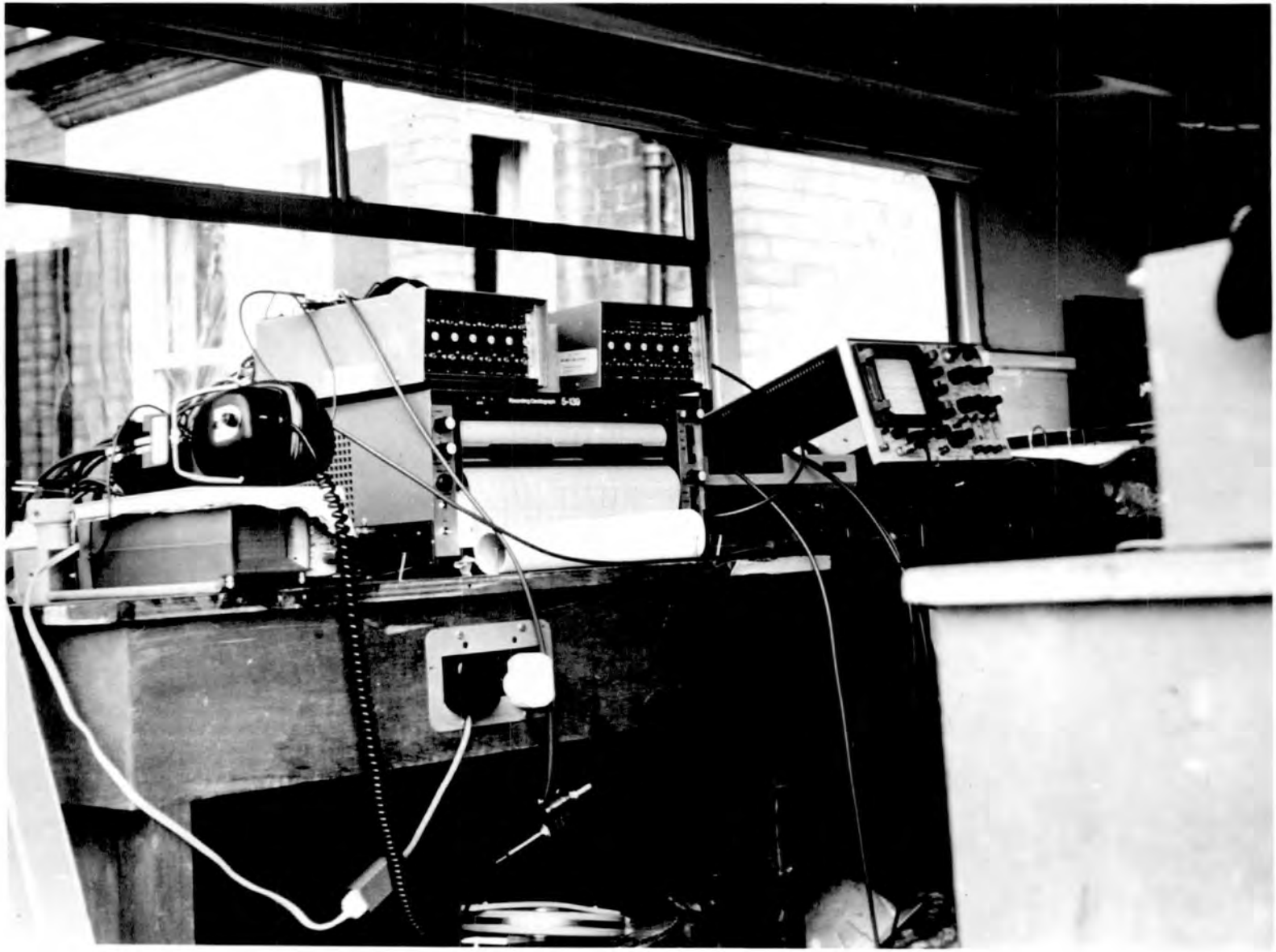

PLATE 4.4 MONITORING AND RECORDING EQIPMENT

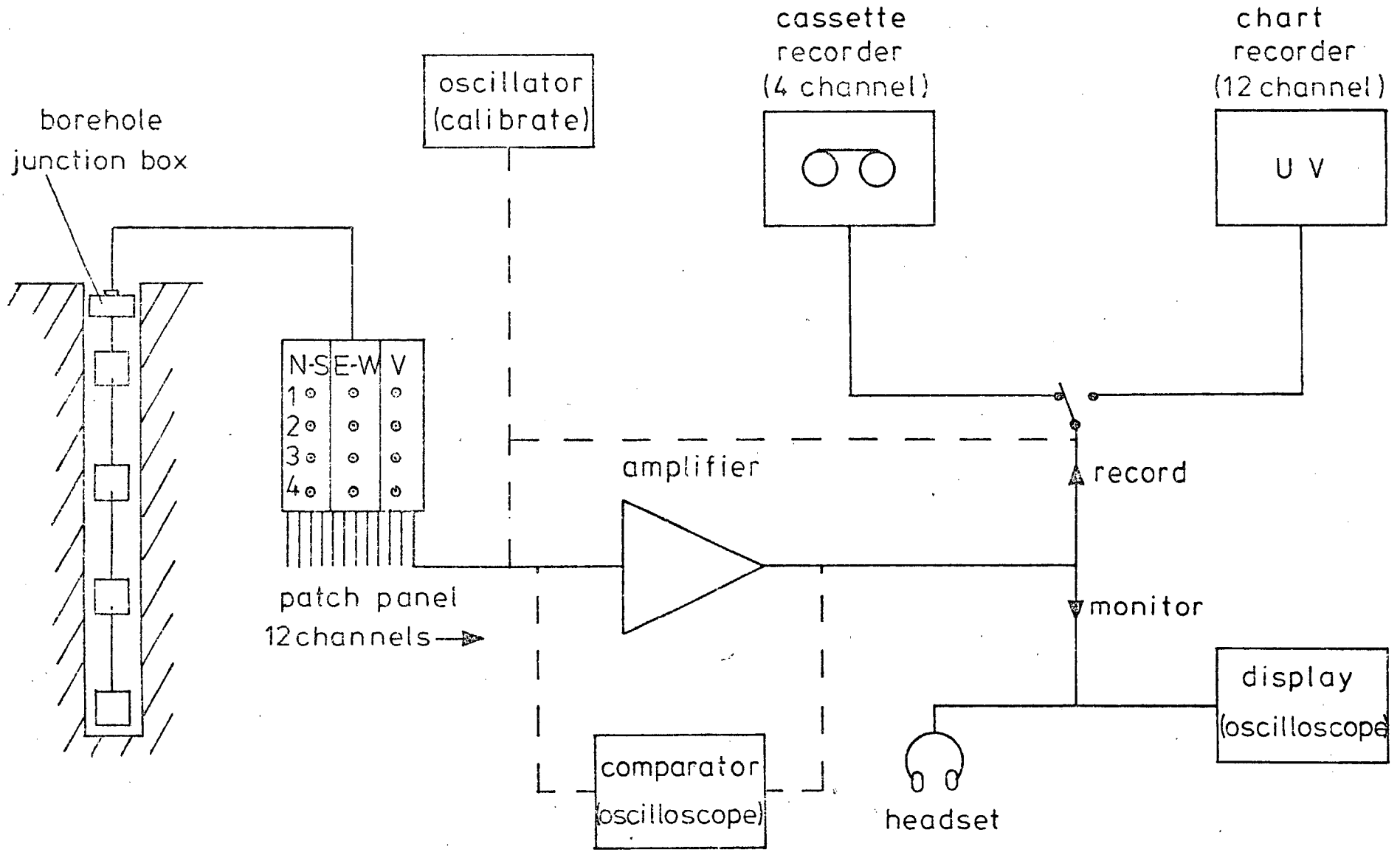

Fig. 4.1. EQUIPMENT SCHEMATIC

Gain (voltage)	switched	x 20, 50, 100, 200, 500, 1000
	accuracy	±1 per cent maximum
	linearity	< 0.1 per cent deviation from best straight line
	stability	better than .02 per cent better than .1 per cent long term

The above ranges may be attenuated by a factor of 100:1

Input impedance	> 2 MΩ balanced differential
Output voltage	± 8 volts maximum
current	± 10 mA
Common mode rejection	> 100 dB
Bandwidth	DC to 20 kHz

The signal was monitored on an oscilloscope at inputs and outputs of the amplifiers to ensure that whilst using the full dynamic range no clipping or other waveform distortion was occurring. A headset was available for listening to the seismic noise and proved a valuable asset. With experience it was possible to recognise, by ear, almost all forms of seismic noise from the tunnel and environmental sources. Viewing the signal on the oscilloscope was not so useful for this purpose.

4.2.2 Recording

All twelve amplifier outputs were fed to a Bell and Howell model 5-139 ultra violet chart recorder fitted with type 7-316 fluid damped galvonometers. This combination has a frequency response flat to 5 per cent for a bandwidth 0-1200 Hz. It was, therefore, possible to produce hard copy in real time of all the geophone outputs from any one borehole. This facility was particularly useful when deciding which were the most

appropriate channels to record on magnetic tape for subsequent spectral analysis. In order to resolve frequencies of up to 500 Hz it was necessary to run the paper at fairly high speeds and this meant that only relatively short bursts of data could sensibly be recorded.

A four-channel instrumentation cassette recorder made by Teac was used to record data from selected geophone channels. This recorder has a high input impedance (100 kΩ) and in its frequency modulated mode an effective bandwidth from DC to 625 Hz. An input voltage of 1v peak to peak gives full tape modulation and on replay results in a 2.3v peak to peak output. This form of data storage allowed a tape library containing many complete 'mucks' (the excavation for one lining ring, 0.615m) to be recorded in a form suitable for direct input to the spectrum analyser or ultra-violet chart recorder.

It was usual to record either all three geophone outputs at one level or one geophone output from each level (all four having a common direction of sensitivity). The raw data were stored on high quality C90 magnetic tape casettes and catalogued with reference to the tape code letter and the three digit tape counter built into the recorder. For example, D187, is the code for position 187 on tape D. To make best use of the dynamic range of the recorder it was desirable to set the gain of the amplifiers to provide as near to full tape modulation as possible. This was achieved by careful monitoring of the signal on the oscilloscope. If, however, the channel with the maximum signal was not correctly predicted overmodulation of the tape could occur. This problem occurred infrequently and was easily detected because all the tape records were checked during processing.

4.3 Processing

4.3.1 Objectives and system choice

The principal objectives of the processing were:

a) to determine the maximum soil particle velocities, and

b) to characterise the seismic energy in terms of its frequency spectrum.

Objective a) was achieved by replaying the data held on cassette and recording on the UV recorder the period of maximum observed particle velocities. From this trace and a knowledge of the overall system calibration the peak particle velocities were determined. Further manual analysis was performed on the twelve channels of UV data recorded directly from the boreholes. These records, however, only covered a very small proportion of the 'mucking' period and were unlikely to detect the important particle velocity maxima.

Two different approaches were considered to perform spectrum analysis of the data. Firstly, the preparation of appropriate software for use with the Laboratory's on-line computer system and, second, the use of a real time spectrum analyser of the type manufactured by Honeywell-Saicor. The latter was chosen for the following reasons:

i. No suitable software packages were available to perform the calculations required and the preparation of new or substantially modified programmes would have been expensive in terms of man hours.

ii. The Honeywell-Saicor analyser performed exactly the processes required and could be used in a real-time mode on-site if required.

iii. The analyser was capable of accepting analogue signals directly, whereas a software-based system would required digitised data.

iv. All processing could be carried out without the delays which seem inevitable with any on-line system.

v. The analyser is extremely flexible and any changes in bandwidth, integrating times or other parameters may be made at the flick of a switch.

In use, all these advantages were apparent and the system chosen was both technically efficient and cost effective.

Spectrum analysis provides a frequency domain characteristic for the applied signal. This characteristic yields the energy or power distribution as a function of frequency. It must be remembered that the relative phase of the individual Fourier components is lost, and as the maximum value of the signal (in this case velocity) may be of interest, this information must be obtained from time domain processing, that is simple direct measurements of particle velocity as described at the beginning of this section.

The information derived from the spectrum analysis allows the principal frequencies to be identified and characterised in terms of the source and the nature of the propagating medium. It also provides a clear indication as to the deployment of the seismic energy over the frequency range.

The Honeywell-Saicor model SAI-52B spectrum analyser is essentially a hard wired computer using a swept filter combined with time compression system which allows a complete 400 point spectrum analysis to be accomplished in 160 msec. A full description of these complex processes, together with detailed specifications and operating instructions, may be found in the handbook supplied by the manufacturers.

The data length required is dependent on the frequency scale selected. As theoretically required, the minimum record length is equal to the reciprocal of the desired resolution, the resolution of this 400 point analyser being 1/400th of the chosen frequency range. Therefore, if the analysis is accomplished on the 500 Hz scale the resolution is $\frac{500}{400}$ = 1.25 Hz and the processed record length is $\frac{1}{1.25}$ = 800 msec.

It is often desirable to produce a spectrum which is characteristic of a long record length. This is accomplished through the digital integrator section of the SAI52B, which accepts the output from the analyser and averages by adding and dividing by a prescribed and selectable number of spectra. The so called 'number of sums' may be 8, 16, 32, 64,.. and the total data length is calculated by multiplying the number of sums chosen by the individual processed recorded length. For example, the processed record length for 32 sums on the 500 Hz bandwidth scale is 32 x 800 msec = 25.6 sec. A particularly useful feature of this analyser is its 'peak hold' facility which, during the processing of data, captures and holds the peak value occurring in each bin. This is particularly useful when the signal comprises a low background noise with high amplitude oscillations occurring with frequent but random periodicity.

4.3.2 The spectrum analysis of field data.

It was decided to simplify the comparison of the frequency spectra by standardising on a single bandwidth for all the processed data. This bandwidth was determined by analysing data when the source (the tunnelling machine) was at its closest to a geophone array. Since high frequencies are selectively attenuated to a higher degree than low frequencies these conditions indicated that the maximum bandwidth required was 500 Hz. The input/ouput gain factors in the processor were also fixed and the relative amplitude of each spectra obtained from the original amplification applied to the geophone signal at the time of recording.

The vertical scale of the spectra is output from analyser in Volts/bin and is proportional to the voltage output from the geophone which, in turn, is proportional to velocity. Owing to the non-stationary nature of the spectra, the unrelated phase distribution of Fourier components, and the finite window size of the processed data, it is not permissible or appropriate to scale the spectra in terms of particle velocity. In this thesis the relative amplitude of the spectra are scaled in terms of a common and arbitrary unit, and when required, the particle velocity should be derived directly from the time domain records as previously stated. As all the records are from a common source, and are processed in the same manner, each spectrum is directly correlated by its common scale with any other, so allowing conclusions to be drawn based on comparative measurements. Owing to the non-linear response of the geophones and the effect of low frequency speed variation of the recorder, the part of the spectrum below 10 Hz should be disregarded. A few records were obtained giving high amplitudes at frequencies below 10 Hz; these were invariably found to be the result of over-modulation of the magnetic tape and were discarded as unreliable. It has been noted earlier

that independent measurements using piezoelectric accelerometers indicated no significant signal amplitude below about 10 Hz.

The raw data were fed directly in analogue form from the tape recorder to the analyser input. The continuous and averaged spectra were displayed throughout the processing period. Headset monitoring was also found to be most useful at this time for identifying particular events noted in the cassette log book, and to ensure that spurious events (such as, a tape stop-start) did not influence the processed data. Having identified the period of seismic noise to be processed, an average and peak hold spectrum was produced together with a UV recording of the period of maximum velocities (observed during the processing period). The records were catalogued and stored for future manual analysis.

Plate 4.5 shows the spectrum analyser with input from the cassette recorder and output to a Bryans X-Y plotter.

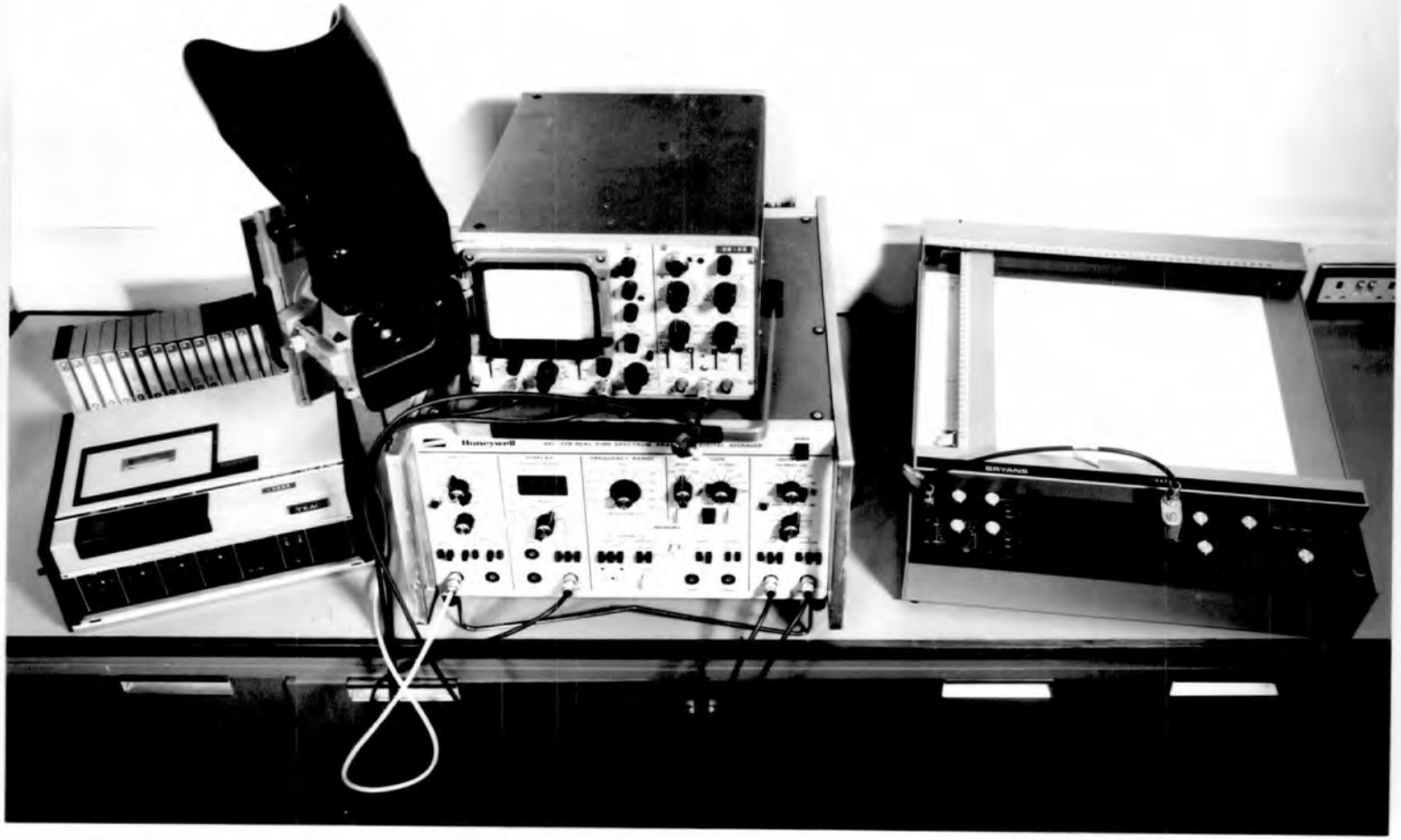

PLATE 4.5 PROCESSING EQUIPMENT

CHAPTER 5

VIBRATION CAUSED BY THE TUNNELLING PROCESS

5.1 Introduction

Data were collected during two periods as the machine approached and passed the instrumented boreholes. The bulk of data at borehole A7 were collected between 15 September 1976 and 23 September 1976, and at borehole B7 between 5 October 1976 and 8 October 1976. Much supplementary data were also collected between May 1975 and May 1977. The volume of data was considerable and was held in magnetic tape and UV chart record form.

To reduce the data to a format suitable for analysis the following procedure was adopted. Each magnetic tape was replayed and significant events reproduced on UV charts and a full spectrum analysis performed (as described in Section 4.3). In all, well over two hundred peak hold and mean spectra were produced. In order to quantify and tabulate the amplitudes shown by the spectra the 500 Hz bandwidth was divided into ten equal parts. An average value was then measured for each 50 Hz bandwidth and tabulated. The relative amplitude and frequency of the principal peaks were also noted. The peak particle velocity was measured from the UV charts and wherever possible the dominant frequency was also noted.

Figure 5.1 shows a typical peak hold and mean spectrum, and illustrates the method of processing the data into tabular form. A data sheet similar to that shown in Figure 5.2 was attached to each spectrum. Figure 5.3 shows a short extract from the UV chart record associated with the spectrum shown in Figure 5.1.

Appendices E, F and G present all the relevant data produced in this way and data are abstracted from these tables for graphical and tabular presentation. Information derived from data held in other forms (that is, 12 channel UV chart or measurements of peak particle velocity from the portable vibration analyser) is reproduced in the text as required. Figure 5.4 is a typical direct record UV chart taken during the muck for ring 1063 (the 1 E-W geophone is not working). A large quantity of data of this type were recorded and were useful in assessing patterns in the data. However, the maximum values which are of particular interest were always to be found and processed from the complete magnetic tape records.

Pilot laboratory experiments, briefly described in the next chapter, had confirmed the findings of other workers (Pyke *et al* 1975) that it was the peak levels of vibration rather than their duration which were of most importance when considering compaction. That is, for a given peak level of vibration, settlement will occur within a relatively short period of time, and until a higher level of vibration is applied no further significant settlements will occur. The emphasis of the experimental effort was, therefore, placed on the determination of peak particle velocities and the majority of the data were recorded in the immediate vicinity of the machine.

5.2 Borehole measurements of machine induced vibration

5.2.1 The type of vibration and peak particle velocities

During the excavation process the vibrations were characterised by periods of low particle velocities with random periods of relatively high velocities. This is shown in Figure 5.5 during 1.8 seconds of a

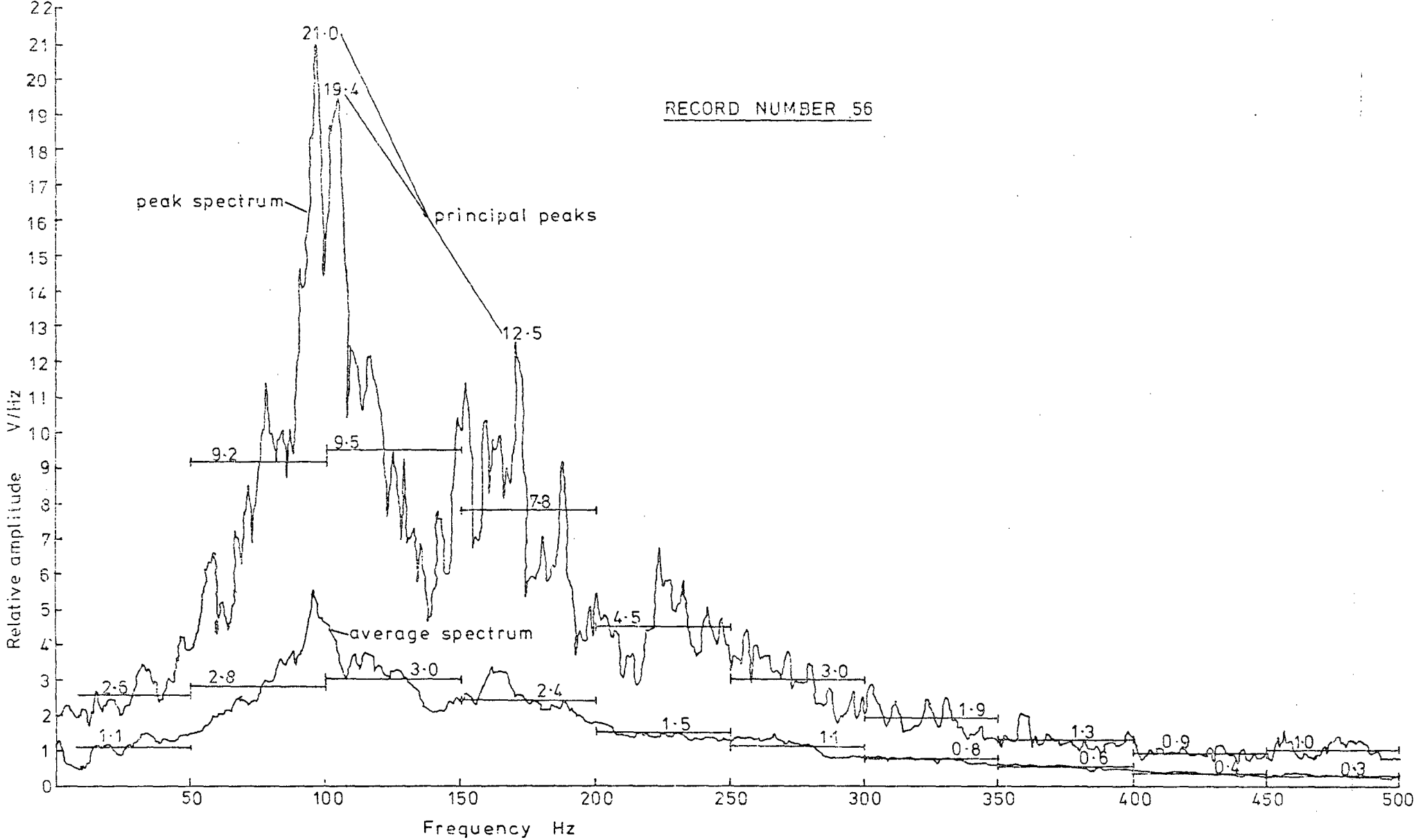

Fig. 5.1 TYPICAL SPECTRA WITH TABULATED VALUES

ANALYSER

RECORD NUMBER 56
GEOPHONE REFERENCE B7 4 Vertical
SOURCE M/c cut ring 1167
Source Dist 4.92 m
AMP GAIN x 100
REMARKS

BANDWIDTH Hz	0-50	50-100	100-150	150-200	200-250	250-300	300-350	350-400	400-450	450-500
MEAN PEAK	2.6	9.2	9.5	7.8	4.5	3.0	1.9	1.3	0.9	1.0
MEAN AVE	1.1	2.8	3.0	2.4	1.5	1.1	0.8	0.6	0.4	0.3

PRINCIPAL PEAK	AMP	FRE Hz
a)	21.0	93
b)	19.4	103
c)	12.5	168

UV

PEAK PARTICLE VELOCITY mm/s 1·1 P to P
at Hz

Fig. 5.2 TYPICAL DATA SHEET

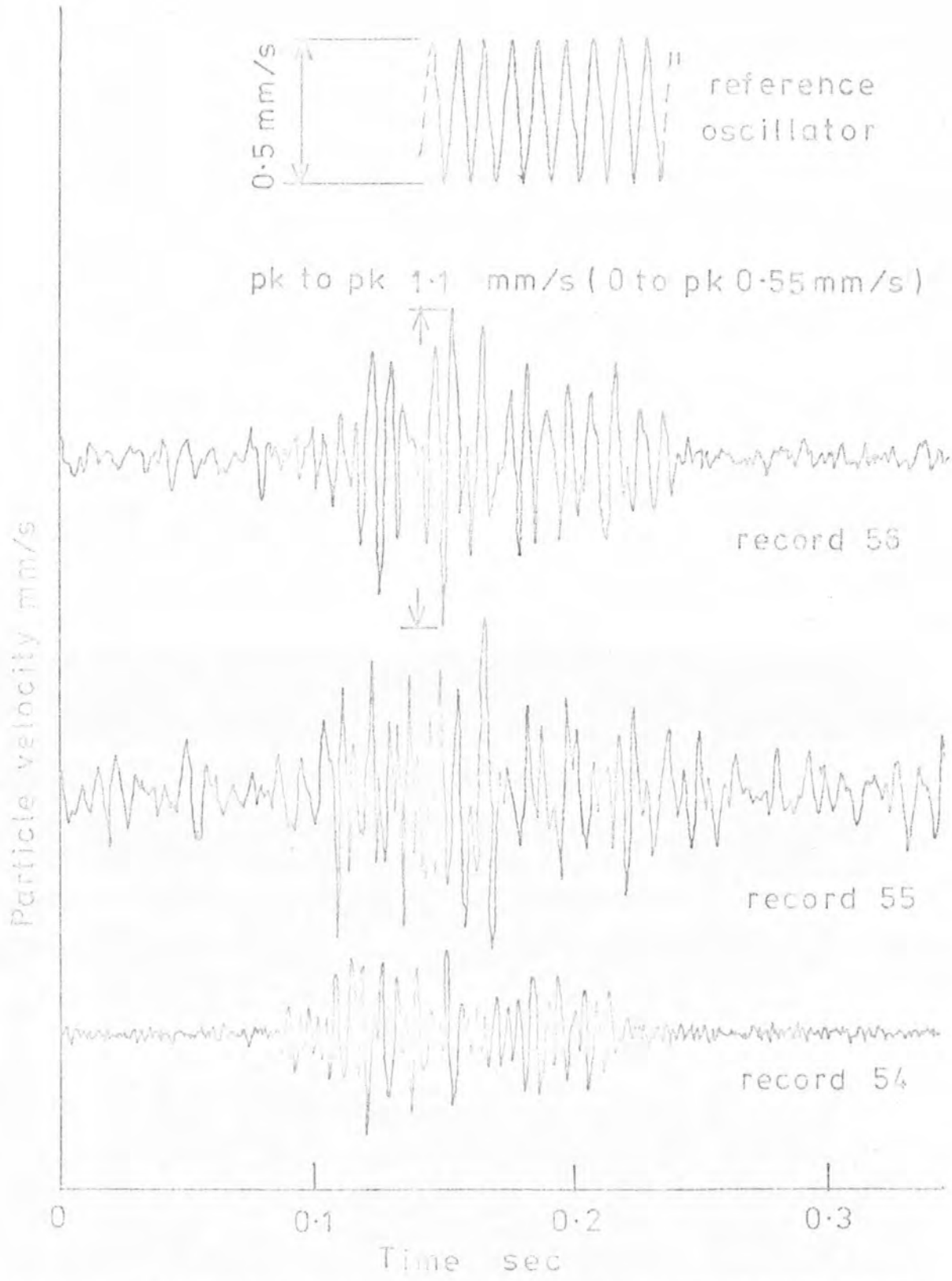

Fig. 5.3 TYPICAL U.V. CHART RECORD DERIVED FROM CASSETTE TAPE

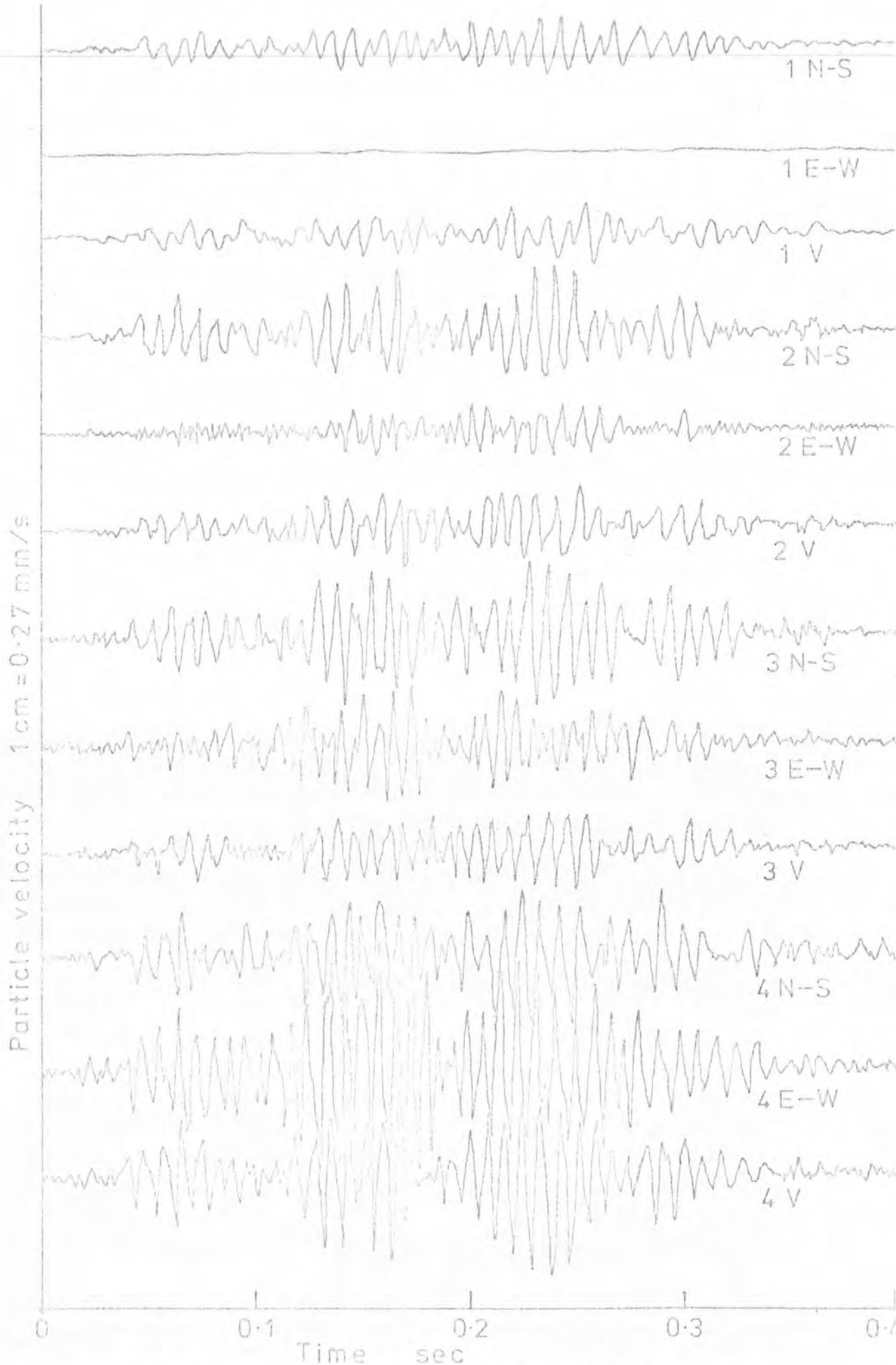

Fig.5.4 TYPICAL UV CHART RECORD (BOREHOLE A 7)

recording typical of the great majority of data collected. The periods of high velocities (in Figure 5.5 between 1.3 and 1.6 secs) were rarely more than 0.5 seconds in duration whereas 'quiet' periods (between 0.42 and 0.88 secs in Figure 5.5) were often as long as 1 or 2 seconds. This cutting action is explained by considering the sandy ground with randomly distributed granite and dolerite boulders. The periods of high particle velocities occur when a boulder is exposed, then pushed into the sand and finally smashed by a disc cutter or by a milling action against other boulders in the face. This cutting action could be heard clearly on the headphones which provided a rather better 'feel' for the mechanism than visual analysis of the UV chart records or oscilloscope trace. A noticeable change in this pattern occurred after the face has passed borehole B7. Although the peak particle velocities remained similar at this time, the periods of high velocities became less frequent than before, giving periods described in the cassette log book as 'quiet cutting'. When standing on the pavement above the tunnel face the vibrations could be felt and heard quite distinctly, and 'clearly perceptible' was considered an appropriate subjective description by site personnel.

Figure 5.4 shows a disc-boulder or boulder-boulder impact during the excavation for ring 1063, with the machine some 5 metres from the borehole. Note the increase of particle velocity with depth. This is typical of most records obtained when the tunnel face approached close to the boreholes. Consequently, the tape records that were made concentrate on the bottom (level 4) geophone array in order to record maximum ground particle velocities.

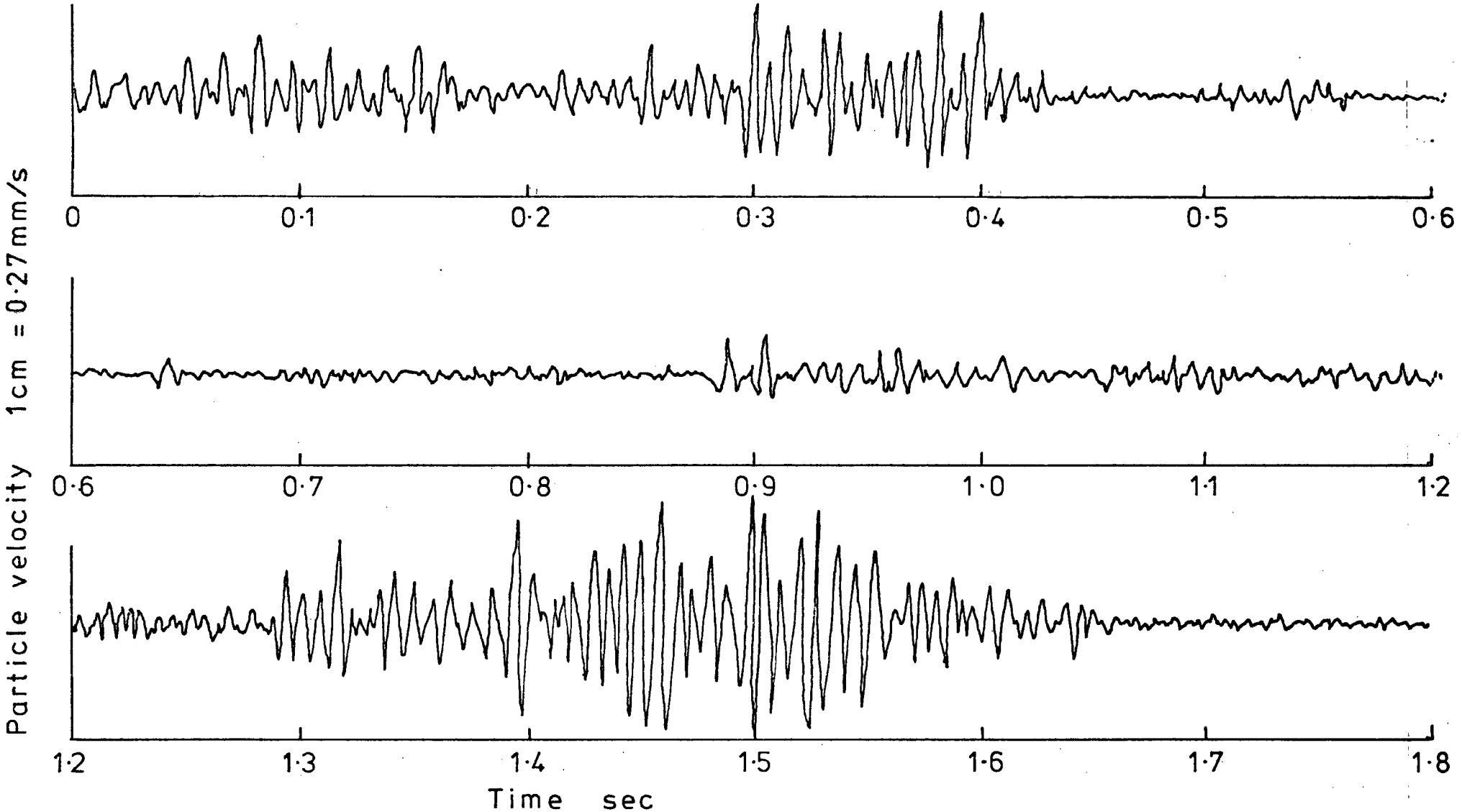

Fig. 5.5 U.V. CHART RECORD SHOWING TYPICAL VIBRATIONS INDUCED BY THE EXCAVATION PROCESS

Figures 5.6, 5.7 and 5.8 show the peak particle velocities recorded in the N-S, E-W and Vertical directions respectively, and demonstrate the increase in particle velocity with tunnel face proximity. The Tables 5.1 and 5.2 give the value plotted in the Figures together with a value of the resultant peak particle velocity calculated as described in Section 4.1.1.

TABLE 5.1

Peak particle velocities at borehole A7

Tunnel face - borehole distance	Peak particle velocities mm/s			
m	4 N-S	4 E-W	4V	Resultant
18.4	0.09	0.06	0.10	0.15
7.4	0.46	0.50	0.29	0.74
4.3	2.07	2.07	0.83	3.04
- 0.6	2.48	2.74	1.34	3.93
- 1.2	2.69	1.19	1.67	3.38
- 2.5	1.11	0.78	0.44	1.43
- 8.0	0.55	0.49	0.49	0.88

TABLE 5.2

Peak particle velocities at borehole B7

Tunnel face - borehole distance	Peak particle velocities mm/s			
m	4 N-S	4 E-W	4V	Resultant
4.9	0.32	0.55	0.54	0.83
0.6	1.13	1.09	1.16	1.95
0	1.85	2.48	1.85	3.60
	(3 N-S)	(3 E-W)	(3V)	
- 5.5	0.34	0.45	0.53	0.77
- 6.1	0.31	0.48	0.54	0.79
- 10.5	0.12	0.15	0.10	0.22
- 11.1	0.17	0.24	0.17	0.34

Fig. 5,6 PEAK PARTICLE VELOCITY (N-S) v TUNNEL FACE DISTANCE

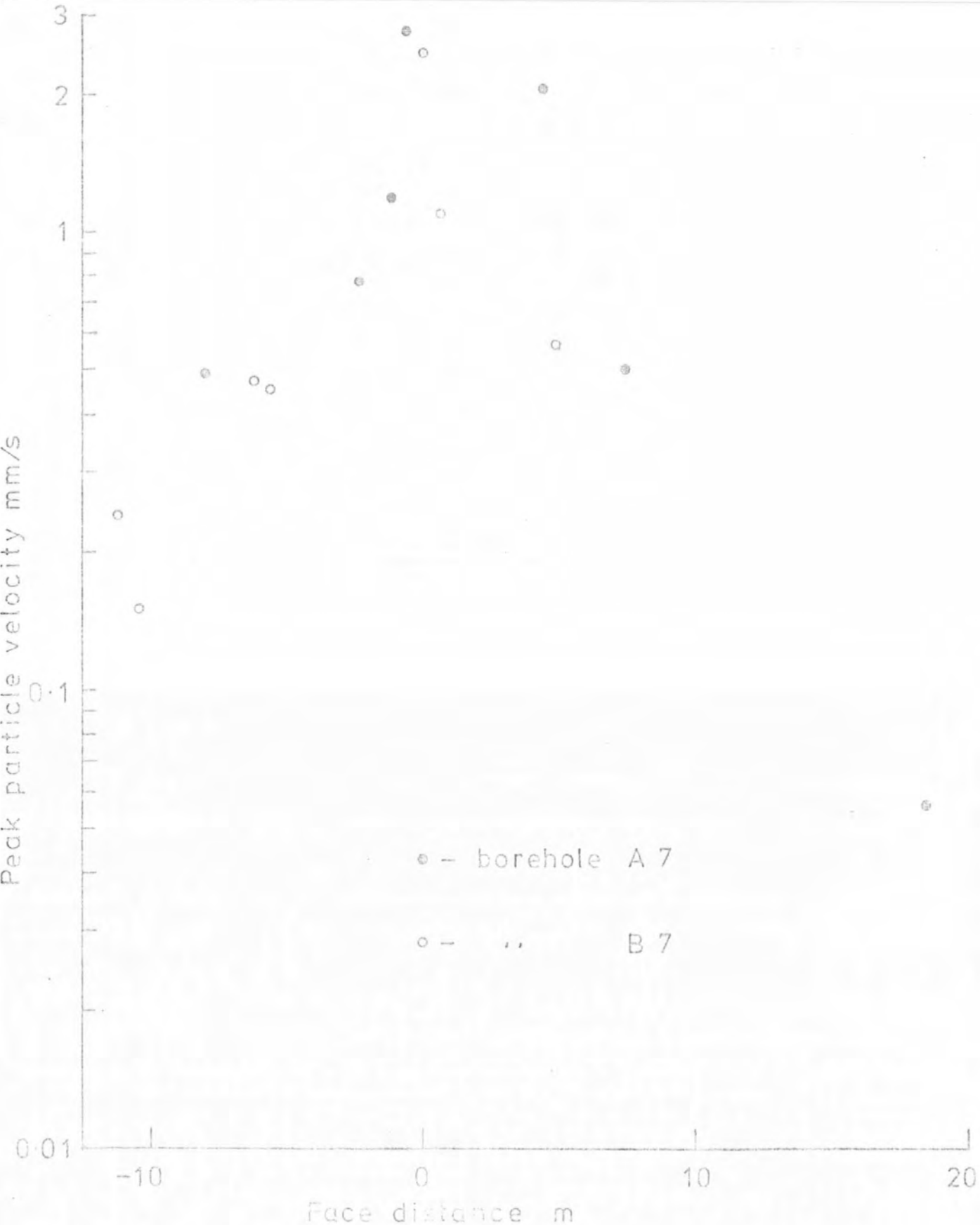

Fig. 5.7 PEAK PARTICLE VELOCITY (E-W) v TUNNEL FACE DISTANCE

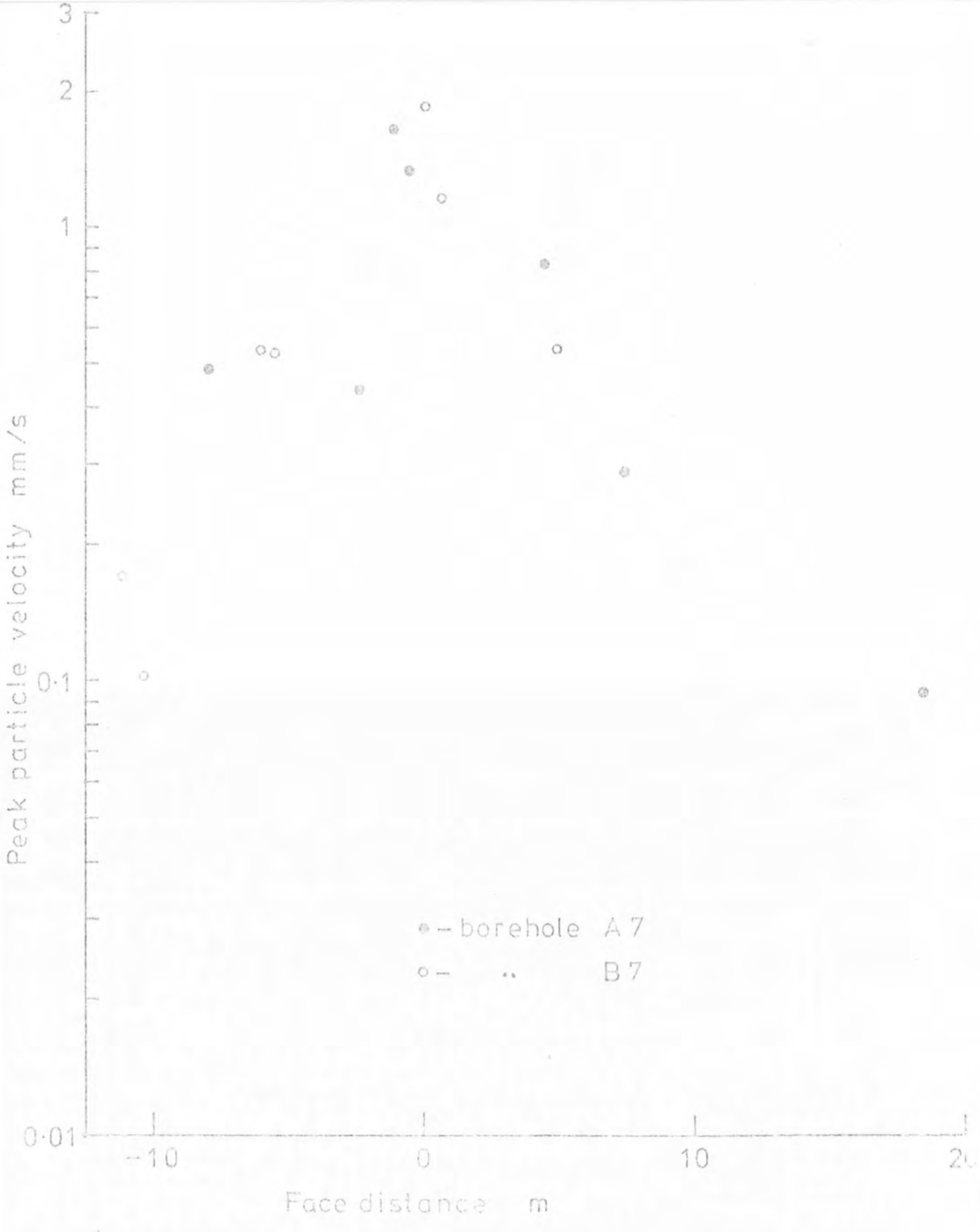

Fig. 5.8 PEAK PARTICLE VELOCITY (VERT) v TUNNEL FACE DISTANCE

The similarity between the results from boreholes A7 and B7 is immediately apparent and the maximum particle velocities recorded in each direction are closely the same. The first of these points may have been expected as we are dealing with the same source in the same type of ground. The second observation is also to be expected if the motions monitored are due to body waves excited in random directions through the process of smashing of boulders by the disc cutters on the rotating machine head.

The level of particle velocity is approximately symmetrically distributed on either side of the 'zero' tunnel face/borehole distance axis. This may suggest that the precise point of impact between disc and boulder is not the exclusive point of energy input to the ground, and that the complete rotating head of the machine is also vibrating on these impacts and exciting the surrounding ground as well.

5.2.2 The spectral distribution of particle velocity

Over 200 detailed spectra similar to that shown in Figure 5.1 were produced, and analysis of these processed records yields much information not directly relevant to this thesis. The simplified presentation and discussion which follows here will serve to indicate general trends observed, and bring out the significance of the data in the context of this work.

Figures 5.9 and 5.10 show the spectral distribution of particle velocities and are representative of the trends shown by other data given in Appendices E and F. These figures were plotted as described in 5.1 with the average relative amplitude for each 50 Hz bandwidth plotted at the midpoint of the bandwidth. As expected, the

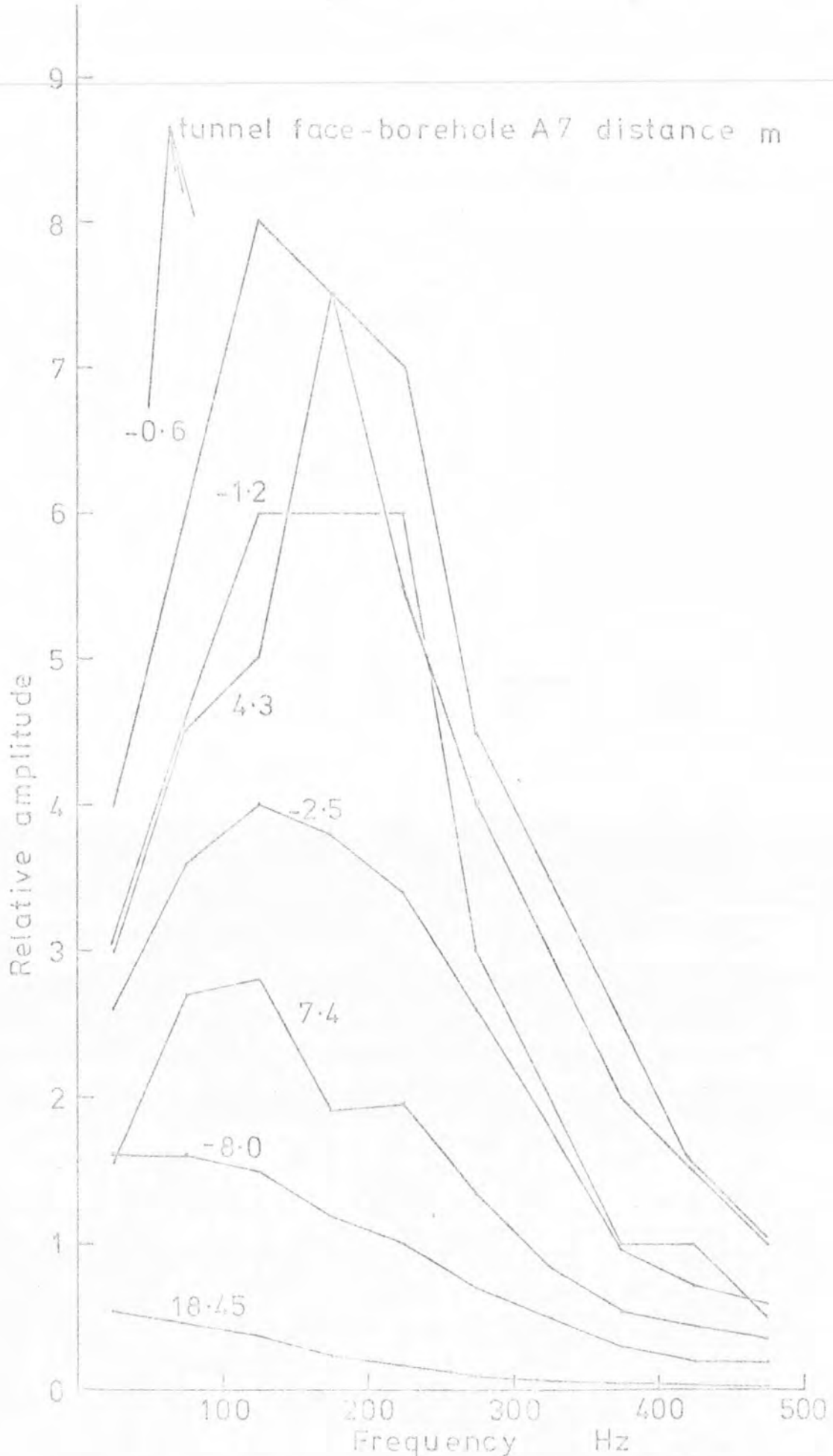

Fig.5.9 AVERAGE (N-S) AMPLITUDE SPECTRA FOR VARIOUS TUNNEL FACE–BOREHOLE A7 DISTANCES

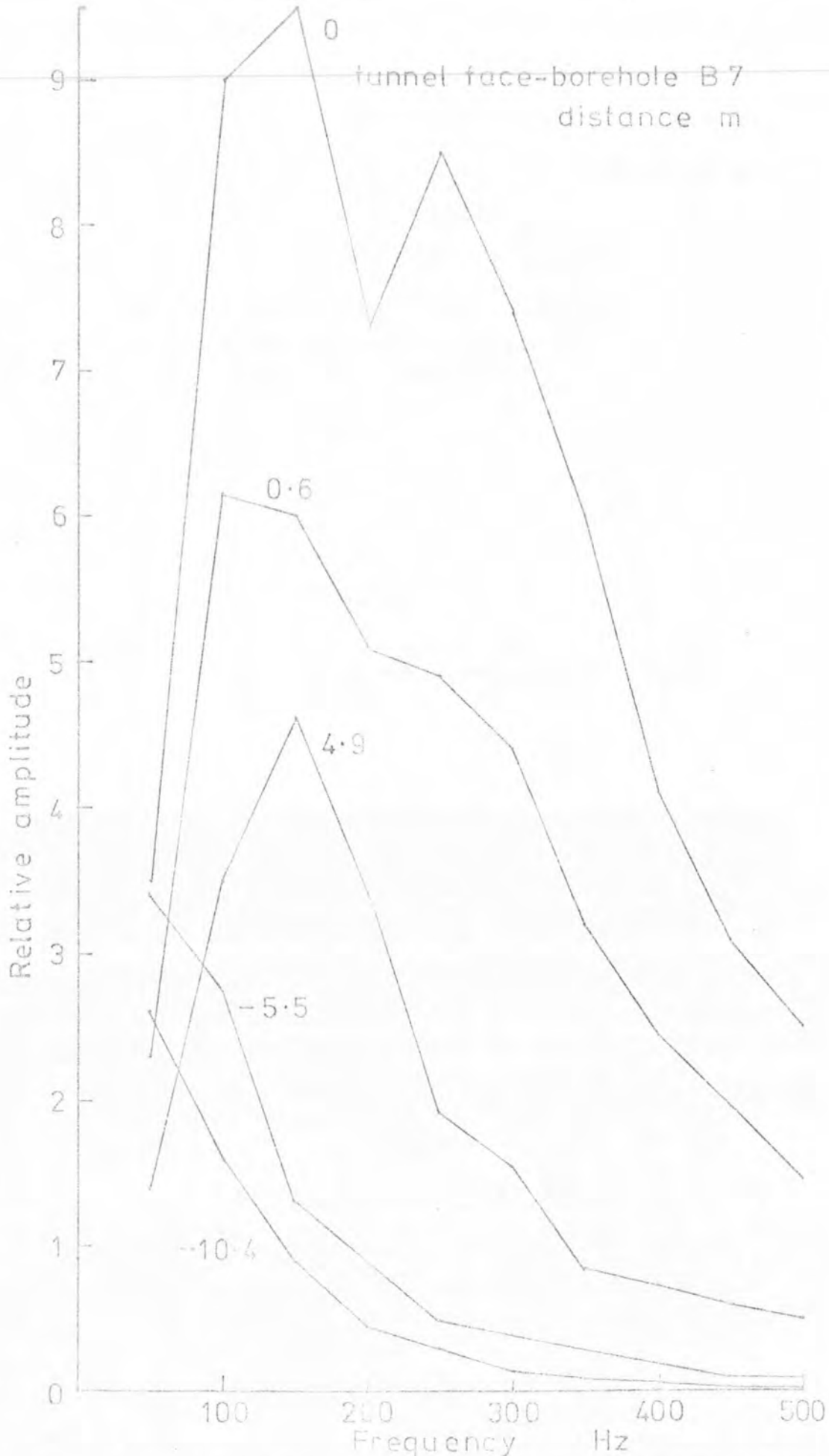

Fig. 5.10 AVERAGE (E-W) AMPLITUDE SPECTRA FOR VARIOUS TUNNEL FACE–BOREHOLE B7 DISTANCES

distribution of energy varies with distance from the source; the closer to the source the greater the proportion of energy at higher frequencies. Again, the similarity between the results from both boreholes and the similar levels of relative amplitude between component velocities, should be noted.

Records number 92 and 93 (see Appendix G) were taken to confirm that the relative amplitude of the spectra beyond 500 Hz was not significant. Spectra were obtained of ambient noise while the machine was idle and there were no other obvious sources (road traffic etc) present. The relative amplitude of these spectra never exceeded 0.01, so indicating that ambient noise levels would not be significant with respect to machine vibration levels.

Table 5.3 is illustrated by Figure 5.11 and shows the variation of relative amplitude in five bandwidths against source distance. The values plotted (in Figure 5.11) are average values of relative amplitude in 100 Hz bandwidths. In order to obtain values for the attenuation coefficient α the slope of a line between the values at 18.4 m and 4.3 m is considered for each bandwidth. Similar values for α are also obtained between values of relative amplitude at 7.4 and 4.3 metres from the tunnel face. Table 5.3 gives the calculated α values. The effect of geometrical spreading is not allowed for in the calculation of α owing to the complex and largely unknown geometry of the source and the refractive and guiding effects of the free ground surface and underlying bedrock. This approach to the calculation of α from field data serves only to describe empirically the order of attenuation as the effects of the site geology and geometry and the deployment of energy into surface waves renders largely invalid the assumptions made in the development of the theory. It is unlikely that the values obtained for the attenuation

Table 5.3

Values of relative amplitude in 100 Hz bandwidths derived from average spectra at borehole A7

Record Number	Tunnel face - Borehole distance	BANDWIDTH				
		0-100	100-200	200-300	300-400	400-500
10	18.4	0.50	0.31	0.14	0.05	0.02
16 & 19	7.4	2.1	2.36	1.65	0.7	0.4
22	4.3	3.75	6.25	4.75	2.5	1.25
26	- 0.6	5.0	7.75	5.75	3.0	1.25
29	- 1.2	3.75	6.0	4.5	1.5	0.75
32	- 2.5	3.1	3.9	3.0	1.4	0.65
43	- 8.0	1.6	1.35	0.85	0.4	0.2
$\log_e$ (rel. amp. rec. 22 ÷ rel. amp. rec. 10) nepers		2.01	3.00	3.52	3.91	4.14
'α' nepers/$_m$		0.14	0.21	0.25	0.28	0.29
$\log_e$ (rel.amp.rec.22 ÷ rel.amp.rec. 16 & 19) nepers		0.57	0.98	1.06	1.27	1.14
'α' nepers/$_m$		0.18	0.31	0.34	0.41	0.37

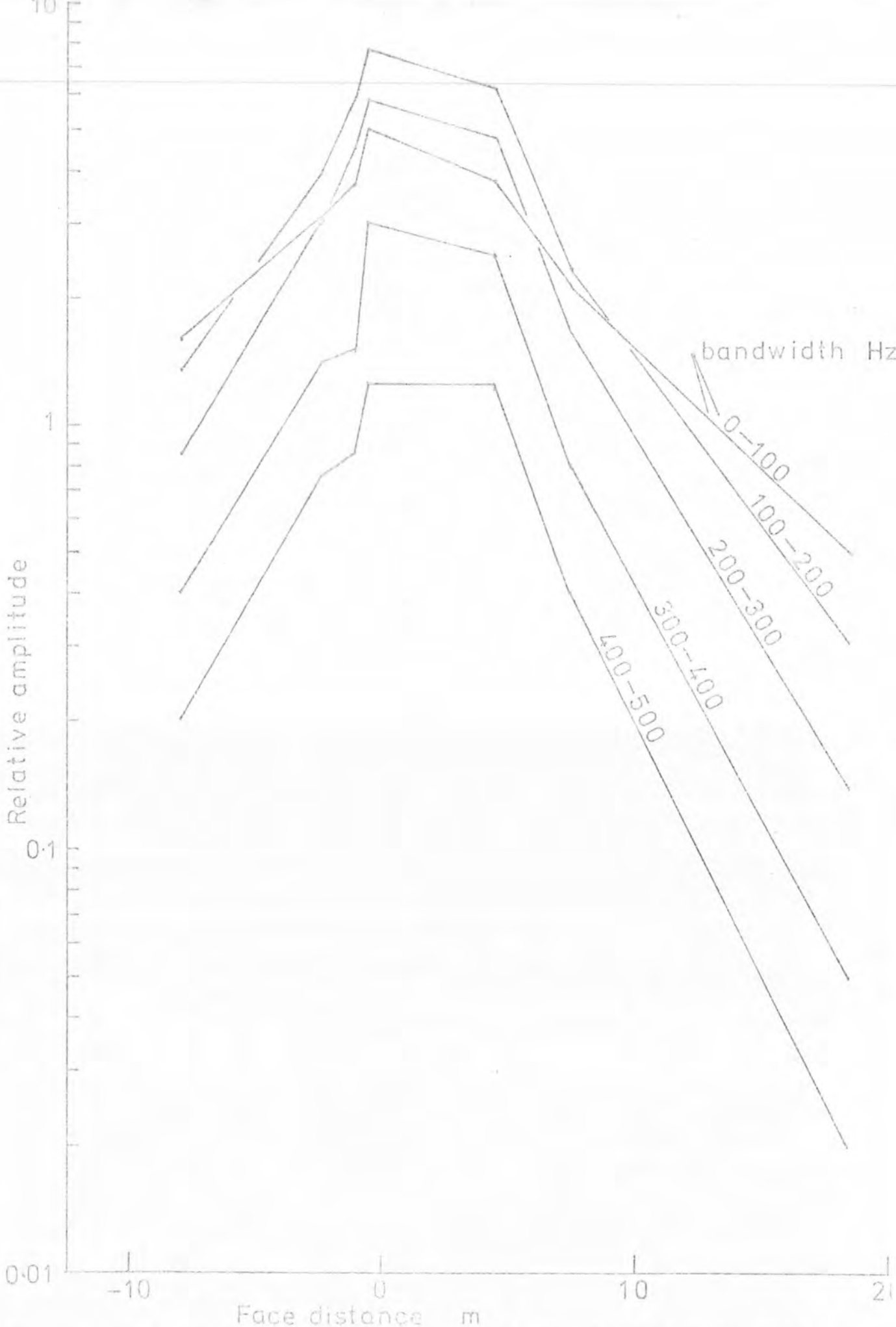

Fig. 5.11 RELATIVE AMPLITUDE (N-S) IN 5 BANDWIDTHS v TUNNEL FACE – BOREHOLE A7 DISTANCE

coefficient are an accurate reflection of the true value. It should be noted that for surface measurements made at distances in excess of a few tens of metres from the source, the effects of surface waves become predominant and the attenuations of the wave energy will be significantly less than that associated with body wave motion.

5.2.3 Other borehole measurements

The process of tunnel construction produced little significant ground vibration other than that directly associated with excavation. The only exception to this was the 'dropping' of the tunnel lining segments into the invert during the building of a ring. Figure 5.12 shows a segment-invert impact when the tunnel face was approximately 3 rings past the borehole. As the lowest level (4) geophone array is just above the crown of the tunnel, the source to a geophone distance was approximately 3 metres. The maximum particle velocity produced by this impact was about 0.33 mm/sec but velocities of up to 0.6 mm/sec were occasionally observed during ring construction.

Vibrations produced by traffic at the Warrington site have been reported by Handsley (1975). He found that the vibrations produced by heavy lorries were largest at the shallowest geophone array and were predominantly vertical in direction. The maximum resultant particle velocity he recorded was 0.25 mm/sec. Numerous recordings of road traffic were collected between periods of tunnel excavation and the results were similar to those of Handsley quoted above. A maximum resultant velocity of 0.18 mm/sec was recorded from a heavily laden articulated lorry travelling at about 35 mph. The frequency of this velocity maxima was approximately 20 Hz and the vibrations from the lorry were measurable for a period of about 5 seconds. Passing cars produced resultant velocities

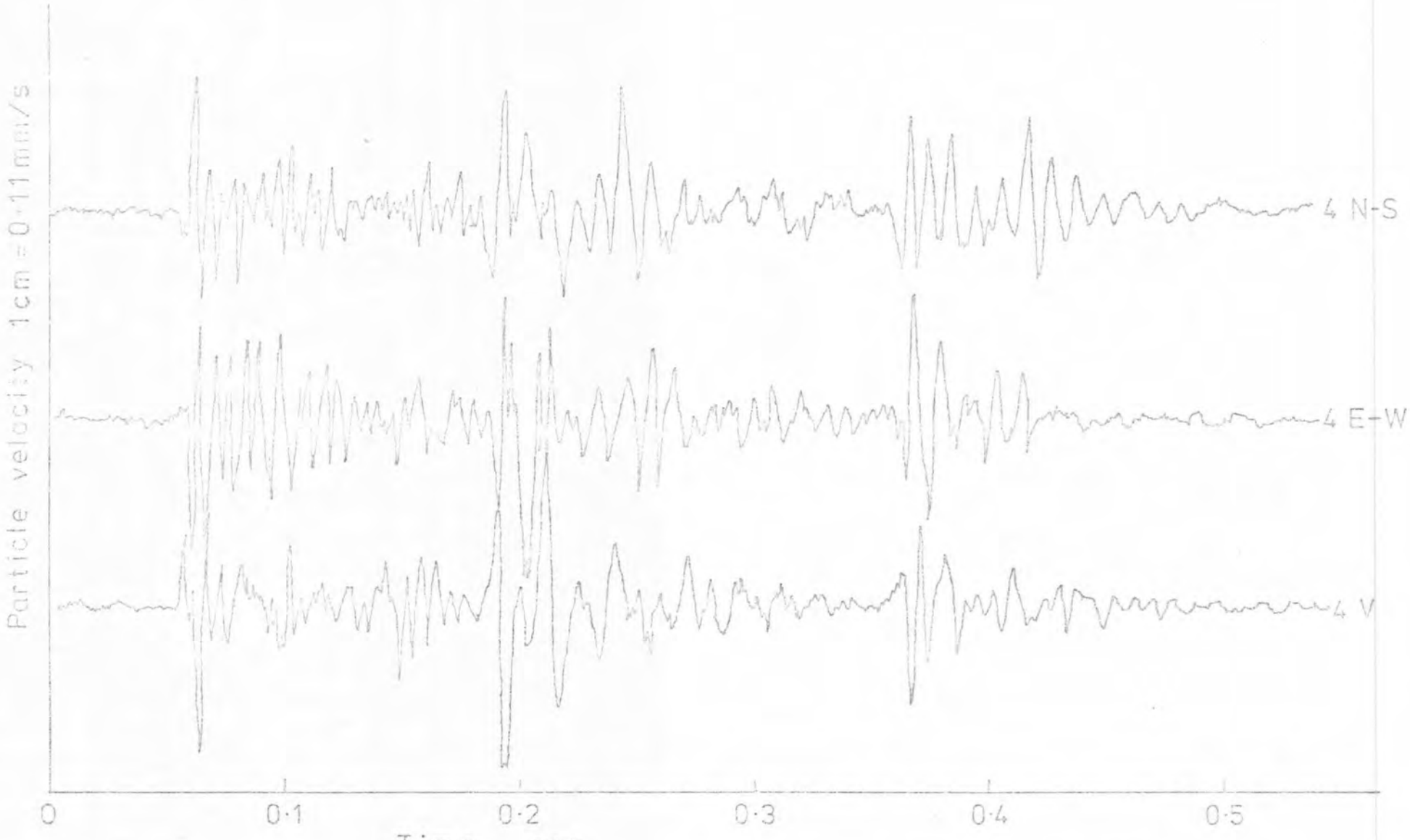

Fig.5.12 LINING SEGMENT DROPPING INTO INVERT DURING CONSTRUCTION OF RING 1075 (BOREHOLE A7)

well below 0.1 mm/sec. Most of the large motions from passing traffic occurred close to the surface and showed the general characteristics of a retrograde ellipse with a principal axis close to vertical. This indicates the predominance of surface waves over body waves from surface sources between approximately 10 and 50 metres distant.

5.3 Surface vibration measurements

5.3.1 Vibration measurements in Number 54 Ellesmere Road

At the invitiation of the householder, vibration measurements were made on the cellar floor at 54 Ellesmere Road during the excavation for the build of ring 1039. At this point the tunnel face is directly beneath the front garden wall and at its closest to this property. The geophone array (shown in Plate 4.2) was placed on the cellar floor about 150 mm from the front wall at some 2 metres below pavement level. Plate 5.1 shows a general view of site A and number 54. Borehole A7 is immediately in front of the parked car and number 54 is the third house from the junction with Francis Road. Figure 2.5 gives a plan of this site and the line $x\text{-}x^1$ shows the position of the tunnel face during the acquisition of this data. Table 5.4 is derived from records 4-9 and gives the peak particle velocities caused by the two largest impacts during the excavation for ring 1039. These vibrations were similar in character (as shown by their frequency spectra) to those recorded by the borehole geophone arrays and had a maximum peak particle velocity of 0.5 mm/s.

PLATE 5.1 GENERAL VIEW AT SECTION A

Table 5.4

Peak particle velocities in cellar of

No 54 Ellesmere Road

Peak particle velocities mm/s			
N-S	E-W	V	Resultant
0.20	0.17	0.37	0.45
0.24	0.24	0.37	0.50

5.3.2 Pavement vibration measurements

This sub-section mentions data which were obtained to allow the determination of seismic wave velocity by a cross-correlation technique and the evaluation of body wave attenuation over the entire bandwidth of energy produced by the tunnelling machine. Although this information is not particularly relevant to this work, it does provide some confirmation of other results quoted earlier in this Chapter.

Vibrations measured on the pavement were found to be similar in character and magnitude to those recorded at level 1 in each borehole and records 50-53 (see Appendix G) are typical of those obtained from geophones mounted directly on the pavement. These records comprise two pairs of simultaneously recorded data sets designated numbers 50, 51 and 52, 53. Numbers 50 and 52 were taken directly above the tunnel face, whilst numbers 51 and 53 were derived from geophones some 18 metres ahead of the face. This arrangement allowed direct comparison of vibrations from identical impact events at a geophone-source distances of about 6 and 18 metres respectively. The values for the attenuation coefficient 'α' obtained from this data were consistent with those given in Table 5.3,

which were derived from the geophones in borehole A7 with varying source distances. However, the results are subject to similar limitations to those described in Section 5.2.2 and should only be used in an empirical manner; and correlation with any theoretical models is not likely to be very meaningful. The maximum vertical particle velocity recorded was 0.5 mm/sec and is in agreement with the subjective description of 'just perceptible' given by site personnel during this period of excavation.

5.3.3 Disturbance by noise

Vibration from the tunnelling machine was transmitted through the ground and resulted in noise in the houses along Ellesmere Road. The sound was similar to distant thunder and was estimated by the author to be less than 40dBA. The sound appeared to result from resonances of floors and ceilings within the houses and the direction of the source was not at all apparent. Occasionally, windows, doors and household items were caused to rattle. The sound was clearly audible in houses for some 20 m behind and in front of the tunnel face and was at its loudest when the face was at its closest to the property. Few if any complaints were made during the day shift working; however, many complaints were made between 22.00 and 24.00 hours. Due to the reduced level of ambient noise, and the fact that they were trying to sleep, the noise seemed, to the residents, to be more severe at night. The vibration from the tunnelling machine was more noticeable indoors than it was standing on the pavement above the machine.

The residents presented their complaints to the Resident Engineer or his Clerk of Works who explained the causes of the noise and performed

the public relations exercise so important to this type of contract. To the author's knowledge no tunnelling 'down-time' resulted from noise complaints.

Several rather obvious conclusions were drawn from the author's experience on site:

a) A tactful and good humoured approach by the man dealing with the residents was vital. A surly or officious attitude would clearly have provoked residents to further action.

b) The noise upset residents because of its unusual source and type but its level was so low that serious problems only occurred at night.

c) With unimpeded tunnel face advance, the noise problem was only present in a given house for about one week. Good driving rates reduced the duration of the noise and hence the disturbance to the residents.

5.4 In-tunnel vibration

The portable vibration analyser described in Section 4.1.4 was used to determine the level of vibration on the tunnelling shield, on various parts of the machine, and on the tunnel lining during the excavation process. Table 5.5 gives the values found and the locations of the points of measurement.

The level of vibration on the tunnelling shield and the lining rings was found to be lower than expected, although certain parts of the machine

resonated at high peak particle velocities. There were few vibrations of the shield or the lining that were directly attributable to any individual source, although there was considerable evidence that the area of the machine around each main motor was excited at about 12-13 Hz. It should be noted in this context that the main motors rotate at 720 revs per minute (12 Hz).

As the data from borehole and surface geophones became available it quickly became clear that it was the random impacts between the disc-cutters and boulders that were the major source of energy transmitted through the ground, and that other machine induced vibrations were not particularly significant. It is of interest to note, however, that the spectra of borehole and surface recordings taken when the main motors were running, but excavation was not taking place, show peaks at approximately 13 Hz and higher modes. These peaks, of course, have a very low relative amplitude in relation to those obtained from data recorded during excavation.

Table 5.5

In-tunnel vibrations

Probable source of vibration energy	Location of measurement	Peak particle velocity mm/s	Dominant frequency Hz
Excavation	Shield tailskin (parallel to tunnel line)	0.1	15-50 (with other peaks between 150-900)
Excavation	Shield tailskin (normal to tunnel line)	0.08	20-40 (with other peaks between 200-800)
Excavation	Rear bulkhead of shield	0.12	15-100
Excavation	Last lining ring erected	0.08	10.35
No 2 main motor	On motor	27	12.3
No 2 main motor	Rail adjacent to motor	4.0	12.4
Erector pump	Rail adjacent to pump	0.25	24.5
Excavation ?	Erector (parallel to tunnel line)	2.7	15
Excavation ?	Erector (normal to tunnel line)	0.7	15-50
Main motors	Lining ring by main motors (parallel to tunnel line)	Below 0.05	-
Main motors	Lining ring by main motors (normal to tunnel line)	Below 0.05	-
Grout mixer	Rail by grout mixer	Below 0.05	-

CHAPTER 6

GROUND SETTLEMENT

6.1 Soil density assessment

Standard penetration tests (SPT) values obtained during the site investigation had indicated that the soil at the Warrington site varied between 'loose' and 'very dense' (see Section 2.3.2). Penetration tests carried out by the contractors more recently, however, have revealed that the soil in the vicinity of the tunnel at Sections A and B might be more accurately described as 'very loose' to 'medium dense' (see Figure 3.4). SPT values of below 10 were often found, and values of 1 to 5 were not uncommon. This indicates areas of very loose ground with considerable potential for settlement due to compaction.

During the excavation of a trench for a feeder sewer to the main tunnel the opportunity arose to measure the *in situ* density of the soil on the proposed tunnel line at a depth of 4.5 metres. The author initiated a series of tests carried out and reported by A S Nagarkatti (1977). Twenty two *in situ* density determinations were made using a sand replacement method (7 tests) and modified core cutter method (15 tests). No significant difference was found between the results given by the two methods, but the core cutter method was preferred because of its relative simplicity. This was important because of the difficult site conditions and the limited access periods. Table 6.1 gives the summarised results, and the standard deviations shown reveal the extremely varied nature of the soil. The dry density, moisture content and air content varied considerably, even over distances of less than 1 metre, and reflected not only changes in the stacking geometry of the particles but

also variations in the material itself. For instance, bands of silty clay were often clearly visible in the trench floor.

Table 6.1

Results of *in situ* density measurements

Type of test	No. of tests	Dry density Mg/m^3		Moisture content per cent		Air content per cent	
		Mean	Std. Dev.	Mean	Std. Dev.	Mean	Std. Dev.
Sand replacement	7	1.59	0.08	17.7	2.4	11.3	3.4
Core cutter	15	1.55	0.09	10.9	6.4	24.3	8.9
Both	22	1.57	0.09	13.1	6.3	19.9	9.7

Figure 6.1 gives the laboratory compaction curve using a 4.5 kg rammer (test number 13 of BS 1377:1975) and shows the individual dry density determinations summarised in Table 6.1. Note the maximum dry density of 1.80 Mg/m^3 occurs at a moisture content of about 11 per cent. The mean 'relative compaction' for the soil is the ratio of the field dry density and the maximum dry density found in the BS compaction test.

$$\text{Relative compaction} = \frac{1.57}{1.80} \times 100 = 87.2 \text{ per cent}$$

This is subjectively described as loose/medium and corresponds to the SPT values of 10 and under, which were found at similar levels in the vicinity of sections A and B (see Figure 3.4).

From the values in Table 6.1 the mean void ratio was found to be 0.681 and the porosity 0.405 (see Appendix D). Several tests involving

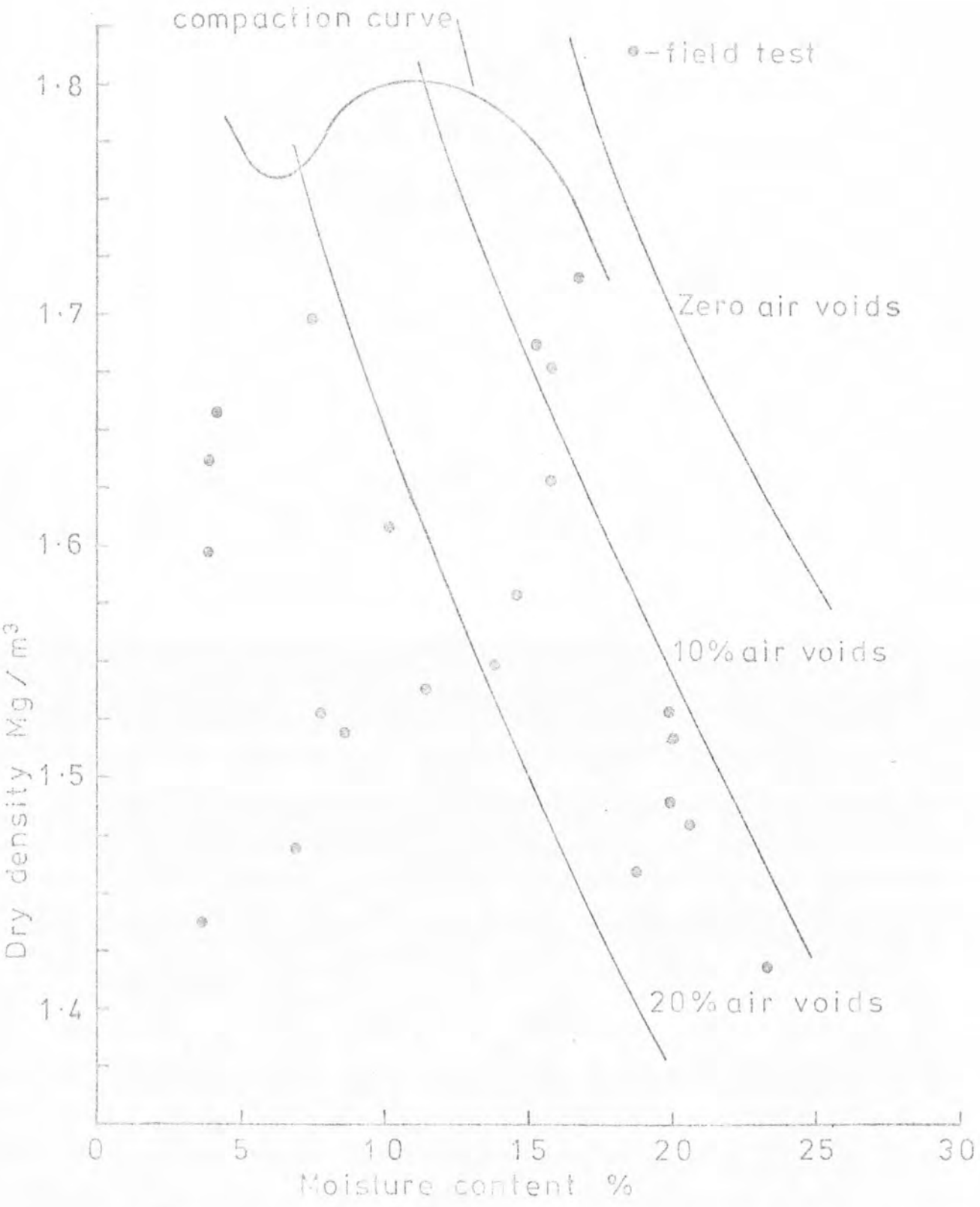

Fig. 6.1 IN SITU DENSITY TEST RESULTS AND B.S. (HEAVY) COMPACTION CURVE

various fast pouring techniques were carried out to find the minimum possible dry density. These tests proved difficult to replicate and the minimum value found of 1.37 Mg/m^3 was not considered an accurate reflection of the 'field' minimum dry density. The resulting value of relative density was 46 per cent which, despite the inadequacies of the method (see Section 3.3.3), is in reasonable agreement with that found for relative compaction (if the relation shown in Figure 3.4 is used).

These density measurements confirm that there is scope for an increase in the *in situ* density of the soil at Warrington and, consequently, settlements at the ground surface.

The wide variation of density values indicates the inhomogeneous nature of the lensed Drift deposits, although the spread may in part reflect the well known difficulties in obtaining an accurate measure of *in situ* density.

6.2 Laboratory tests of vibration induced settlements

In order to obtain some feel for the level of vibration at which settlement may begin to occur, a brief series of experiments was carried out on the rig shown in Plate 6.1. Samples of the soil from the Warrington site were prepared at dry densities and moisture contents similar to those found on the tunnel line. These samples were contained in a steel mould 150 mm in diameter and 125 mm high. The mould was clamped to a vibrating table which had a fixed frequency of 100 Hz and whose amplitude of motion could be controlled. The motion of the mould was measured by an accelerometer mounted directly on the mould and output on the vibration analyser shown on the extreme left of Plate 6.1. A plaster disc was placed on top of the sample to provide a small surcharge which prevented loosening of the surface sand. The settlement of the sample was measured using a

PLATE 6.1 LABORATORY SHAKE TABLE RIG

linear potentiometer which rested on the centre of the plaster surcharge disc.

The sample was subjected to increasing levels of vibration until the first sign of settlement was observed. The vibrations were held at this level for 2 minutes and the total settlement was then measured. The level of vibration was then raised in stages to a peak level of 2 to 3g and settlements again recorded after periods of 2 minutes at each level.

Table 6.2

Laboratory vibration induced settlements

Test Number	Dry density Mg/m^3	Moisture content %	Direction of vibration	Peak accel. g	Settlement %
1a	1.52	12.0	Vert	1.4	0.20
1b	1.52	12.0	Vert	2.8	3.84
2a	1.79	6.7	Horiz.	0.1	0.04
2b	1.79	6.7	Horiz.	3.0	4.26
3a	1.59	9.6	Horiz.	0.2	0.22
3b	1.59	9.6	Horiz.	2.0	7.50
4a	1.50	11.7	Horiz.	0.2	0.22
4b	1.50	11.7	Horiz.	2.0	5.45
5a	1.37	9.2	Horiz.	0.05	0.44
5b	1.37	9.2	Horiz.	2.0	23.24

Table 6.2 summarises the results for 5 samples. The tests sufficed 'a' give the threshold levels at which the first settlements were observed and those suffixed 'b' indicate the settlements after the maximum accelerations had been applied.

It was not possible to apply a substantial surcharge stress to the sample to simulate true field conditions. However, these experiments were useful and allow the following observations to be made:

i. Samples 3 and 4 had very similar dry densities and moisture contents to the soil at Warrington and under horizontal unidirection shaking at 100 Hz began to compact at a peak acceleration level of 0.2 g. This corresponds to a peak particle velocity of 3mm/sec.

ii. Samples 2 and 4, which are similar to the extremes of dry density found on the site, began to settle at 0.1 and 0.05 g (1.6 and 0.8 mm/sec) respectively.

iii. As expected, the higher the initial dry density of the sample, the lower was the final settlement.

iv. The samples were far less affected by unidirectional vertical shaking than by horizontal shaking.

v. It was noted that the settlement due to a given level of vibration occurred within a few seconds of the start of shaking and thereafter no significant settlements occurred until the vibration level was increased.

The results of this brief series of tests are similar to the results of other workers and conform to the broad principles of compaction by vibration discussed in Section 3.3.3.

Vibration thresholds of 0.8, 1.6 and 3.0 mm/sec caused the samples to settle. As the level of vibration in the ground due to the tunnelling process was often in excess of these values, it is possible that settlements due to compaction will occur.

It should be noted that in the field two factors not simulated in the laboratories will have an important influence on the vibration induced settlements.

a) The effective stress in the soil due to the cover will increase the strength of the soil and increase the energy levels required to re-order the particle structure (see Figure 3.3).

b) The multi-directional shaking present in the field will tend to reduce the vibration threshold levels observed for unidirectional motions.

These effects are opposite in character and will be, to some extent, self cancelling.

6.3 Ground settlements at Sections A and B

6.3.1 Introduction

An important part of the TRRL research programme at Warrington was the measurement of surface and subsurface ground movements due to tunnel construction. The following paragraph forms the conclusions to Tunnels Division Working Paper No. 3 (Barratt 1976) and adequately summarises surface subsidence measurements made prior to work at the main instrumented sections A and B:

'Settlements above the sandstone and above the start of the chemically consolidated ground have been reported in TRRL Internal Note IN 0123/75. The maximum and minimum values measured were 2.3 and 1.3 mm in the sandstone and 2.2 and 1.4 mm in the chemically consolidated ground. The amount of chemical treatment in the zone where these settlements were measured was up to 40 per cent of the area of the face. Measurements reported in this Paper show that towards the end of the chemically treated ground the settlement measured was between 2.5 and 4.8 mm, with an area of treated face of up to 65 per cent. This shows an increase in settlement as the extent of the treated ground increases. The surface settlements measured above the tunnel excavated using the bentonite system gave values of 19.9 and 14.2 mm on the centreline and 10.2 and 8.6 mm at the shoulders, values considerably higher than in all previous cases at Warrington: the corresponding slope values were 1/210 and 1/360. If it is assumed that the subsidence profile at the surface can be approximated by a normal distribution curve, the cross-sectional areas of the subsidence troughs developed at the two survey locations are 0.086m^2 and 0.071m^2'.

The data given in Sections 6.3.2 and 6.3.3, were derived from measurements given to the author by D Barratt in the form of personal communications and will be published in due course.

6.3.2 Surface settlement

At sections A and B a series of six studs were fixed into the road surface on a line normal to the tunnel axis as shown in the site plans (Figures 2.5 and 2.6). The upper parts of Figures 6.2 and 6.3 show the

settlement of the 'o' road stud (directly above the centre line of the tunnel) as the tunnel face passed beneath. These data with their date and time (where relevant) of acquisition, are also given in Table 6.3. The lower parts of Figures 6.2 and 6.3 give the settlement profiles of the ground when the face was more than 20 metres beyond the measuring points. By this time the great majority of the settlement had occurred and for our purposes the ground level had stabilised.

The settlements at both sections A and B showed very similar characteristics which were as follows:

a) At both sections over 95 per cent of the total settlement occurred during the excavation of material from approximately 5 m before the road studs to 15 m beyond the road studs.

b) The maximum settlement at section A was 18.7 mm and at section B, 25.3 mm.

c) The settlement profiles at A and B were distinctly assymmetrical. Settlements 2 m north of the tunnel centre line were appreciably lower than those 2 m to the south. This effect may be due to the greater degree of initial compaction of the ground beneath the main road (Ellesmere Road) or some other difference in ground conditions. Preferential 'take' of material related to the direction of rotation of the cutting head offers another possible cause.

d) At sections A and B the volume of ground 'lost' expressed as a percentage of the volume of ground excavated was 1.1 per cent and 1.5 per cent respectively.

e) The ground slopes, calculated on a stud to stud basis, are given in Table 6.4.

6.3.3 Sub-surface settlements

Sub-surface ground settlements at sections A and B were measured by direct ground anchors and by magnetic rings placed on the outside of the inclinometer tubes, (see Figures 2.5 and 2.6). The equipment is described and the full results of the ground movement survey are given by Barratt (1977). This section summarises the ground movements only where relevant to the objectives of the thesis.

Figure 6.4 shows the settlements of magnetic rings at tunnel invert level offset about $1\frac{3}{4}$ metres south of the tunnel centre line at sections A and B (boreholes A2 and B2). The Figure also shows the settlements of magnetic rings some 2 m below invert level which were thought to be on fairly competent rock at the bottom of each borehole. As expected, the lower magnetic rings show no significant movement, however the invert level rings settled by some 7 mm at section A and 10 mm at section B. It is considered that this settlement was caused by compaction. Settlements at these points due to the redistribution of effective stresses during excavation were not considered likely owing to the non-cohesive, granular nature of the ground and the constant support given to the tunnel cover.

The direct ground anchors above the tunnel crown (shown in Figure 6.4) settled by closely similar amounts. At section A they both settled 25 mm

Table 6.3

Surface settlement above tunnel axis

Section	Date	Time	Distance to tunnel face m	Settlement at 'o' road stud mm
A	21.9.76	10.30	5.5	0
A	21.9.76	17.50	1.8	1.8
A	22.9.76	09.30	3.1	11.9
A	23.9.76	11.00	9.8	17.3
A	23.9.76	16.30	11.1	17.6
A	24.9.76	09.07	14.8	17.5
A	24.9.76	15.00	16.6	17.8
A	25.9.76	10.30	20.3	17.9
A	27.9.76	-	20.9	18.7
B	5.10.76	13.45	4.3	0
B	6.10.76	14.10	3.1	10.8
B	7.10.76	10.00	6.2	21.3
B	8.10.76	10.15	13.6	24.1
B	18.10.76	-	16.6	25.2

Table 6.4

Surface slopes of settlement profiles

Section	Slope between road studs				
	2-0	0-2	2-4	4-6	6-8
A	1:125	1:220	1:250	1:1000	1:1000
B	1:90	1:145	1:200	1:1000	1:1000

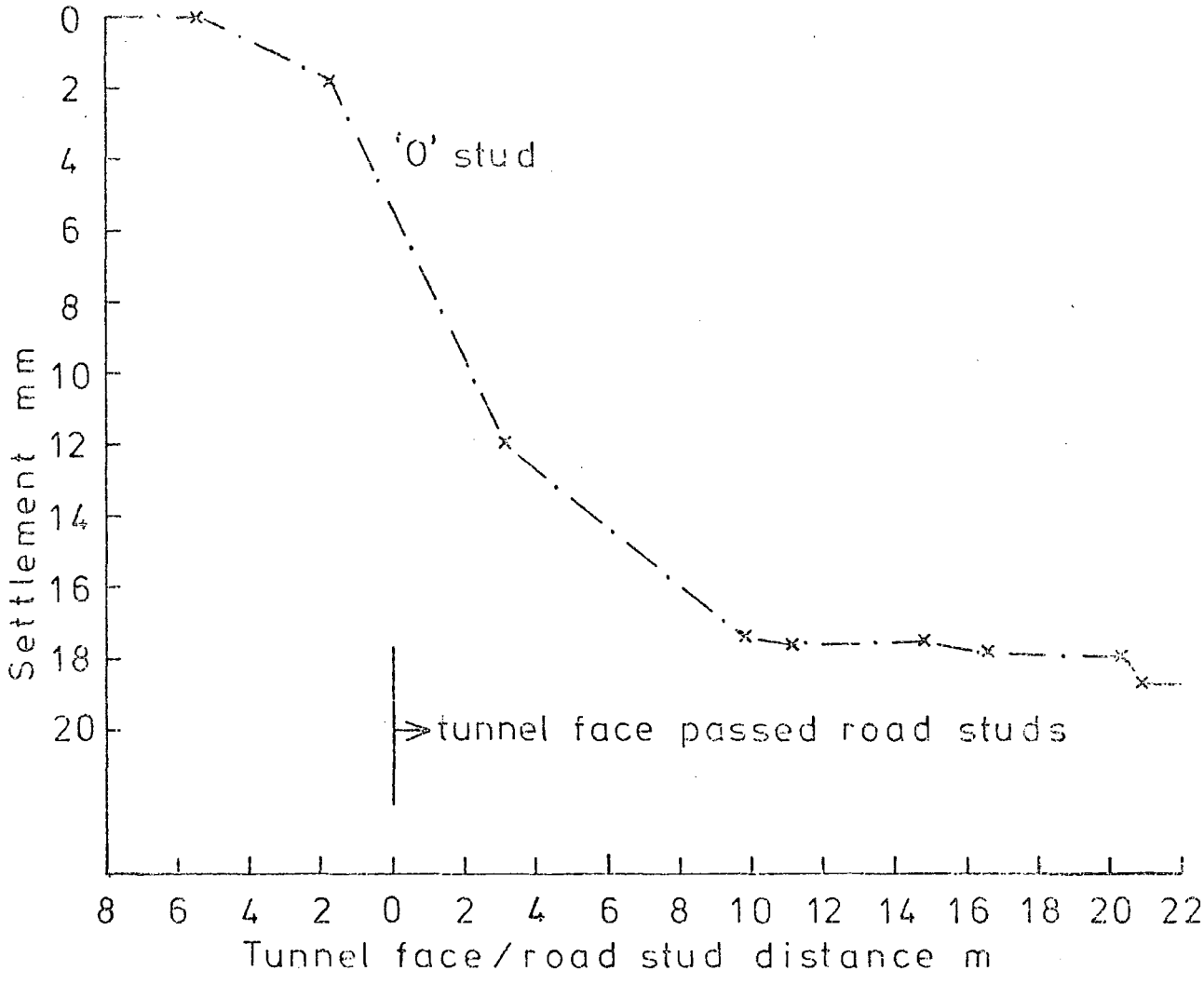

a) Settlement development profile

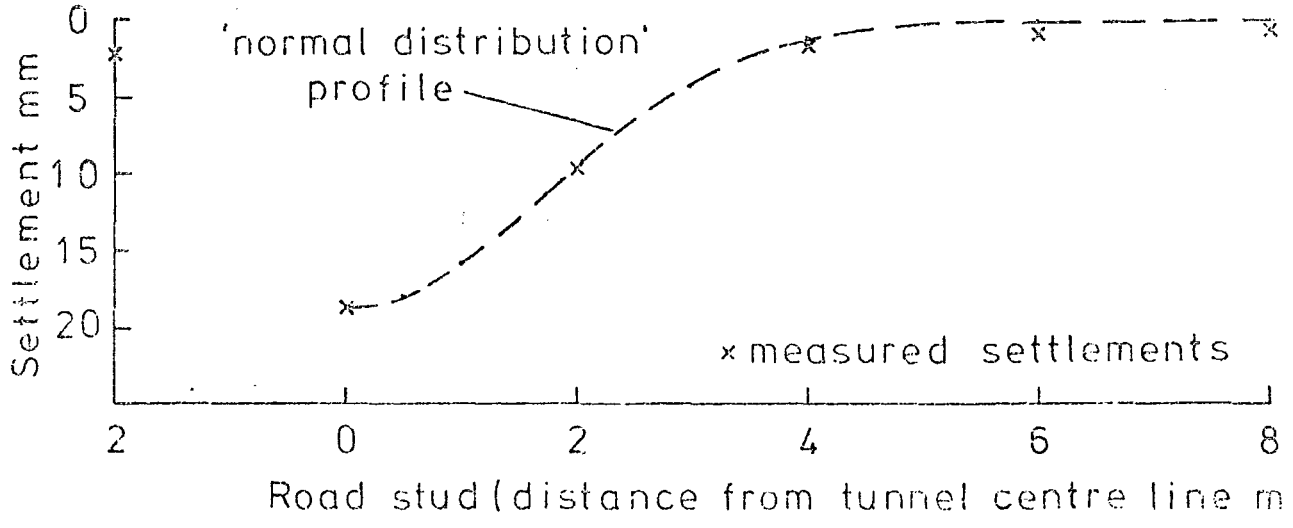

b) Transverse settlement profile

Fig. 6.2. SURFACE SETTLEMENT AT SECTION A

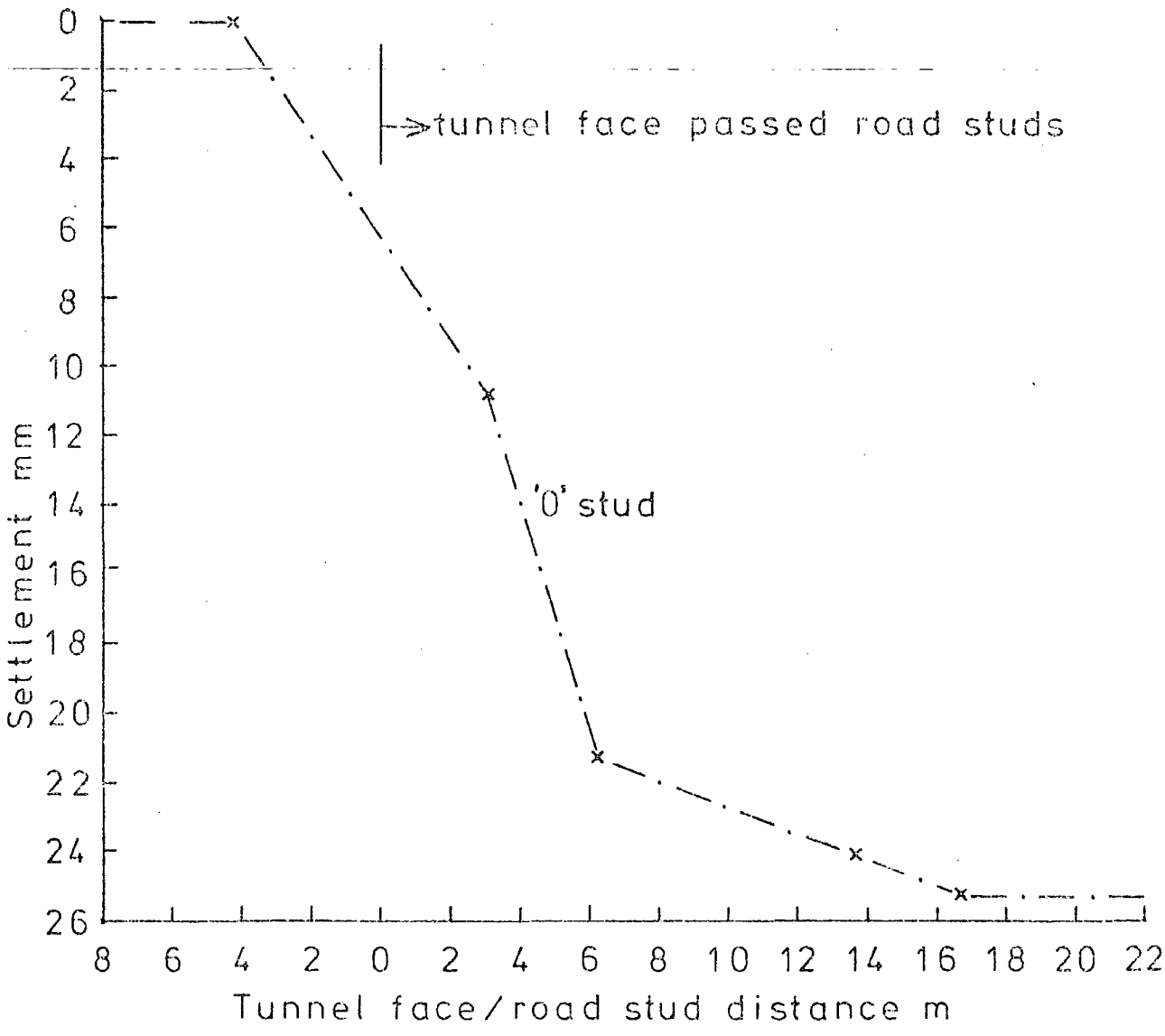

a) Settlement development profile

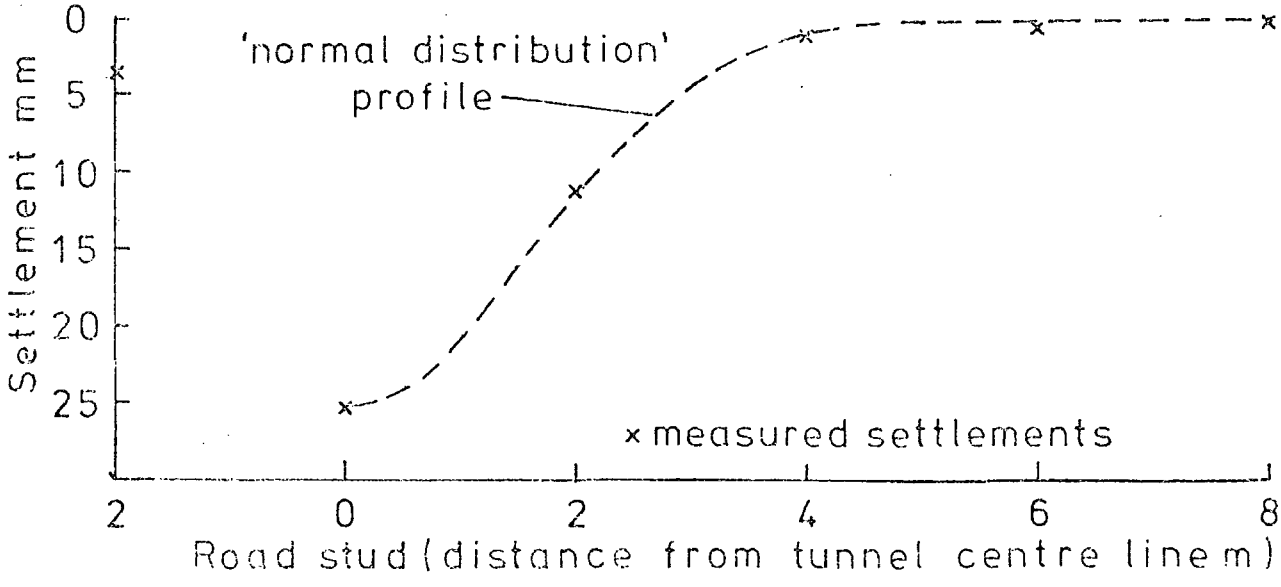

b) Transverse settlement profile

Fig. 6.3 SURFACE SETTLEMENT AT SECTION B

and at section B, 34 mm. It is common in ground of this type for the material close to the tunnel crown to settle rather more than that toward the surface. This dilation is due in part to the broadening of the settlement trough in the upper regions of the cover.

The absence of this dilation may be partially due to some re-compaction of the soil. However, the movements above the crown were complex and no firm conclusions regarding compaction, should or need, be drawn from data obtained in this area.

The inclinometer results from boreholes A2 and B2 showed that the ground in the vicinity of the tunnel below shoulder level moved away from the approaching tunnel face. Bearing in mind the stresses imposed by the bentonite this ground movement is also consistent with a compaction process.

6.3.4 Structural damage due to settlement

The lower parts of Figures 6.2 and 6.3 also show 'best fit' theoretical subsidence profiles based on the assumption that such profiles can be approximated by a normal distribution curve (Peck 1969). The settlement S developing at a lateral distance y from the centre line of the tunnel is defined by $S = \hat{S}\, e^{-y^2/2i^2}$ where $\hat{S}$ is the subsidence above the tunnel crown and i is the lateral distance to the point of inflexion of the normal distribution curve. It follows that the slope of the ground is given by:

$$\frac{dS}{dy} = -\frac{\hat{S}y}{i^2}\, e^{-y^2/2i^2}$$

and the rate of change of slope is:

$$\frac{d^2S}{dy^2} = \frac{\hat{S}\, e^{-y^2/2i^2}}{i^2}\left(\frac{y^2}{i^2} - 1\right)$$

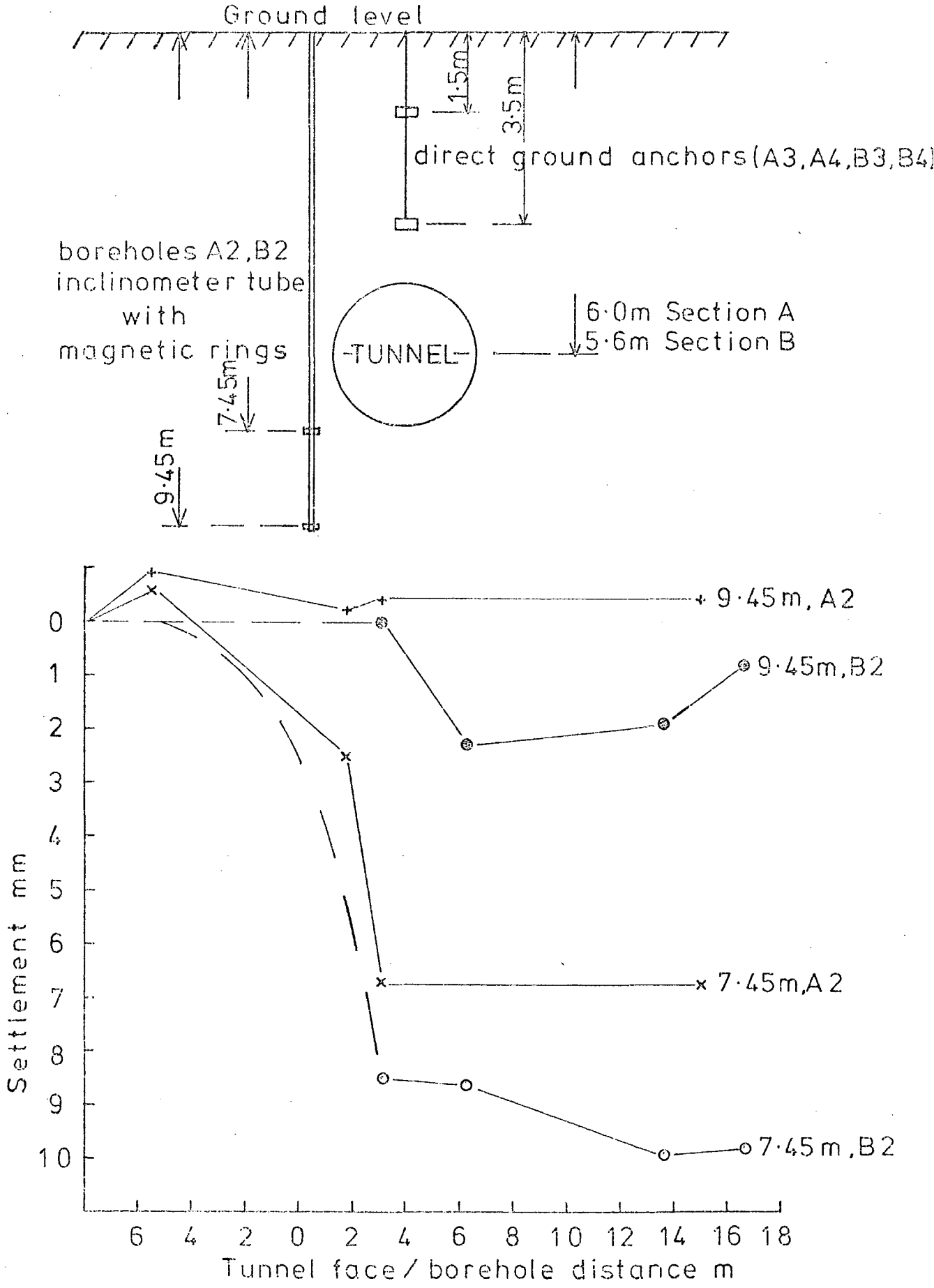

Fig. 6.4 SUB-SURFACE SETTLEMENT

At the point of inflexion (where y = i) this expression is equal to zero. This is the point of maximum slope. However, it may be expected that damage will be greatest where the rate of change of slope is a maximum, that is where $\frac{d^3S}{dy^3} = 0$

$$\frac{d^3S}{dy^3} = \frac{\hat{S}\, e^{-y^2/2i^2}}{i^4} \left(3y - \frac{y^3}{i^2}\right)$$

this expression equals zero when $3y = \frac{y^3}{i^2}$ that is, when $y = \sqrt{3}\, i$. The value of i was found by iteration to be 1.75 m for the semi-profile at section A and 1.6 m at section B.

The shapes of the theoretical curves show good agreement with the measured settlements confirming the validity of the theory in this case.

The distance from the tunnel centre line to the points of maximum rates of change of slope ($\sqrt{3}\, i$) were 3.03 m at section A and 2.77 m at section B. At section A only very minor damage to property occurred due to settlement. This principally took the form of cracked garden walls and paths. However, at section B the first structural damage to a house occurred at No. 40A Ellesmere Road (see Figure 2.6). Plate 6.2 is taken from a position some 3 m south of the tunnel looking west. Note the cracked pavement and bay window and the tilt of the gatepost away from the gate. It is understood that the damage visible inside the house was considerable. The contractor erected the temporary supports shown to prevent any further movement of the bay window. It is of particular interest to note that the cracks in the footpath and the front footings for the bay windows lay within ½ m of the calculated point of maximum rate of change of slope. Although it is not possible to accurately

PLATE 6.2 STRUCTURAL DAMAGE AT SECTION B

predict the settlement profile at the tunnel planning stage, the siting of this tunnel seems particularly unfortunate.

6.4 Disturbances due to ground treatment

As a result of the problems which arose between chainages 725 m and 740 m (see section 2.4.2 and 6.3.4) the tunnel drive was temporarily halted. It was decided to treat the 'loose' ground ahead of the machine for about 150 metres with cementitious and chemical grouts to reduce the possibility of settlement and further damage to property. These works are generally beyond the scope of this thesis but it is relevant to quote the ground settlements caused by the drilling of the 4-inch diameter holes necessary for the injection of the grouts. Groups of five holes up to 9 metres deep, were drilled beneath the pavement at 4 foot centres along the tunnel line. The 75hp air flushed drill rig (see Plate 6.3) advanced a steel casing with the drill bit. Unfortunately, measurements of ground vibration caused by the drilling were not obtained as the drill rig had left site before it was made known to the author that this process was causing substantial settlements. However, it was the opinion of the site engineer that any ground vibration caused by the drill rig was considerably less than that associated with the tunnelling machine.

At various stages during the treatment process the contractor measured the settlement at each end of the garden parting wall between each house.

Table 6.5 gives the settlements measured after the holes had been drilled but before the injection of grout. The majority of these substantial settlements must have been caused by compaction of the soil as excessive take of material could and did not occur.

PLATE 6.3 THE DRILL RIG

On grouting the ground heaved, rising in many places by over 25 mm. Plate 6.4 shows the footpath above the tunnel during grout injection. The grout tubes are visible in the path and along the kerb line.

The four houses (Numbers 29-32) shown in the left foreground of Plate 6.4 are shown again in Plate 6.5 with the scaffold shoring erected to prevent further structural damage. The ground settlement and subsequent heave had caused some damage to the front wall of the terrace at its junctions with the party walls. Plates 6.3, 6.4 and 6.5 clearly illustrate the severe nuisance caused to householders and road users due to the ground treatment operation.

Plate 6.4 Nos 29-32 ELLESMERE Rd DURING GROUND TREATMENT

Plate 6.5 Nos 29-32 ELLESMERE Rd AFTER GROUND TREATMENT

Table 6.5

Settlements due to drilling grout holes

Location Parting wall between houses No /No	Settlement mm	
	Adjacent to house	Adjacent to footpath
34/35	1	1
33/34	3	6
33/Brackley St	4	7
Brackley St/32	5	-
32/31	8	9
30/31	21	32
29/30	10	14
28/29	9	23
27/28	13	20
26/27	3	13
25/26	2	18
25/Roman Road	3	4
Roman Road/24	8	12
23/24	17	14
22/23	8	11
21/22	8	3
20/21	1	1
19/20	1	3
18/19	3	4
17/18	7	10
16/17	9	4
Egerton St/16	2	2

CHAPTER 7

CONCLUSIONS AND RECOMMENDATIONS

7.1 Introduction

This thesis has described the construction of the AGTOS tunnel and, in particular, has discussed the factors affecting vibration induced ground settlement. The experimental results have been analysed and commented upon in the text and the objective of this Chapter is to summarise and correlate the most important aspects of the research and to provide concise conclusions and recommendations.

7.2 Vibration induced ground settlement

The tunnel excavation process resulted in maximum ground vibrations (expressed in terms of resultant peak particle velocity) of 3.90 mm/s and 3.60 mm/s at boreholes A7 and B7 respectively. Close to the tunnel face the majority of the vibrational energy lay in the bandwidth 50 Hz - 350 Hz. The vibration was characterised by random heavy 'impacts' separated by periods of low amplitude vibration. The large amplitude motions showed no preferred direction of particle motion and were due to a combination of:

a) the impacts between the cutting discs and the granite and dolerite boulders;

b) The impacts between boulders in the face; and possibly,

c) the impacts between the cutting discs and the weak sandstone occasionally present in the tunnel invert.

It was the interaction between the cutting head and the ground which was the major source of ground vibration, and other sources of periodic type (generated, for example,by the main motors) were small by comparison. It follows that the spectra produced were of a non-stationary nature with a complex and varied frequency and amplitude content. These body wave ground vibrations were quickly attenuated with spatial progress and were reduced to less than 1 mm/s (resultant peak particle velocity) when the tunnel face was more than 5 metres distant from the recording point.

Because of the complex nature of the site geology and geometry, and the deployment of body wave energy into surface waves, no directly useful conclusions are drawn regarding the attenuation of the vibration energy over distances in excess of 20 metres. However, the results given in Chapter 5 do indicate that high frequencies are attenuated more than low frequencies and may be used empirically to predict maximum peak particle velocities at distances up to 20 m from the tunnel face.

Structural damage to a house occurred due to ground settlement at section B, and evidence of minor damage (cracking of garden walls, paths and road surface) was present at section A. The surface settlement was 18 mm and 25 mm at sections A and B respectively. Also, sub-surface ground settlements of between 7 and 10 mm occurred at tunnel invert level some 2 m from the tunnel centre line.

It is an important feature of the bentonite tunnelling process that an absolute minimum of excess take of material occurs. The pressure in the plenum chamber was capable of supporting the cover and the immediate grouting of the lining to the rear of the shield should have ensured complete ground support. It was thought that compaction of the ground, caused by vibration from the excavation process, in the vicinity of the

tunnel face was the most likely cause of these ground settlements.

This hypothesis was further supported by results from drilling and laboratory settlement tests described in Chapter 6. The drilling of holes for ground treatment prior to tunnelling caused settlements similar to those which resulted from the tunnelling in untreated ground. The majority of these drilling induced settlements must have been caused by compaction of the soil as excessive take of material did not occur. This confirms that the ground has considerable potential for settlement as indicated by the measurement of relative compaction and Standard Penetration Tests. The laboratory vibration tests on samples of the Warrington sand (at similar dry density and moisture content to that *in situ*) showed that settlement could occur at vibration levels of less than the peak values measured in the field.

This work has shown that only the ground close to the tunnel face was subjected to vibration levels likely to produce compaction, and it is therefore difficult to assess the relative contributions of compaction and excess material take to the total ground settlement. However, bearing in mind the nature of the bentonite process we may infer that the vibration from the tunnelling process caused ground compaction which contributed substantially to the settlement produced and the ensuring damage to the overlying structures. It is recommended that:

a) When tunnelling in non-cohesive ground, compaction (that is, densification through vibration) must be considered as an important potential source of ground settlement.

b) Some reliable measure of the initial density of the ground in the vicinity of any proposed tunnel should be obtained during

the site investigation in order to assess the degree of possible settlement. The 'relative compaction' of the material *in situ* seems to be the best measure of settlement potential. However, Standard Penetration Tests may be a more practical means of assessment in the field (Figure 3.4 may be of use in this context).

c) Broader and more rigorously controlled laboratory investigations should be carried out to determine the effect of vibrations, similar in magnitude and frequency to those produced by excavation processes, on the densification and settlement of sands.

7.3 The direct effect of vibrations

7.3.1 Damage to structures

Measurements of vibration in the cellar of a house when the tunnel face was only some 4 m away revealed a maximum resultant peak particle velocity of 0.5 mm/s. The results from the borehole measurements indicate that the peak particle velocity of the ground at foundation level for houses 5 m or more from the tunnel was not likely to exceed 1 mm/s. These levels are well below the established thresholds cited in Section 3.4, for either architectural or structural damage. It would, therefore, seem to be extremely unlikely that the tunnelling process caused any damage to the property in this area by dynamic stressing of the structures.

7.3.2 Nuisance to residents

The vibration from the tunnelling machine caused low level noise and minor vibrations within the houses situated close to the tunnel. The

noise was less than that caused by some passing road traffic, but was of an unusual nature and was often present for periods throughout the night. The sound appeared to result from resonances of floors and ceilings, and was similar to that of distant thunder. The nuisance was at its worst when the tunnel face was at its closest and gave rise to little complaint when more than 20 m from the houses. The reaction of the householders to the same stimulus was extremely varied, some complaining bitterly whilst others found no cause to visit the site offices and object.

Most of the noise complaints that were received were related to the disturbance at night. Owing to the reduced level of ambient noise and the fact that they were trying to sleep, the noise seemed to the residents to be more severe. This reaction from the local population is fairly typical and similar to that found by other workers (see Chapter 1).

The unusual noise from the tunnel construction worried and caused actual nuisance to residents even though its level was lower than that associated with familiar ambient sources. A tactful and good humoured approach by the man dealing with the residents (in this case the Resident Engineer or Clerk of Works) was of vital importance. A surly or officious attitude would clearly have provoked the residents to further action which may have materially hindered the progress of the works.

It is recommended that considerable effort is made to achieve good public relations and that the nuisance to residents is minimised by achieving unimpeded tunnel advance to reduce the overall period of the disturbances.

LIST OF REFERENCES

ANON. 1974 Suppression of noise and vibration on L.T. underground link with Heathrow airport. Rail Engineering International. 4, No. 6, 285-287.

ATTEWELL, P B and FARMER, I W. 1976 Principles of engineering geology. Chapman and Hall Ltd, London.

ATTEWELL, P B and RAMANA, Y V. 1966 Wave attenuation and internal friction as functions of frequency in rocks. Geophysics, 31, No. 6, 1049-1056 .

BARKAN, D D. 1962 Dynamics of bases and foundations. McGraw-Hill, New York.

BARRATT, D A. 1976 Further notes on subsidence levelling at Warrington. Tunnels Division Working Paper No. 3. Transport and Road Research Laboratory, Crowthorne.

BARRATT, D A 1977 (To be published).

BARTLETT, J V, BIGGART, A R and TRIGGS, R L. 1973. The bentonite tunnelling machine. Proc. Inst. Civ. Eng. 54. Pt 1, Nov, 605-624.

BARTLETT, J V and KING, J R J. 1975 Soft ground tunnelling. Proc. Inst. Civ. Eng. 58.Pt 1, Nov, 615-628.

BASORE, C E and BOITANO, J D. 1969 Sand densification by piles and vibroflotation. Journal of the Soil Mechanics and Foundations Division. ASCE, 95, Nov, 1303-1323.

BEAN, R and PAGE J. 1976 Traffic induced ground vibration in the vicinity of road tunnels. Department of the Environment. TRRL Report SR 218UC. Crowthorne (Transport and Road Research Laboratory).

BENDER, E K. 1972 Noise from construction, home appliances and building equipment. Journal of Environmental Science. Sept - Oct. 9-18.

BIOT, M A. 1956 Theory of propagation of elastic waves in a fluid saturated porous solid. J. Acous. Soc. Amer. 28, 168-191.

BODEN, J B and McCAUL, C M. 1974 Measurements of ground movements during a bentonite tunnelling experiment, Department of the Environment, TRRL Report LR 653. Crowthorne (Transport and Road Research Laboratory).

BOYES, R G H. 1972 Uses of bentonite in civil engineering, Proc. Inst. Civ. Eng. 52 Part 1, May, 25-32.

BRADLEY, J J and FORT Jr, A N. 1966 Internal friction in rocks. Handbook of physical constants. Editor S P Clark Jr. The Geological Society of America, New York.

BRUMUND, W F and LEONARDS, G A. 1972 Subsidence of sand due to surface vibration. Journal of the Soil Mechanics and Foundations Division. ASCE, 98, Jan, 27-42.

BRE/TRRL. Committee on Tunnelling. 1974 Future tunnelling in Britain. Building Research Establishment Current Paper 39/74

BULLEN, K E. 1963 Introduction to the theory of seismology. 3rd ed. Cambridge University Press.

D'APPOLONIA, E. 1970 Dynamic loadings. Journal of the Soil Mechanics and Foundations Division, ASCE, 96, Jan, 49-72.

DIECKMAN, D. 1958 A study of the influence of vibrations on man. Ergonomics, 1, 4, 347-355.

DONOVAN, H J. 1968 Modern Tunnelling methods. Pub. Wks. Mun. Serv. Congr. 472-507.

DUFFY, J and MINDLIN, R D. 1957 Stress-strain relations and vibrations of a granular medium. Jour. Appl. Mech. 24, 585.

DUVALL, W I and FOGELSON, D E. 1962 Review of criteria for estimating damage to residences from blasting vibrations. US, Bur. Min. Rep. Invest. 5968. 1962.19.

FORSSBLAD, L. 1965 Investigations of soil compaction by vibration, Civil engineering and building construction series No 34. Acta Polytechnica Scandinavica Publishing Office, Stockholm, Sweden.

FOUNTAIN, L S and OWEN T E. 1967 Investigation of seismic parameters related to shallow tunnel detection. Report AD 820-238. July. Defense Documentation Centre, Virginia, USA.

GASSMAN, F. 1951 Elastic waves through a packing of spheres. Geophysics, 16, 673-685.

GIBBS, H J and HOLTZ, W G. 1957 Research on determining the density of sand by spoon penetration testing. Proc. 4th International Conference on Soil Mechanics and Foundation Engineering. 1, 35-39.

GUIGNARD, J C and GUIGNARD, E. 1970 Human response to vibration - a critical survey of published work. Univ. Southampton, Inst. Sound and Vibn. Res. Memo 373.

HANDSLEY, S. 1975 Low amplitude ground vibration from road traffic, M.Sc. Dissertation, Advanced Course in Engineering Geology. University of Durham.

HARDIN, B O and RICHART, F E. 1963 Elastic wave velocities in granular soils. Journal of the Soil Mechanics and Foundations Division. ASCE. 89, Feb, 33-65.

HOLMES, A. 1965 Principles of physical geology. Ch.25. Thomas Nelson and Sons Ltd. London.

JACKSON, M W. 1967 Thresholds of damage due to ground motion. Proc. Internat. Symp. Wave Prop. Dyn. Props. Earth. Mats, New Mexico, 961-969.

JACOB, E. 1976 The bentonite shield: Technology and initial application in Germany. Proc. Symp. Tunnelling 76. Institution of Mining and Metallurgy, London.

JAEGER, J C and COOK, N G W. 1976 Fundamentals of Rock Mechanics. 2nd Edition. Chapman and Hall. London.

JONES, R, LISTER N W and THROWER, E N. 1966 The dynamic behaviour of soils and foundations. Proc. Symp. Vibration in Civil Engineering. British national section of the International Association for Earthquake Engineering. Butterworths, London.

JUMIKIS, A R. 1967 Introduction to soil mechanics. D Van Nostrand Co. Inc, New Jersey, USA.

KOCH, H W. 1953 Determining the effects of vibrations in buildings. VDI-Z. 95 (21), 744-747. (Building Research Station translation LC 597).

KOLSKY, H. 1963 Stress waves in solids. Dover Publications Inc. New York, USA.

KOLBUSZEWSKI, J. 1965 Sand particles and their density. Symp. on the densification of particulate materials. The Materials Science Club. London.

LACROIX, Y and HORN, H M. 1973 Direct determination and indirect evaluation of relative density and its use on earthwork construction projects. ASTM. STP523, 251-280.

LAMBE, T W and WHITMAN, R V. 1969 Soil mechanics. Wiley, New York, USA.

LEE, K L and ALBAISA, A. 1974 Earthquake induced settlements in saturated sands. Journal of the Geotechnical Engineering Division, ASCE. 100, April, 387-406.

LEE, K L and SINGH, A. 1971 Relative density and relative compaction. Journal of the Soil Mechanics and Foundations Division. ASCE. 97, 1049-1052.

LEECH, SIR BOSDIN. 1895 The History of the Manchester Ship Canal.

LORENZ, H. 1938 Dagebo. Deutsche Gesellschaft fur Bodenmechanik. 4, Springer, Berlin.

LUNA, W A. 1967 Ground vibration due to piling. Foundation facts, 111(2), Raymond Pile Co.

MILLER, G F and PURDSEY, H. 1954 The field and radiation impedance of mechanical radiators on the free surface of a semi-infinite isotropic solid. Proc. Roy. Soc. London. A223, 521-541.

NAGARKATTI, A S. 1977 Density measurements at Warrington. Tunnels Division Working Paper No. 15 - Transport and Road Research Laboratory, Crowthorne.

PAKES, G. 1976 Edinburgh sewage disposal scheme; Tunnelling works. Proc. Symp. Tunnelling 76. Institution of Mining and Metallurgy, London.

PECK, R B. 1969 Deep excavations and tunnelling in soft ground. Proc. 7th International Conference on Soil Mechanics and Foundation Engineering. State of the art report. 225-290, Mexico.

POULOS, S J and HED, A. 1973 Density measurements in a hydraulic fill, ASTM. STP 523, 403-424.

PYKE, R, SEED, H B and CHAN, C K. 1975 Settlement of sands under multidirectional shaking. Journal of the Geotechnical Engineering Division, ASCE, 101, 379-398.

REIHER, H and MEISTER, F J. 1931 Human sensitivity to vibrations. Forsch. auf dem Geb, des Ingen, 2, 11, 381-386.

ROAD RESEARCH LABORATORY. 1952 Soil mechanics for road engineers. Dept. of Scientific and Industrial Research. HMSO. London.

ROBERTS, A. 1969 Vibrations produced by engineering processes. Construction Industry Research and Information Association (CIRIA) Technical note, No. 6, London.

SCHEIDIG, A. 1931 Tests on the deformation of sand and their application to the settlement analysis of buildings. M.S. Thesis. Vienna. Cited by Terzaghi and Peck (1967)

SEED, H B and LUNDGREN, R. 1954 Investigation of the effect of transient loadings on the strength and deformation characteristics of saturated sands. Proc ASTM 54, 1288-1306.

SELIG, E T and LADD, R S (editors). 1973 Evaluation of relative density and its rôle in geotechnical projects involving cohesionless soils. ASTM. Special technical publication 523.

SILVER, M L and SEED, H B. 1971 Deformation characteristics of sands under cyclic loading. Journal of the Soil Mechanics and Foundations Division. ASCE, 97,1081-1098.

SIOR, G. 1961 The damaging effects of vibration due to pile driving operations. Bauterchnik 38(6), 181-185 (Building Research Station translation LC 1283)

SNODGRASS, J J, and SISKIND, D E. 1974 Vibrations from underground blasting. RI 7937 US Bureau of Mines. Washington. USA.

SOLIMAN, J T. 1968 A scale for the degrees of vibration perceptibility and annoyance. Ergonomics, 2, 101-122

STEFFENS, R J 1974 Structural vibration and damage. Building Research Establishment Report. HMSO. London.

SZECKY, K. 1966 The art of tunnelling. Akademial Kiado, Budapest (revised edition 1973)

TAYLOR, A G. 1975 Quarry blast acoustic wave (concussion) response of structures and human annoyance. Paper presented at 89th meeting Acoustical Society of America. April.

TAVENAS, F A, LADD, R S and La ROCHELLE, P. 1973 Accuracy of relative density measurements: Results of a comparative test program. ASTM. STP 523, 18-60.

TERZAGHI, K and PECK, R B. 1967 Soil mechanics in engineering practice John Wiley and Sons Inc. New York.

TIMOSHENKO, S P, YOUNG, D H and WEAVER Jr, W. 1974 Vibration problems in engineering (4th Ed). John Wiley and Sons, New York.

VOLTERRA, E and ZACHMANOGLOU, E C. 1974 Dynamics of Vibrations. Charles E. Merrill Books Inc. Ohio. USA.

WHIFFIN, A C and LEONARD, D R 1971 A survey of traffic induced vibrations. Department of the Environment, RRL Report LR418, Crowthorne.

WHITE, J E and SENGBUSH, R L. 1953 Geophysics 18, 54.

WHITMAN, R V. 1970 Response of soils to dynamic loading, Report AD-708-625, May, Defence Documentation Centre, Virginia, USA.

WINTER, T G. 1972 A survey of sound propagation in soils. Acoustical holography. 5. Plenum Publishing Corporation, New York, USA.

WISS, J F. 1967 Damaging effects of pile driving vibrations. Highway Res. Record 155, 14-20.

WRAY, D A. 1948 The Pennines and adjacent areas. British Regional Geology Series. HMSO, London.

APPENDIX A

BENTONITE

Bentonite is a clay mineral comprising principally montmorillonite with small amounts of other minerals. It is formed by the alteration *in situ* of volcanic ash or scoria and usually occurs in seams and beds from a few inches to a few feet thick in clays. It has a soapy feel, is highly plastic and is smooth and free from grit. The best known deposits are found at Fort Benton, Wyoming, USA.

Bentonite is chemically described as hydrous aluminium silicate ($Al_2\ O_3\ 5\ Si\ O_2\ 5\text{-}7\ H_2o$). The crystals structure is formed of mica-like layers, built up from sheets of silica and gibbsite as shown below:

Silica
Gibbsite
Silica
nH_2o
Silica
Gibbsite
Silica

The adsorbed ions are principally sodium and give a very great swelling capacity. Water may be taken in between the layers until they are completely dissociated forming a thixotropic gel.

In South East England, important beds occur in the Lower Greensand which are minerals rich in montmorillonite and are known as Fullers Earth.

The adsorbed ions are, however, mostly calcium and the material is described as sub-bentonite. The calcium may be exchanged for sodium to give bentonite.

Bentonite has a liquid limit of about 400 per cent and forms a stable suspension in water at very low solids concentrations. This suspension acts as a Bingham plastic and as such requires a definite shear stress to be applied before the fluid will flow.

Bentonite is dried and ground to a fine powder for commercial supply as pellets, powder or a suspension. Various manufacturing processes are employed to produce a range of grades for different purposes.

In civil engineering, bentonite has been used since the late 1920s when it was used as a drilling fluid. It is used principally for soil stabilisation and as a lubricant (e.g. for sinking caissons). However, it has a number of other important uses. A review of the 'Uses of Bentonite in Civil Engineering' has been published by Boyes (1972).

APPENDIX B

HARMONIC PARTICLE MOTION

Consider the motion of a particle (of weight W, mass m) due to a strain wave passing through an elastic solid. Let the restoring force on the particle be proportional to its displacement and the dissipation of energy be proportional to its velocity. These are the fundamental assumptions of linear elasticity and viscous damping. This approach is the one used most commonly to model internal friction in solids. The terms viscous used in this context does not imply that viscous processes are necessarily causing attenuation but that the result is similar.

The forces acting upon the particle are:-

W, the particle weight and

$-(W+ky)$, the elastic restoring force,

where k is an elastic constant and y is the particle's displacement from the position of equilibrium.

$-(c\dot{y})$ is the viscous force

where c is a coefficient of viscous damping and $\dot{y} = \frac{dy}{dt}$, the particle velocity.

If P is an impressed force,

then force on particle $= W - (W+ky) - c\dot{y} + P$

This model is analogous to that used to describe mechanical vibrations of a spring-dashpot-mass system as shown in the diagram below.

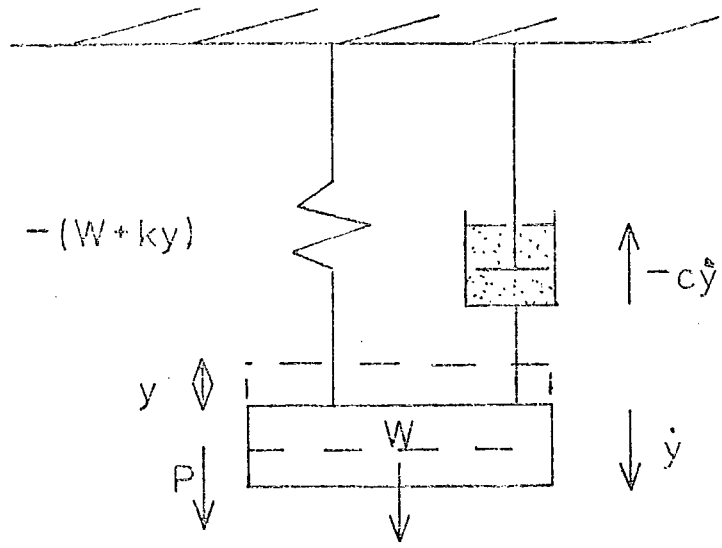

From Newtons 2nd law this applied force will accelerate the mass $m\left(\frac{w}{g}\right)$

$$\therefore \quad m\ddot{y} = -ky - c\dot{y} + P \qquad \ldots\ldots\ldots (1)$$

where $\ddot{y} = \frac{d^2y}{dt^2}$, the particle acceleration.

$$\therefore \quad P = m\ddot{y} + c\dot{y} + ky \qquad \ldots\ldots\ldots (2)$$

Considering only free vibrations (P = 0)

$$m\ddot{y} + c\dot{y} + ky = 0 \qquad \ldots\ldots\ldots (3)$$

to simplify let $p^2 = \frac{k}{m}$ and $2n = \frac{c}{m}$

$$\therefore \quad \ddot{y} + 2n\dot{y} + p^2y = 0 \qquad \ldots\ldots\ldots (4)$$

This is a second order linear differential equation with constant coefficients and may be solved in the usual manner

Assume a solution where,

$$y = B\, e^{rt} \qquad \ldots\ldots\ldots (5)$$

and where r is a constant that allows equation (5) to satisfy equation (4)

Putting (5) into (4) we obtain

$$Br^2e^{rt} + 2n\beta re^{rt} + p^2\beta e^{rt} = 0$$

$$\therefore \quad r^2 + 2nr + p^2 = 0 \qquad \ldots\ldots\ldots (6)$$

By quadratic solution

$$r = \left[-2n \pm (4n^2 - 4p^2)^{\frac{1}{2}}\right] \Big/ 2$$

$$= n \pm (n^2 - p^2)^{\frac{1}{2}} \qquad \ldots\ldots\ldots (7)$$

Equation (7) allows three types of solution which define the character of the damping

a) where $n^2 < p^2$ periodic motion

b) where $n^2 = p^2$ critical damping

which represents the level of damping where the motion first loses its vibratory character.

and c) where $n^2 > p^2$ overdamped

In this latter case the viscous resistance is so large that when the particle is displaced from its equalibrium position it does not vibrate but only creeps gradually back to that position. The aperiodic motions b and c are not relevant to this work and we shall consider only a).

Now, as $n^2 < p^2$, the quantity $p_d = p^2 - n^2$ is positive and we obtain two complex roots for r

$$r_1 = -n + i\,p_d \quad \text{and} \quad r_2 = -n - i\,p_d$$

substituting these roots into equation (5) we obtain

$$y' = B\,e^{(-n+ip_d)t} \quad \text{and} \quad y'' = B\,e^{(-n-ip_d)t}$$

The sum or the difference of these two solutions multiplied by any constant will also be a solution of equation (4)

Therefore, $y' + y'' = y = \frac{1}{2}B_1\ e^{-nt}\left(e^{ip_dt} + e^{-ip_dt}\right)$ after simplification

$$\therefore \quad y_1 = B_1\,e^{-nt}\cos p_d t \qquad \ldots\ldots\ldots (8)$$

and similarly

$$y' - y'' = y_2 = \frac{1}{2i}\ B_2\,e^{-nt}\left(e^{ip_dt} - e^{-ip_dt}\right)$$

$$\text{Therefore } y_2 = B_2\,e^{-nt}\sin p_d t \qquad \ldots\ldots\ldots (9)$$

By adding these two solutions we obtain the general solution of equation (4)

$$y = e^{-nt}\left(B_1\cos p_d t + B_2\sin p_d t\right) \qquad \ldots\ldots\ldots (10)$$

B_1 and B_2 must be determined from the initial conditions (of particle displacement and velocity) and the factor e^{-nt} decreases with time, damping

y as a negative exponential. To determine B_1 and B_2 assume that at the initial instant (time t_o) the particle is displaced from its equilibrium position by a distance y_o and has a velocity $\dot{y}_o$

Substituting t = 0 into equation (10)

$$y_o = B_1 \qquad \ldots\ldots\ldots (11)$$

Therefore, $y = e^{-nt}\left(y_o \cos p_d t + B_2 \sin p_d t\right)$

and $\dot{y} = \frac{dy}{dt} = -y_o e^{-nt} p_d \sin p_d t - y_o n e^{-nt} \cos p_d t$

$$+ B_2 e^{-nt} p_d \cos p_d t - B_2 n e^{-nt} \sin p_d t \qquad \ldots\ldots\ldots (12)$$

Substituting t = 0 into equation (12)

$$\dot{y}_o = -y_o n + B_2 p_d$$

Therefore $B_2 = \left(\dot{y}_o + y_o n\right) \Big/ p_d \qquad \ldots\ldots\ldots (13)$

Substituting for B_1 and B_2 in equation (10) we obtain

$$y = e^{-nt}\left(y_o \cos p_d t + \frac{\dot{y}_o + n y_o}{p_d} \sin p_d t\right) \qquad \ldots\ldots\ldots (14)$$

Note that the first term depends only on the initial displacement y_o whilst the second term depends both on the initial displacement and velocity $\dot{y}_o$

The oscillations may be considered as a cosine wave of amplitude y_o with another wave of amplitude $(\dot{y}_o + n\, y_o)/p_d$ (with a 90^o phase lag) superimposed.

To determine the resultant amplitude A and the phase angle ϕ_d consider the vector diagram in figure B.1. Note that the rotating vector OQ lags OP by 90^o and the resultant vector OR (A) lags OP by the phase angle ϕ_d

By Pythagorus $$A = \left[y_o^2 + (\dot{y}_o + n y_o)/p_d \right]^{\frac{1}{2}} \quad \ldots\ldots\ (15)$$

also $$\phi_d = \tan^{-1} \frac{\frac{\dot{y}_o}{y_o} + n}{p_d} \quad \ldots\ldots\ (16)$$

Thus, equation (14) becomes

$$y = A\, e^{-nt} \cos (p_d t - \phi_d) \quad \ldots\ldots\ (17)$$

We have a motion with an exponentially decreasing amplitude $A\, e^{-nt}$, a phase angle ϕ_d and a period $T_d = \frac{2\pi}{p_d}$

Note that for free undamped vibrations, $n = 0$, $p_d \to p$ and $\phi_d \to \phi$ giving

$$y = A \cos (pt - \phi) \quad \ldots\ldots\ (18)$$

From equation (17), the ratio of two successive amplitude maxima y_{mi} and $y_{m(i+1)}$ is

$$\frac{y_{mi}}{y_{m(i+1)}} = A\, e^{-nt_i} \Big/ A\, e^{-n(t_i+T_d)} = e^{nT_d} = e^{\delta} \quad \ldots\ (19)$$

where δ is the logarithmic decrement

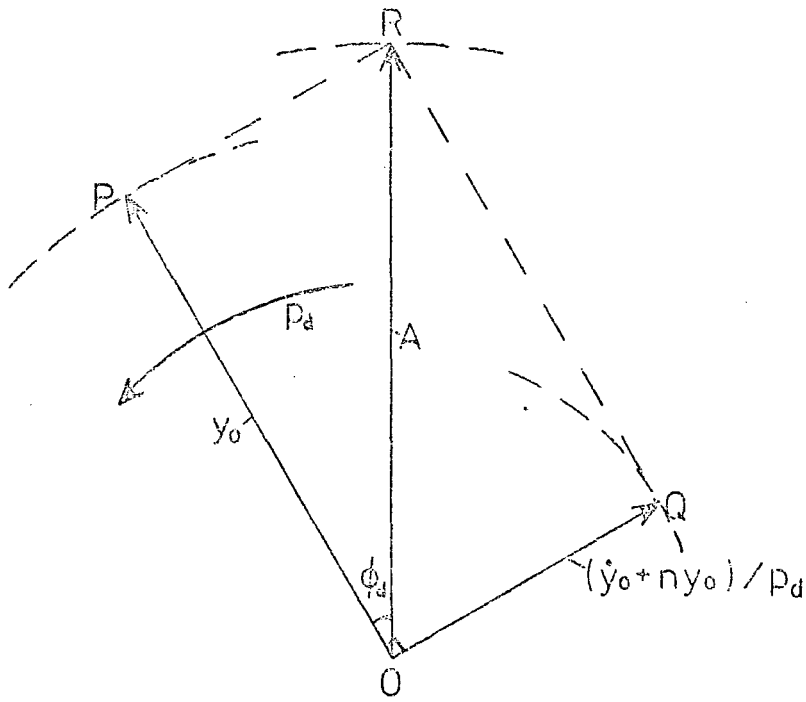

Fig. B.1 VECTOR DIAGRAM FOR HARMONIC MOTION

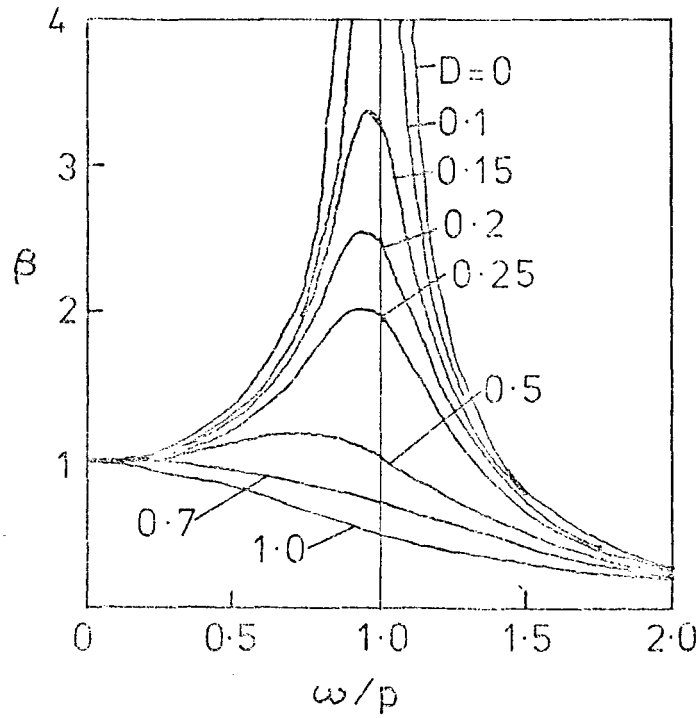

Fig. B.2. FORCED-DAMPED MOTION MAGNIFICATION FACTOR FOR VARIOUS LEVELS OF DAMPING(TIMOSHENKO)

It follows that

$$\delta = \ln\left(y_{mi}/y_{m(i+1)}\right) = nT_d = \frac{2\pi n}{p_d} \simeq \frac{2\pi n}{p} \qquad \ldots\ldots\ldots (20)$$

As the frequency $f = \frac{1}{T} = \frac{p}{2\pi}$, $\delta = \frac{n}{f}$ ..... (21)

Now the elastic energy stored in the particle is proportional to the square of the amplitude (as is the kinetic energy).
Therefore if we define the specific energy loss as $\Delta W/W$, then

$$\Delta W/W = \left(y_{mi}^2 - y_{m(i+1)}^2\right) \Big/ y_{mi}^2 \qquad \ldots\ldots\ldots (22)$$

when this is small compared to unity we have

$$\Delta W/W \simeq 2\left(y_{mi} - y_{m(i+1)}\right) \Big/ y_{mi} \simeq 2\ln\left(y_{mi}/y_{m(i+1)}\right) = 2\delta \qquad \ldots\ldots\ldots (23)$$

Forced vibrations with viscous damping

Consider equation (2) and let $P = Q \cos \omega t$ and $q = \frac{Q}{m}$

then $\ddot{y} + 2n\dot{y} + p^2 y = q \cos \omega t$ ..... (24)

The solution of this equation is now the sum of two terms, a complementary function and a particular integral. The complementary function is given by equation (10) and dies away as t increases. The particular integral corresponds to the steady state solution and is

$$y = M \cos \omega t + N \sin \omega t \qquad \ldots\ldots\ (25)$$

which, when expressed in terms of its amplitude and phase angle, becomes (as before)

$$y = A \cos (\omega t - \theta) \qquad \ldots\ldots\ (26)$$

$$\text{where } A = (M^2 + N^2)^{\frac{1}{2}} = q \Big/ \left[(p^2 - \omega^2)^2 + 4n^2\omega^2 \right]^{\frac{1}{2}} \qquad \ldots\ldots\ (27)$$

$$\text{and } \theta = \tan^{-1}\left(\frac{N}{M}\right) = \tan^{-1} 2\omega n/(p^2 - \omega^2)$$

$$= \tan^{-1} \frac{2n\omega/p^2}{1 - \omega^2/p^2} \qquad \ldots\ldots\ (28)$$

$$\text{Let the damping ratio } D = \frac{n}{p} = \frac{C}{C_{cr}} \qquad \ldots\ldots\ (29)$$

Where C_{cr} is defined as critical damping when n = p and the motion just becomes aperiodic

Subsituting equation (27) into (26)

$$y = \frac{Q}{k} \beta \cos (\omega t - \theta) \qquad \ldots\ldots\ (30)$$

where β is the magnification factor,

$$\beta = \left[(1 - \omega^2/p^2)^2 + (2D\omega/p)^2 \right]^{-\frac{1}{2}} \qquad \ldots\ldots\ (31)$$

and equation (28) becomes

$$\theta = \tan^{-1}\left(\frac{2D\omega/p}{1 - \omega^2/p^2}\right) \qquad \ldots\ldots\ (32)$$

From equation (30) the amplitude of the steady state forced vibration is obtained by multiplying the static load displacement $\frac{Q}{k}$ by β. This factor depends on D and the frequency ratio ω/p. Figure B2 shows the inter-related effects of the magnification factors and the frequency and damping ratios. Note that:-

when ω is small compared to p, β is close to unity;

when ω is large compared to p, β tends to zero regardless of damping;

when ω is close to p the amplitude is very sensitive both to β and p. Large amplitude particle motions are therefore to be expected.

Note also that the maximum value of β occurs when ω/p is slightly less than unity.

Setting $\frac{d\ \beta}{d\omega/p} = 0$ we find that the maximum occurs when $\omega/p = (1 - 2D^2)^{\frac{1}{2}}$

APPENDIX C

TRAVELLING WAVE MOTION

Consider a solid through which a strain wave is travelling. At some time, say $t = 0$ the shape of the wave can be represented by $y = f(x)$, $t = 0$ where y is the displacement at the position x.

Let this wave propagate to the right with a constant velocity C. At some time t later the wave will have travelled a distance Ct. The wave equation at this time (t) is therefore

$$y = f(x - Ct) \; ; \; t = t \qquad \ldots\ldots\ldots (34)$$

This is the same waveform about the point $x = Ct$ at time t as we had about $x = 0$ at time $t = 0$.

Equation (34) is the general equation for any wave travelling to the right. It follows that $y = f(x + Ct)$ represents a wave travelling to the left.

If we wish to determine the progress of a particular part (or *phase*) of the wave we must fix y and examine the effect of increasing t. Now if y is fixed then as t increases so must x increase such that

$x - Ct = \text{constant}$

$$\therefore \quad x = \text{constant} + Ct$$

and $$\frac{dx}{dt} = C$$

Thus the velocity C is the *phase* velocity in the x direction.

Note that for any fixed value of time equation (34) gives y as a function of distance x (from t = 0, x = 0). Also if we choose to investigate the motion of a particle at a fixed distance x then the equation gives the variation of amplitude with time.

Now consider the particular wave motion whose amplitude at time t = 0 is given by

$$y = A \sin 2\pi x/L \qquad \ldots\ldots\ldots \quad (35)$$

Note that the displacement y is the same at x as it is at x + L, x + 2L... ie L is the *wavelength*.

Let this wave travel to the right with a phase velocity C.

$$\text{Then } y = A \sin \frac{2\pi}{L}(x - Ct) \qquad \ldots\ldots\ldots \quad (36)$$

The period T is the time required for the wave to travel one wavelength so L = CT

Substituting into equation (36)

$$y = A \sin 2\pi(x/L - t/T) \qquad \ldots\ldots\ldots \quad (37)$$

This equation is often expressed in terms of the *wave number* K and angular frequency ω where

$$K = 2\pi/L \quad \text{and} \quad \omega = 2\pi/T$$

$$\therefore \quad y = A \sin (Kx - \omega t) \qquad \ldots\ldots\ldots \quad (38)$$

This analysis has assumed the displacement y to be zero at x 0, t = 0. This need not be the case and the general expression for a wave travelling to the right is

$$y = A \sin \left[(Kx - \omega t) - \phi \right] \qquad \ldots\ldots\ldots \quad (39)$$

where ϕ is the phase angle.

This equation is similar to equation (18), the additional term Kx allowing for the spatial dimensions required for a travelling wave rather than stationary simple harmonic motion.

Differentiating equation (36) with respect to time we find that the particle velocity of the wave is

$$\frac{dy}{dt} = \frac{-2\pi AC}{L} \cos \frac{2\pi}{L} (x - Ct) \qquad \ldots\ldots\ldots \quad (40)$$

The strain due to the wave (the rate of change of displacement with respect to distance) is

$$\frac{dy}{dx} = \frac{2\pi A}{L} \cos \frac{2\pi}{L} (x - Ct) \qquad \ldots\ldots\ldots \quad (41)$$

The energy propagated by a wave is part potential and part kinetic. Consider an element, dx, of a filament of unit cross-section extending in the direction of wave propagation. The kinetic energy of the element is

$$\frac{1}{2} \rho \left(\frac{dy}{dt} \right)^2 dx = \frac{2}{L} \pi^2 C^2 A^2 \rho \cos^2 \left[\frac{2\pi}{L} (x - Ct) \right] dx \qquad \ldots\ldots\ldots \quad (42)$$

Now the strain energy in the same element depends upon whether the wave is one of distortion or dilatation. The strain energy for a wave of dilatation is

$$\tfrac{1}{2}(\lambda + 2G)\left(\frac{dy}{dx}\right)^2 dx = \frac{2\pi^2}{L^2} A^2(\lambda + 2G)\cos^2\left[\frac{2\pi}{L}(x - Ct)\right] dx \quad \ldots\ldots\ldots \quad (43)$$

where $C = \left(\frac{\lambda + 2G}{\rho}\right)^{\frac{1}{2}}$ the velocity of a wave dilatation and λ and G are Lamés constants.

Therefore, $\frac{1}{2}\rho C^2\left(\frac{dy}{dx}\right)^2 dx = \frac{2\pi^2}{L^2} A^2C^2\rho\cos^2\left[\frac{2\pi}{L}(x - Ct)\right] dx \quad \ldots\ldots\ldots \quad (44)$

as $C^2 = \left(\frac{dx}{dt}\right)^2$ equation (44) becomes identical to equation (42)

The strain energy for a wave of distortion is

$$\tfrac{1}{2} G\left(\frac{dy}{dx}\right)^2 dx = \frac{2\pi^2}{L^2} G A^2 \cos^2\left[\frac{2\pi}{L}(x - Ct)\right] dx \quad \ldots\ldots\ldots \quad (45)$$

where $C = \left(\frac{G}{\rho}\right)^{\frac{1}{2}}$ the velocity of a wave of distortion
Substituting for G in equation (45) again yields an equation identical to equation (42).

These results show that for a wave of dilatation or distortion the kinetic and potential energies at any instant are equal. It follows that the energy propagated by a wave is divided equally between its kinetic and potential energies. This result is quite different from that obtained from a simple vibrating spring-mass system where the energy oscillates between pure strain energy when the mass is at rest and pure kinetic energy when the mass is at its maximum velocity.

Consider the energy flux passing through unit area perpendicular to the direction of propagation. For a single harmonic component, the energy passing through such an area in unit time is found by integrating the energy in a filament of length C.

$$E = \int_{x-C}^{x} 2\left(\frac{2\pi^2}{L^2} C^2A^2\rho\right) \cos^2\left[\frac{2\pi}{L}(x - Ct)\right] dx$$

$$= 2\pi^2\rho C^3A^2/L^2 \qquad \ldots\ldots\ (46)$$

For a spherical wave the total flux E' passing in unit time through an envelope of large radius r is

$$E' = 8\pi^3\rho C^3A^2r^2/L^2 \qquad \ldots\ldots\ (47)$$

Consider equation (17) and putting the phase angle = -90^o,

then $y = A e^{-nt} \sin p_d t$

$$= A e^{-nt} \sin 2\pi f_d t \qquad \ldots\ldots\ (48)$$

where f_d is the frequency.

Now consider this wave propagating through a solid with a phase velocity C $(t = \frac{x}{C})$

Then, spatially, equation (48) becomes

$$y = A e^{-nx/C} \sin 2\pi f \left(\frac{x}{C} - t\right)$$

or $$y = A e^{-\alpha x} \sin 2\pi f \left(\frac{x}{C} - t\right)$$

where α (the spatial attenuation coefficient) = n/C (unit m^{-1})

and n is the temporal attenuation coefficient (unit t^{-1}).

Now considering only amplitude maxima

$$y = A e^{-\alpha x}$$

and the ratio of two successive maxima at

$$\frac{x_i}{x_{i+L}} = A e^{-\alpha x_i} \Big/ A e^{-\alpha(x_i+L)} = e^{-\alpha L} = e^{-\alpha C/f} = e^{\delta}$$

where, again, δ is the logarithmic decrement.

Consider the attenuation of seismic waves from a point source. The wavefront will be spherical, and, if there is no damping, the energy in unit solid angle will remain constant and the energy passing unit area will vary as $1/r^2$ (where r is the radius of the wavefront). Now the energy is proportional to y^2 . Therefore the amplitude of the motion will decrease as $1/r$. Thus for attenuation of amplitude due to *geometrical spreading* y is proportional to $1/r$. Consider, for example, two distances r_1 and r_2 from a point source, then with damping

$$y_1 = \frac{A}{r_1} e^{-\alpha r_1} \text{ and } y_2 = \frac{A}{r_2} e^{-\alpha r_2}$$

$$\text{Therefore, } y_2 = y_1 r_1 e^{-\alpha r_2} \Big/ e^{-\alpha r_1} r_2 = y_1 \frac{r_1}{r_2} e^{-\alpha(r_2-r_1)}$$

where A is the amplitude at the source

y_1 is the amplitude at r_1

y_2 is the amplitude at r_2

APPENDIX D

PHYSICAL PROPERTIES OF A GRANULAR SOIL

Consider a volume, V_f, of soil weight W_f. Conventionally a soil may be regarded as a three-phase system comprising solids, liquid (usually water) and gas (usually air).

Using subscripts to weight W and volume V as follows g - gas, w - water, v - voids, s - solids.

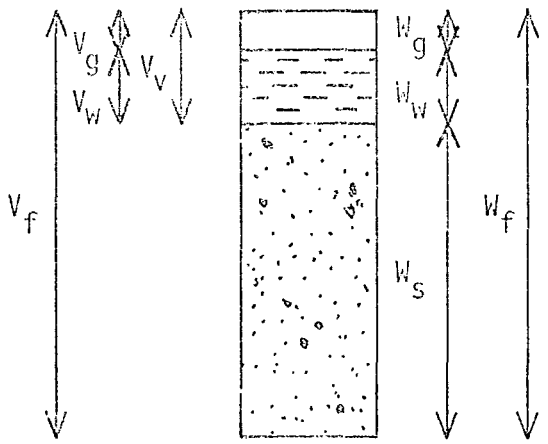

The porosity $n = V_v/V_f$

and void ratio $e = V_v/V_s$

Hence $n = e/1+e$ and $e = n/(1-n)$

Saturation $S = V_w/V_v = W_w/\gamma_w V_v$

where γ_w is the density of water

Moisture content $m = W_w/W_s$

Bulk density $\gamma = W_f/V_f$

Dry bulk density $\gamma_d = W_s/V_f = \gamma/(1+m)$

Specific gravity (solids) $G_s = \gamma_s/\gamma_w$

Hence $G_s m = Se = V_w/V_s$

Calculation of void ratio and porosity for samples of Warrington soil

Considering 1cc of *in situ* material

$$m = W_w/W_s$$

$$\therefore \quad W_w = m\, W_s = 13.1 \times 1.57/100 = 0.206 \text{ gm}$$

$$\therefore \quad V_w = 0.206 \text{ cc}$$

Now $V_s = \gamma_d/G_s = 1.57/2.64 = 0.595\text{cc}$

$$V_g = 1 - (V_s + V_w) = 0.199\text{cc}$$

Void ratio $e = V_v/V_s = (V_w+V_g)/V_s = 0.405/0.595 = 0.681$ and

Porosity $n = V_v/V_f = 0.405$

APPENDIX E

PROCESSED DATA FROM BOREHOLE A7

Record No.	Geophone (Level and direction)	Source (Cutting for ring -)	Tunnel-face/ borehole separation m	Peak particle velocity		Average relative amplitude									
				Zero to peak mm/s	Frequency Hz	0-50	50-100	100-150	150-200	200-250	250-300	300-350	350-400	400-450	450-500
10	4N-S	1041	18.4	0.09	150	0.54	0.46	0.38	0.24	0.18	0.10	0.06	0.04	0.02	0.02
16	4N-S	1059	7.4	0.37	180	1.5	2.5	2.6	1.9	2.0	1.4	0.8	0.5	0.4	0.3
19	4N-S	1059	7.4	0.56	230	1.6	2.9	3.0	1.9	1.9	1.3	0.9	0.6	0.5	0.4
22	4N-S	1064	4.3	2.10	190	3.0	4.5	5.0	7.5	5.5	4.0	3.0	2.0	1.5	1.0
25	4N-S	1072	- 0.6	2.50	150	4.0	6.0	8.0	7.5	7.0	4.5	3.5	2.5	1.5	1.0
29	4N-S	1073	- 1.2	2.70	200	3.0	4.5	6.0	6.0	6.0	3.0	2.0	1.0	1.0	0.5
32	4N-S	1075	- 2.5	1.10	150	2.6	3.6	4.0	3.8	3.4	2.6	1.8	1.0	0.7	0.6
42	4N-S	1084	- 8.0	0.55	-	1.6	1.6	1.5	1.2	1.0	0.7	0.5	0.3	0.2	0.2
11	4E-W	1041	18.4	0.06	100	0.22	0.42	0.28	0.26	0.22	0.12	0.08	0.02	0.00	0.00
17	4E-W	1059	7.4	0.49	200	0.9	2.1	2.4	2.4	2.5	1.6	0.8	0.5	0.4	0.3
20	4E-W	1059	7.4	0.50	240	0.9	2.5	2.9	2.5	2.4	1.7	0.9	0.6	0.4	0.3
25	4E-W	1064	4.3	2.10	200	2.0	5.0	8.0	7.5	6.0	3.5	2.5	1.5	1.0	1.0
27	4E-W	1072	- 0.6	2.74	160	2.0	4.5	7.0	9.0	7.0	4.0	2.5	2.5	2.0	2.0
30	4E-W	1073	- 1.2	1.20	140	1.5	3.5	5.0	6.0	5.0	3.0	2.0	1.5	1.0	1.0
33	4E-W	1075	- 2.5	0.78	180	1.5	2.6	3.2	3.2	2.5	2.0	1.2	0.8	0.5	0.4
44	4E-W	1084	- 8.0	0.49	95	0.9	1.3	1.2	1.2	1.0	0.7	0.5	0.3	0.2	0.2
12	4V	1041	18.4	0.10	160	0.20	0.40	0.28	0.22	0.14	0.06	0.04	0.02	0.02	0.02
18	4V	1059	7.4	0.24	160	1.3	2.5	1.9	2.3	1.4	1.0	0.9	0.6	0.5	0.4
21	4V	1059	7.4	0.34	200	0.9	2.3	1.8	1.4	1.1	0.8	0.7	0.4	0.3	0.2
24	4V	1064	4.3	0.83	190	1.5	3.0	4.5	4.5	3.5	2.5	2.0	1.3	1.0	1.0
28	4V	1072	- 0.6	1.34	140	2.0	3.5	4.8	4.0	2.5	2.0	1.5	1.5	1.5	1.5
31	4V	1073	- 1.2	1.67	130	1.5	3.0	3.5	3.0	2.0	1.5	1.0	1.0	0.5	0.5
34	4V	1075	- 2.5	0.44	-	1.6	2.4	2.0	2.2	1.8	1.3	0.9	0.6	0.2	0.2
46	4V	1084	- 8.0	0.49	-	1.2	1.2	1.0	0.8	0.5	0.4	0.2	0.2	0.2	0.1
38	1N-S	1076	- 3.1	0.39	125	1.8	1.4	1.4	1.3	1.0	1.0	0.8	0.8	0.7	0.4
35	2N-S	1076	- 3.1	0.60	-	1.6	3.0	2.4	2.0	2.0	1.7	1.2	0.9	0.5	0.4
36	3N-S	1076	- 3.1	0.99	140	1.8	3.1	4.1	4.0	2.9	2.1	1.5	1.0	0.8	0.6
37	4N-S	1076	- 3.1	0.70	120	2.4	2.4	2.2	2.3	2.4	1.6	1.2	0.8	0.5	0.4
42	1N-S	1084	- 8.0	0.20	100	1.2	0.8	0.7	0.5	0.4	0.3	0.3	0.2	0.1	0.1
39	2N-S	1084	- 8.0	0.54	85	1.1	1.6	1.2	1.2	0.9	0.8	0.7	0.6	0.3	0.2
40	3N-S	1084	- 8.0	0.54	-	1.2	1.8	1.8	1.7	1.6	1.5	1.1	0.7	0.5	0.3
41	4N-S	1084	- 8.0	0.44	85	1.4	1.8	1.7	1.8	1.8	1.2	0.9	0.6	0.4	0.2

APPENDIX E

Processed data from borehole A7 (continued)

Record No.	Relative amplitude and frequency of principal peaks						Peak relative amplitude									
	Amp	Hz	Amp	Hz	Amp	Hz	0-50	50-100	100-150	150-200	200-250	250-300	300-350	350-400	400-450	450-500
10	3.2	110	3.1	25	-	-	1.20	1.14	1.26	0.66	0.52	0.24	0.16	0.12	0.08	0.06
16	28.2	90	19.3	240	15.3	150	4.1	9.2	9.5	8.4	10.4	6.5	4.1	1.6	1.5	1.3
19	28.6	90	21.2	240	-	-	3.4	11.0	9.0	5.3	9.8	4.7	3.0	1.9	1.4	1.2
22	89	180	68	160	47	230	5.5	11.5	12.5	47.0	30.0	19.0	12.5	7.0	5.0	4.0
26	75	150	70	130	53	210	9.0	21.0	39.0	35.0	33.0	15.5	9.5	7.0	5.0	4.0
29	83	205	74	215	55	172	7.5	13.0	24.0	33.0	39.0	10.0	4.0	3.5	4.0	3.5
32	37	123	25	180	23.4	85	8.0	15.6	19.2	14.0	13.2	9.4	7.0	3.2	2.6	2.0
43	13.9	130	12.5	95	11.3	75	4.9	7.1	7.4	3.8	3.2	2.1	1.6	1.4	1.1	0.9
11	2.0	70	1.8	55	-	-	0.62	1.10	0.74	0.72	0.70	0.46	0.20	0.10	0.06	0.04
17	29	250	20.3	220	18.8	180	4.2	7.8	8.4	11.7	14.5	10.5	3.5	1.8	1.7	1.2
20	21.9	290	18.2	160	17.0	120	2.5	8.2	10.5	7.6	10.0	5.6	2.8	1.7	1.4	1.0
23	80	160	64	210	61	180	4.5	14.0	22.5	45.0	33.0	13.0	9.0	5.0	3.5	4.5
27	90	150	70	207	45	240	8.0	19.0	44.0	50.0	30.0	15.0	9.5	12.0	8.5	8.5
30	43	170	40	135	40	205	4.0	9.5	25.0	24.0	23.0	11.5	4.5	4.5	3.5	2.5
33	29	100	23	85	22.6	170	4.4	12.6	13.2	13.6	8.0	8.8	5.8	3.0	1.8	1.6
44	12.2	95	10.7	112	10.0	127	2.3	5.7	6.2	4.6	3.6	2.2	1.2	0.8	0.7	0.6
12	1.7	75	1.5	95	1.26	110	0.58	1.02	0.82	0.64	0.40	0.20	0.14	0.08	0.08	0.06
18	20.3	180	16.7	160	12.5	70	2.5	8.4	5.6	11.0	4.3	2.5	2.7	1.4	0.8	0.8
21	11.3	70	8.3	190	-	-	2.0	7.3	5.2	5.2	3.3	2.5	1.9	1.3	0.8	0.7
24	29	210	24	180	23	130	3.0	7.5	14.0	14.5	13.0	9.5	5.5	4.5	3.0	2.0
28	55	140	42	130	28	185	5.0	10.0	30.0	19.5	10.5	6.0	5.0	4.5	4.5	4.5
31	58	135	45	155	-	-	4.5	9.0	26.0	17.0	10.0	5.0	3.0	2.5	2.5	2.5
34	16.2	60	14.4	85	14.0	140	4.4	10.6	8.0	8.2	8.1	5.2	3.7	1.9	1.4	2.0
45	12.0	85	11.9	76	10.1	46	3.2	6.7	5.2	3.0	2.0	0.9	0.8	0.7	0.6	0.4
38	8.0	25	7.6	135	-	-	3.8	3.3	5.2	4.8	2.9	2.7	2.5	2.3	2.1	1.3
35	22.2	130	11.6	80	-	-	3.4	7.8	7.2	6.2	5.6	4.8	4.2	2.6	1.3	1.2
36	46.8	130	16.8	160	-	-	3.8	8.0	16.5	11.8	8.2	5.8	5.2	3.4	2.3	1.9
37	12	130	12	210	10.6	160	5.0	5.2	7.2	7.0	7.3	3.8	3.2	2.1	1.4	1.0
42	5.1	22	5.0	50	4.5	110	3.4	2.4	2.6	1.7	1.6	1.2	1.2	0.6	0.6	0.4
39	13.6	80	8.3	115	7.1	50	3.5	6.0	4.8	4.5	2.5	2.3	2.7	2.5	0.9	0.5
40	14.4	265	12.0	120	9.5	192	3.5	5.5	6.7	6.1	6.1	7.5	3.6	2.7	2.3	2.0
41	13.9	90	13.3	215	-	-	5.5	7.0	5.9	6.4	7.7	5.0	4.4	2.6	2.1	0.8

APPENDIX F

PROCESSED DATA FROM BOREHOLE B7

Record No.	Geophone (Level and direction)	Source (Cutting for ring -)	Tunnel-face/ borehole separation m	Peak particle velocity		Average relative amplitude									
				Zero to peak mm/s	Frequency Hz	0-50	50-100	100-150	150-200	200-250	250-300	300-350	350-400	400-450	450-500
54	4N-S	1167	4.9	0.31	200	0.2	0.8	1.4	1.5	1.8	1.1	0.9	0.7	0.6	0.5
57	4N-S	1167	4.9	0.34	120	0.3	0.8	1.4	1.4	1.5	1.2	0.8	0.7	0.6	0.5
60	4N-S	1174	0.6	1.14	250	1.2	3.2	4.0	3.8	4.0	3.6	2.6	1.8	1.6	1.4
63	4N-S	1174	0.6	1.11	60	1.0	2.7	3.7	3.4	3.6	3.0	2.4	2.8	1.6	1.1
66	4N-S	1175	0	1.85	-	2.0	4.0	5.2	5.3	6.5	6.0	4.8	3.2	3.0	2.1
84	3N-S	1184	- 5.5	0.34	-	3.2	3.5	1.8	1.1	0.6	0.4	0.2	0.2	0.1	0.1
87	3N-S	1185	- 6.1	0.31	-	2.4	2.7	1.5	1.2	0.6	0.4	0.3	0.2	0.1	0.1
90	3N-S	1192	- 10.5	0.12	60	2.3	1.8	0.9	0.45	0.3	0.15	0.05	0	0	0
95	3N-S	1193	- 11.1	0.17	-	1.8	1.6	0.7	0.4	0.2	0.1	0	0	0	0
55	4E-W	1167	4.9	0.56	-	1.4	3.5	4.3	3.4	1.9	1.6	0.9	0.8	0.6	0.5
58	4E-W	1167	4.9	0.64	-	1.4	3.5	4.9	3.4	1.9	1.5	0.8	0.7	0.6	0.5
61	4E-W	1174	0.6	1.07	230	2.2	6.0	5.6	5.0	5.0	4.8	3.4	2.8	2.2	1.6
64	4E-W	1174	0.6	1.11	60	2.4	6.3	6.4	5.2	4.8	4.0	3.0	2.1	1.7	1.3
67	4E-W	1175	0	2.48	105	3.5	9.0	9.5	7.3	8.5	7.4	6.0	4.1	3.1	2.5
82	4E-W	1184	- 5.5	0.44	45	2.8	3.1	1.2	0.9	0.5	0.4	0.3	0.2	0.1	0.1
85	3E-W	1184	- 5.5	0.46	-	4.0	2.4	1.4	0.9	0.5	0.4	0.3	0.2	0.1	0.1
88	3E-W	1185	- 6.1	0.48	-	3.3	2.1	1.3	0.9	0.6	0.4	0.3	0.2	0.1	0.1
93	3E-W	1192	- 10.5	0.15	-	2.6	1.6	0.9	0.45	0.3	0.15	0.1	0.05	0	0
96	3E-W	1193	- 11.1	0.24	-	2.5	1.5	0.8	0.4	0.2	0.1	0	0	0	0
56	4V	1167	4.9	0.54	-	1.1	2.8	3.0	2.4	1.5	1.1	0.8	0.6	0.4	0.3
59	4V	1167	4.9	0.54	95	1.4	3.4	3.6	2.3	1.4	1.2	0.7	0.6	0.4	0.3
62	4V	1174	0.6	1.10	-	3.4	6.0	4.7	3.2	3.3	2.4	1.7	1.6	1.2	1.0
65	4V	1174	0.6	1.24	55	3.6	5.5	5.0	3.6	3.0	2.3	1.5	1.2	1.0	0.8
68	4V	1175	0	1.35	-	7.0	7.5	7.8	5.2	5.5	5.0	3.8	5.0	4.7	1.7
83	4V	1184	- 5.5	0.78	-	5.2	3.1	1.9	1.0	0.7	0.3	0.2	0.2	0.1	0.1
86	3V	1184	- 5.5	0.29	120	2.8	2.4	1.7	1.0	0.5	0.4	0.3	0.2	0.1	0.1
89	3V	1185	- 6.1	0.64	100	2.1	2.2	1.5	1.0	0.6	0.5	0.3	0.2	0.1	0.1
94	3V	1192	- 10.5	0.10	-	1.9	1.6	0.9	0.45	0.3	0.15	0.10	0.05	0	0
97	3V	1193	- 11.1	0.17	60	1.6	1.5	0.8	0.4	0.25	0.1	0	0	0	0
69	1V	1177	- 1.2	0.54	55	3.0	2.8	1.9	1.0	0.5	0.4	0.3	0.2	0.1	0.1
70	2V	1177	- 1.2	0.56	-	3.1	3.8	2.9	1.8	1.2	0.7	0.6	0.4	0.3	0.2
71	3V	1177	- 1.2	0.46	50	1.1	1.6	1.5	1.2	1.0	0.6	0.4	0.3	0.2	0.2
72	4V	1177	- 1.2	0.53	-	3.7	2.3	1.8	1.5	1.2	1.0	0.7	0.6	0.5	0.5
73	1V	1181	- 3.7	0.27	50	3.0	2.1	1.2	0.7	0.4	0.3	0.2	0.1	0.1	0
74	2V	1181	- 3.7	0.34	90	3.1	2.8	1.9	1.0	0.6	0.5	0.4	0.3	0.1	0.1
75	3V	1181	- 3.7	0.20	100	1.9	1.8	1.3	1.2	0.8	0.7	0.4	0.2	0.1	0.1
76	4V	1181	- 3.7	0.31	-	2.5	2.1	1.2	1.1	0.9	0.7	0.5	0.4	0.4	0.4
77	1V	1183	- 4.9	0.34	30	3.5	2.0	1.0	0.5	0.3	0.2	0.1	0.1	0.1	0
78	2V	1183	- 4.9	0.34	-	3.4	3.2	1.6	0.9	0.5	0.3	0.2	0.1	0.1	0.1
79	3V	1183	- 4.9	0.41	80	2.6	2.1	1.1	0.9	0.5	0.4	0.3	0.2	0.1	0.1
80	4V	1183	- 4.9	0.44	40	6.4	2.9	1.3	0.8	0.5	0.4	0.2	0.2	0.1	0.1

Processed data from borehole B7 (continued)

Record No.	Relative amplitude and frequency of principal peaks						Peak relative amplitude									
	Amp	Hz	Amp	Hz	Amp	Hz	0-50	50-100	100-150	150-200	200-250	250-300	300-350	350-400	400-450	450-500
54	16.1	195	10	100	10	125	0.8	3.7	6.2	6.4	5.3	2.9	1.9	1.6	1.1	1.1
57	19.7	128	14.0	145	-	-	1.0	3.7	8.1	4.9	4.9	3.1	2.0	1.5	1.3	1.2
60	17.8	208	17.4	80	17.2	180	5.4	11.2	11.6	12.2	12.6	10.8	7.4	5.2	6.4	5.8
63	29.1	55	24.6	100	16.4	250	3.4	12.6	11.4	9.0	10.8	10.0	8.0	6.1	4.0	3.7
66	34	122	28.5	112	23	235	6.0	11.0	18.0	15.5	18.0	15.0	12.5	8.0	6.0	5.0
84	16.2	24	11.2	48	11.2	72	8.5	8.4	4.7	2.5	1.2	0.7	0.5	0.4	0.3	0.2
87	10.3	60	9.3	29	8.7	88	5.1	6.8	3.5	2.9	1.4	0.9	0.6	0.4	0.4	0.4
90	8.3	40	5.8	77	5.1	125	4.9	4.0	2.5	1.2	0.6	0.4	0.2	0.2	0.2	0.2
93	8.0	53	7.0	62	6.5	22	4.2	4.2	1.8	1.1	0.5	0.4	0.2	0.2	0.2	0.1
56	29.0	112	19.5	93	15.5	165	4.4	9.7	14.2	9.0	5.1	5.0	3.0	2.0	1.7	1.9
58	25.4	95	20.8	138	19.5	114	4.6	10.7	15.6	9.4	4.8	3.7	2.5	2.4	1.8	1.7
61	35	235	31.6	210	29	88	6.0	16.2	15.0	15.6	21.8	18.2	12.0	11.8	14.0	7.4
64	28.8	98	28.4	55	28.4	108	6.8	19.4	17.0	13.3	12.0	10.0	8.2	5.0	5.0	5.2
67	63	110	54	124	51	100	7.5	27.5	35.5	19.0	24.0	22.0	20.5	13.0	7.7	5.3
82	16.7	47	11.7	75	11.6	32	7.6	7.9	3.3	2.4	1.5	1.0	0.7	0.5	0.4	0.3
85	20.5	37	16.3	28	15.7	22	8.5	6.2	3.9	3.3	1.2	0.8	0.6	0.5	0.4	0.3
88	13.7	26	11.4	16	9.4	41	8.2	5.3	3.4	2.4	1.4	0.9	1.0	0.8	0.7	0.4
99	9.9	28	8.4	35	8.4	40	6.4	3.9	2.1	1.1	0.7	0.4	0.3	0.2	0.2	0.15
96	12.8	27	9.4	38	7.7	43	3.7	1.8	0.8	0.6	0.3	0.2	0.2	0.2	0.2	0.2
55	21	93	19.4	103	12.5	168	2.6	9.2	9.5	7.8	4.5	3.0	1.9	1.3	1.9	1.0
59	32	95	21.5	72	17.8	118	3.9	12.5	11.3	6.2	3.6	3.0	1.7	1.5	0.9	0.9
62	38.4	80	32.5	65	25.4	122	8.6	22.0	15.2	9.4	10.4	7.0	4.4	6.6	5.2	5.2
65	47	55	33.8	108	23.6	128	9.8	21.6	16.6	9.5	8.6	9.4	4.5	2.9	2.9	4.0
68	32	137	31	85	-	-	16.0	22.0	23.0	13.5	15.0	14.5	9.0	7.5	5.0	4.0
80	24.0	13	18.5	40	13.3	62	13.3	8.0	5.2	3.3	4.9	1.0	0.7	0.7	0.7	0.5
86	9.6	36	9.4	40	8.5	60	6.2	6.1	4.1	2.2	1.2	0.9	0.6	0.4	0.3	0.2
83	10.4	40	8.1	85	7.5	23	5.6	5.6	4.1	2.4	1.2	1.0	0.8	0.5	0.4	0.4
100	7.35	37	6.4	45	6.3	52	4.2	3.9	2.1	1.05	0.75	0.3	0.2	0.2	0.15	0.15
97	7.1	66	6.8	27	6.4	40	4.2	3.9	1.8	0.9	0.6	0.4	0.2	0.2	0.2	0.10
69	16.2	24	13.5	105	13.0	60	7.0	7.7	6.6	3.4	1.6	1.3	1.0	1.0	0.7	0.6
70	18.8	105	17.0	112	16.2	60	7.1	10.6	10.2	5.4	3.5	2.1	1.8	1.3	1.0	0.9
71	11.7	132	11.5	105	10.4	75	2.9	6.6	6.6	3.7	3.1	1.5	1.3	0.8	0.6	0.5
72	19.7	24	12.3	35	11.3	105	9.5	6.2	6.1	4.3	3.6	3.1	2.4	1.5	1.4	1.2
73	11.8	28	9.6	53	8.1	13	5.8	6.0	2.9	1.6	0.9	0.6	0.4	0.4	0.3	0.2
74	14.7	88	12.0	105	11.4	26	6.9	7.9	5.5	2.5	1.4	0.9	0.8	0.6	0.4	0.3
75	7.8	53	7.7	92	7.4	108	4.0	4.3	3.6	2.5	1.7	1.4	0.8	0.4	0.4	0.3
76	7.7	22	6.8	15	6.6	40	5.0	4.5	3.0	2.3	1.8	1.7	1.0	0.9	0.9	0.3
77	13.3	35	11.3	26	10.3	48	7.5	5.2	2.6	1.3	0.7	0.5	0.4	0.3	0.3	0.2
78	18.6	65	17.0	78	13.0	15	7.0	7.0	4.9	2.1	1.1	0.8	0.7	0.4	0.3	0.3
79	10.5	38	10.0	60	9.8	84	5.9	5.8	4.1	2.2	1.2	1.0	0.7	0.5	0.4	0.4
80	21.4	35	20.4	27	16.0	14	14.0	6.9	3.9	2.1	1.0	1.0	0.6	0.5	0.5	0.4

APPENDIX G

SUPPLEMENTARY PROCESSED DATA

Record No.	Geophone (Level and direction)	Source (Cutting for ring -)	Tunnel-face/ geophone separation m	Peak particle velocity		Average relative amplitude									
				Zero to peak mm/s	Frequency Hz	0-50	50-100	100-150	150-200	200-250	250-300	300-350	350-400	400-450	450-500
4	CELLAR FLOOR V	1036	< 5	0.37	80	1.5	2.6	1.9	1.6	1.4	0.7	0.3	0.3	0.1	0.1
7	CELLAR FLOOR V	1039	< 5	0.37	140	1.9	3.0	2.3	2.1	1.6	0.9	0.5	0.4	0.2	0.1
5	CELLAR FLOOR E-W	1039	< 5	0.17	230	1.1	0.9	0.9	0.85	1.0	0.5	0.25	0.1	0.05	0.05
8	CELLAR FLOOR E-W	1039	< 5	0.24	215	1.4	1.0	1.0	1.1	1.2	0.7	0.3	0.2	0.1	0.1
6	CELLAR FLOOR N-S	1039	< 5	0.20	190	1.3	1.4	0.9	1.0	0.8	0.35	0.2	0.1	0.1	0.1
9	CELLAR FLOOR N-S	1039	< 5	0.24	180	1.7	1.7	1.25	1.25	1.0	0.5	0.25	0.15	0.1	0.1
50	PAVEMENT V	1085	6	0.98	115	2.8	2.5	1.8	2.1	2.2	2.0	1.2	1.2	0.9	0.9
52	PAVEMENT V	1085	6	0.61	75	2.6	2.3	1.3	1.2	1.0	0.8	0.8	0.6	0.5	0.4
51	PAVEMENT V	1085	18	0.26	70	0.9	1.25	0.6	0.4	0.3	0.2	0.15	0.1	0.05	0.05
53	PAVEMENT V	1085	18	0.22	80	1.1	1.1	0.5	0.25	0.20	0.15	0.10	0.05	0.05	0.05
91	4N-S	1174	0.6	1.14	250	1.1	2.4	3.2	3.2	3.3	3.0	2.3	1.7	1.4	1.0
						0-100	100-200	200-300	300-400	400-500	500-600	600-700	700-800	800-900	900-1000
92	4N-S	1174	0.6	1.14	250	3.0	4.8	4.7	2.6	1.7	0.9	0.8	0.5	0.2	0.2
93	4N-S	1174	0.6	1.10	60	2.8	4.8	4.4	2.6	1.6	1.1	0.9	0.7	0.4	0.2

APPENDIX G

Supplementary processed data (continued)

Record No.	Relative amplitude and frequency of principal peaks						Peak relative amplitude									
	Amp	Hz	Amp	Hz	Amp	Hz	0-50	50-100	100-150	150-200	200-250	250-300	300-350	350-400	400-450	450-500
4	23.7	80	15.5	68	15.5	85	3.6	11.5	6.4	4.8	4.5	2.4	1.0	0.8	0.4	0.4
7	20.3	145	19.9	190	15.0	60	4.6	9.1	9.5	8.8	5.4	3.2	1.9	1.3	0.8	0.8
5	5.8	30	5.6	215	-	-	2.9	2.7	2.8	2.7	3.5	1.9	0.6	0.35	0.2	0.2
8	7.8	218	7.6	30	-	-	4.2	2.9	3.2	4.2	4.7	2.6	1.2	0.5	0.4	0.4
6	6.5	175	6.3	105	6.0	26	3.4	4.1	3.0	3.6	2.8	1.0	0.45	0.3	0.25	0.25
9	14	140	9.8	60	-	-	3.9	4.7	5.4	4.4	3.4	1.5	0.8	0.6	0.45	0.50
50	32	110	26.6	65	22.8	170	9.0	13.6	14.0	11.8	10.6	10.0	5.6	4.6	3.6	3.6
52	36.6	65	15.0	55	-	-	6.2	12.2	4.8	4.6	3.1	2.4	2.2	1.7	1.9	1.9
51	12.3	103	11.9	65	4.1	24	2.4	5.2	4.0	1.6	1.1	0.9	0.55	0.25	0.25	0.20
53	10.6	63	6.5	92	-	-	2.9	4.8	2.7	1.0	0.55	0.4	0.25	0.2	0.2	0.2
91	28.0	55	26.6	230	24.0	103	7.0	16.2	14.4	14.8	16.0	13.8	10.2	7.2	6.7	6.0
92	30.6	190	27.4	90	26.0	150	16.0	21.4	19.0	10.4	10.4	4.8	3.8	3.8	1.6	1.6
93	52.2	60	41	110	31	250	17.0	18.0	18.5	12.3	6.7	4.3	2.8	1.8	1.8	1.6

APPENDIX H

SIMPLIFIED ANALYSIS OF SIMPLE HARMONIC MOTION

Consider a line OB, length r, rotating about point O at ω rads/sec. BC is the vertical projection of the point B which intersects OA at C.

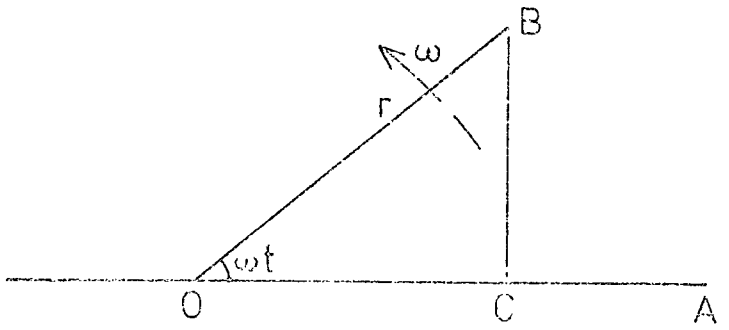

Let the displacement OC = y

At the initial instant, t_o, let point B be coincident with A then after t seconds

displacement $y = r \cos \omega t$

velocity $\frac{dy}{dt} = -\omega r \sin \omega t$

and acceleration $\frac{d^2y}{dt^2} = -\omega^2 r \cos \omega t = \omega^2 y$

$$\omega = 2\pi f = \left(\frac{\text{acceleration}}{y}\right)^{\frac{1}{2}}$$ where f = frequency

Maximum displacement (amplitude) = r

Maximum velocity = $-\omega r = 2\pi f r$

Maximum acceleration = $\omega^2 r = 4\pi^2 f^2 r$